

We thank the reviewers for their time and effort reviewing this manuscript. All reviewer comments are reproduced below in ***bold, italicized font***. Our responses are shown in regular font. Changes to the text are indicated as underlined text for insertions or are ~~crossed-out~~ for deletions. Line numbers given below are for the revised version with all markups shown. We numbered the reviewer comments for easier cross-referencing.

Anonymous Referee #1

This manuscript measured a variety of air pollutants at a surface site in the oil sands region in summer 2013. PCA approach was used to elucidate major sources of these air pollutants, in particular, IVOCs. Using the 95% cumulative percentage of variance criterion, ten components were categorized, among which 3 components correlated with IVOCs, most likely related to the unearthing and processing of raw bitumen. The authors also found the association of secondary variables with the primary components, implying rapid formation of these secondary products on a time scale that is similar to the transit time of the pollutants to the measurement site. The study was specifically carried out in an oil sand region, which constrained the extension of the implication of the findings to other regions. The PCA with different number of sources was tested, and the identification of source types was discussed and elucidated in detail.

Though this manuscript was for a special issue of ACP, this manuscript still needs significant improvement, and could only be considered for potential publication after the following major concerns are well addressed.

1) The aim of this study was to identify IVOC sources. However, none of the peaks of IVOC species in Ion Chromatograms was identified, which subsequently biased or even wronged the identification of the IVOC sources.

The goal of this manuscript was to identify sources of IVOCs, but not to identify the compounds that make up the IVOCs. The identities of individual IVOCs do not need to be known to determine their origin as a group, through PCA, and does not imply, as the reviewer suggests, that our analysis was biased or wrong.

We agree with the reviewer, however, that identification of individual IVOC may provide useful information; however, this was not possible for this measurement campaign, since the IVOCs did not resolve on the chromatographic column. The more important feature is the volatility range of these species, which was constrained based on their retention times.

We note on line 779 that "future studies should focus on characterizing the VOCs in the above mentioned volatility range using a greater mass and time resolution instrument, such as a time-of-flight mass spectrometer (TOF-MS) or higher resolution separation methods (e.g., multi-dimensional gas chromatography)".

No changes were made in response to reviewer's comment.

2) It is doubtful that CO was mainly generated from VOC oxidation given many industrial sources in the oil sand region.

We apologize for the misunderstanding, which was probably triggered by the entry in Table 6 and the discussion of component 9 in the S.I.

The main source of CO in the atmosphere is undoubtedly the incomplete oxidation of hydrocarbons, to which a variety of sources contribute – e.g., fuel combusted in car engines, generators, forest fires, etc. or VOCs oxidized photochemically. For the oil sands region, it is, as Marey et al. (2015) state, generally "assumed that CO spatial variations in northern Alberta are associated with oil sands industrial activities and forest fires". We certainly agree that in the vicinity of large industrial sources such as the AOS industrial sources ought to be the largest source of CO. Our analysis suggests that factor 9 is dispersed over a wide geographical area, which could be due to a combination of numerous CO point sources (generators, pump stations, motor vehicles, etc.), i.e., the size of the geographical area covered by oil sands operations, but could also include the oxidation of biogenic and anthropogenic VOCs. Accordingly, we state in the main text that "Carbon monoxide is a tracer of biomass burning and fossil fuel combustion, in particular in automobiles with poorly performing or absent catalytic converters, but is also a byproduct of the oxidation of VOCs, in particular of methane and isoprene which are oxidized over a wide area upwind of AMS 13 (Miller et al., 2008)."

The assignment to component 9 to a particular source is somewhat tentative as noted on lines 378-380 that "components 6 through 10 are somewhat tentative as many (i.e., 7 – 9) are single variable components and have eigenvalues close to or below unity, i.e., account for less variance than any single variable."

In response to the reviewer's comment, we have modified the text as follows:

In Table 6, component 9 (Enhancement of CO) now lists as possible source(s) "incomplete hydrocarbon oxidation" instead of "VOC oxidation".

We have also modified the paragraph starting on line 376 as follows:

"Components 1 through 4 emerged regardless of the number of components used to represent the data, whereas the structure of components 5 through 10 only fully emerged in the 10-component solution (see S.I.). Hence, components 6 through 10 are somewhat tentative as many (i.e., 7 – 9) are single variable components and have eigenvalues close to or below unity, i.e., account for less variance than any single variable. As a result, the interpretations of these components are subject to more uncertainty and are more speculative but are presented in the S.I. for the sake of completeness and transparency. For the purpose of this manuscript, this is inconsequential as components 6 – 10 are not associated with IVOCs."

We have also slightly modified a paragraph in the S.I. (starting on line 366):

"Component 9: ~~Background CO from VOC oxidation~~ Incomplete hydrocarbon oxidation
Component 9 is another single variable component and strongly correlates with CO ($r = 0.87$). The variables with the next largest correlation coefficients are CH_4 ($r = 0.17$), 1,2,3- and 1,2,4-TMB (both $r = 0.18$), and o-xylene ($r = 0.16$).

The conventional interpretation of CO is as a byproduct of incomplete hydrocarbon oxidation, as it is found in fossil fuel combustion exhaust or in biomass burning plumes. Component 9, however, is not associated with NO_y (r = -0.08) or CO₂ (r = 0.05), which rules out this conventional interpretation. Recently, Marey et al. (2015) examined the spatial distribution of CO in Northern Alberta using a combination of satellite and ground station data and found that most CO is derived from anthropogenic sources, biomass burning and the photochemical oxidation of methane and other VOCs."

3) The criteria for the degree of correlations, i.e., correlation coefficient r value, are unclear. $r = 0.3$ indicated very poor correlation to me.

The criteria for the degree of correlations were stated on lines 362-364 in the text: 'Associations with $r > 0.7$, $r > 0.3$, and $r > 0.1$ are referred to as "strong", "moderate", and "weak", respectively.' We chose a cut-off value of 0.3 because of the non-negligible correlations of IVOCs with components 1 and 2 (Table 5). The labels "weak", "strong", and "moderate" were used for the purpose of keeping the discussion consistent when referencing degrees of correlation.

In light of the reviewer's concern (which was echoed by reviewer 3), we have modified the text, starting with the sentence on lines 362-364, as follows:

'Associations with $r > 0.7$, $r > 0.3$, and $r > 0.1$ are referred to as "strong", "~~moderate~~weak", and "~~weak~~poor", respectively.'

Specific comments:

1a. Page 9, Figure 2. The gray area showed unsolved HCs in the volatility range of C11-C17 with saturation vapor concentration from $105 \text{ g m}^{-3} < C^* < 107 \text{ g m}^{-3}$. It is not clear how the retention time for C11, C12, ..., C16 was obtained in the figure.

Our apologies – this important experimental detail should have been provided. The retention times were obtained by analyzing a standard hydrocarbon mixture with the same temperature program and carrier gas flow rate as deployed in the field. We have added the following to the figure caption:

"Figure 2. (Top) (Bottom) Retention times of n-alkanes, determined after the measurement intensive by sampling a VOC mixture containing a C₁₀ – C₁₆ n-alkane ladder."

1b. The marked retention time for C11-C16 n-alkanes is actually doubtful, because for n-alkanes IVOCs, the distance between C11 and C12, C12-C13, C13-C14, ... C15-C16 in the chromatograms should be generally equal. Also, their retention time in Figure 2 seems too high (25 min later) as they usually appear at 10-15 mins (of course it depends on the methods and columns used).

The reviewer is assuming that the GC was operated using a single temperature ramp. However, we used a somewhat unusual temperature program that resulted in uneven spacing of the n-alkanes; the temperature program is described in the S.I. on line 87:

"The GC oven was programmed as follows: hold at 40° C for 3.00 min, heat at 1.5° C min⁻¹ to 70° C, heat at 5° C min⁻¹ to 200 °C and hold for 4 min (total 53.00 min)."

We have modified this description slightly as follows:

"The GC oven was programmed as follows: hold at 40 °C for 3.00 min, heat at 1.5 °C min⁻¹ to 70° C (reached at 23.00 min), heat at 5° C min⁻¹ to 200 °C (reached at 49.00 min) and hold for 4 min (total 53.00 min)."

No further changes were made in response to reviewer's comment.

1c. Furthermore, why were some IVOC species not identified (even could not be quantified) when this study was designed because the focus of this manuscript is about IVOC sources? If the focus was based on something unknown, the speculation could be very wrong.

Please see our response above to major comment #1 above.

1d. In this study, the headspace sample of bitumen indeed showed an unsolved signal in the IVOC range, but this does not mean bitumen is definitely the IVOC source in this study because nalkanes IVOCs have many other sources such as vehicular emissions, biogenic IVOCs (e.g. sesquiterpenes) and petroleum enterprises.

The reviewer is correct that IVOCs may originate from all of these sources. However, our analysis (see Table 5) suggests that the IVOCs in this study originated mainly from a standalone component (#5), were not associated with a biogenic source (#3) and only very weakly with vehicular sources (#2). Since these associations are described and discussed at length in the manuscript, no changes were made in response to reviewer's comment.

1e. In fact, there are mature analytical methods such as TAG-GC-ToF-MS for gas- and particle-phase IVOCs, SVOCs and SOA tracers.

This is correct. However, identification of individual compounds that make up the IVOC signature was not the goal of this work, nor was it possible with the instrumentation on hand during the time of the study. We agree that future TAG-GC-ToF-MS measurements at this site would be useful. In response to the reviewer's comment, we modified a paragraph in the conclusion section:

"Finally, there is a need for improved monitoring methods for IVOCs. For instance, future studies should focus on characterizing the VOCs in the above mentioned volatility range using a greater mass and time resolution instrument, such as a time-of-flight mass spectrometer (TOF-MS), higher resolution separation methods (e.g., multi-dimensional gas chromatography), and also include measurement of speciated aerosol organic composition by, for example, thermal desorption aerosol GC (TAG) analysis (Williams et al., 2006). "

2a. I have to admit that the PCA results in this study were quite impressive no matter how many factors were extracted (5-11 factors) because it is common that PCA often gives collocated factors and it is very difficult to identify 10 or above individual sources with this method, especially when 22-28 variables were input.

We agree that this is a somewhat unusual, though note that the sources in this region are somewhat unusual as well. In support of the number of components extracted, all solutions are shown in the supplementary information for this reason.

No changes were made in response to this comment.

2b. Certainly more than 200 samples as input could enhance the PCA extraction.

We agree. Unfortunately, we are limited by the temporal resolution of the various instruments on site, data outages, etc. A longer field study over an entire season would be very beneficial for this type of approach. Since we already state on line 764 that "A longer continuous data set with a greater number of variables would have perhaps been able to resolve these different sources", that is, additional components, no changes were made to the manuscript in response to the reviewer's comment.

3. Page 12, Table 3. 4 AVOC and 3 BVOC species were quantified. What were the reasons to select these specific VOC species in this study, due to the limit of GC-ITMS or selection of tracers? In particular, isoprene was not measured (used) in this study as its level in the atmosphere is usually much higher than other BVOCs.

As stated on lines 183-185, we included all quantified non-methane hydrocarbons in the analysis. We agree that inclusion of a larger number of hydrocarbons would have been advantageous; however, the GC-ITMS was the only time-resolved VOC instrument on site that reported final data. Isoprene was not on this list.

The manuscript was not changed in response to the reviewer's comment.

4. Lines 284-289 stated that CH₄ and CO₂ originated from distinct sources while both correlated well with Factor 6 in Table 5, indicating their similar sources/patterns. They are contradictory. Please clarify it.

There are many sources of CH₄ and CO₂ in the region. This is reflected by five different components that correlate with one of CH₄ or CO₂ (but not the other); these are # 1, 2, and 3. Factor 6 is the only one associated with both CH₄ and CO₂ (Table 5). To improve the clarity of the manuscript, we have modified the text on lines 306-307:

"While CH₄ and CO₂ mixing ratios frequently correlated in plumes, their ratios were variable overall, suggesting they often originated from distinct sources."

5. Table 5 claims that coefficients with Pearson correlation coefficients $r > 0.3$ are interpreted as being moderately or strongly associated with a component, which I do not agree.

We apologize for the confusion and have modified the table caption (which contradicted what was stated in the main text) as follows:

"Table 5. Loadings for the 10-factor, optimal solution (primary variables only). Coefficients with Pearson correlation coefficients $r > 0.3$ are ~~interpreted as being moderately or strongly associated with a component and are~~ shown in bold font."

What are the criteria to select $r > 0.3$ to indicate moderate or strong association? To me, r value around 0.3 means very poor correlation. At least r value should be > 0.5 to indicate somewhat correlations.

Please see our response to major comment #3 above.

6. Page 24, Table 6. Component 5 was identified as "surface exposed bitumen and hot-water based bitumen extraction". This is only based on the headspace sample of bitumen without any identification of IVOC species. Could it be other sources?

In Table 6, we show "Hypothesized identifications" and "possible source(s)", i.e., they are not definitive identifications. Other potential sources were considered and discussed on lines 579-618.

In brief, we concluded that surface exposed bitumen and hot-water based bitumen extraction was a likely source contributing to component 5. This is supported by the observations of hydrocarbons that encompassed the same volatility space and produced similar ion fragments in the electron impact mass spectra as observed in the head space analysis above bitumen (Figure 2) and the absence of correlations with variables expected to be associated with other activities, such as CO_2 .

As already stated in our response to major comment #1, identification of individual IVOC species is not necessary in this context.

No changes were made in response to this comment.

If TAG-GC-ToF-MS was used, this source could be better identified.

Please see our responses to major comment #1 and minor comment #1e above.

Furthermore, IVOCs correlated well with LO-OOA (Table 5), implying that some IVOCs might be secondarily formed or the PCA results were collocated. Please comment on these.

This is discussed on lines 516-521:

"Component 1 is also **weakly** associated with the less oxidized oxygenated organic aerosol factor, LO-OOA ($r = 0.45$). Liggio et al. (2016) found that the observed secondary organic aerosol is dominated by

an OOA factor whose mass spectrum was similar to those of aerosols formed from oxidized bitumen vapours. The organic aerosol budget in this study was also dominated by an OOA factor, the LO-OOA (Lee et al., 2018). The association of LO-OOA with component 1 is thus consistent with its association with IVOCs."

It is possible that the IVOCs included species formed by secondary processes. However, given the close proximity to sources (and a bias of the measurement towards non-oxygenated hydrocarbons - see our response to question 2 by reviewer 2), it is reasonable to assume that most of what was observed in this study was primary. To make such a distinction would have required more advanced instrumentation (see comment #1e above).

No changes were made in response to the reviewer's comment.

7a. Page 24, Table 6. Component 9 "enhancement of CO" was categorized as "VOC oxidation". This is questionable. Why?

Please see our response to major comment #2 above.

7b It is apparent that on some days the nighttime CO was quite high, which should not be formed via VOC oxidation due to the fact that nighttime VOC oxidation chemistry is weaker than daytime photochemistry.

The reviewer is correct that at night, CO mixing ratios are enhanced mainly due to anthropogenic emissions of partially oxidized hydrocarbons into a shallow boundary layer. Since we clarified that we view CO as originating from the incomplete oxidation of hydrocarbons by both anthropogenic and natural sources (see response to major comment #2 above), no further changes were made in response to the reviewer's comment.

7c. Moreover, if CO was from VOC oxidation, it would destroy the correlations among VOCs (due to various photochemical reactivity of VOC species), leading to poor factor loadings, while the correlations among AVOCs and BVOCs were strong in Table 5.

A diffuse source such as VOC oxidation would not likely correlate with the (strong) AVOC and BVOC emissions, but likely show up as a stand-alone component similar to what is observed for component #9.

Please also see our response to major comment #2 above.

7d. Though CO did not have correlations with other combustion tracers, could it be caused by the weakness of the PCA method, or the correlation of CO with other combustion tracers is the "must" for the identification of a combustion source?

As stated in our response to major comment #2, the assignment to component 9 to a particular source is tentative as noted on lines 378-380 that "components 6 through 10 are somewhat tentative as many

(i.e., 7 – 9) are single variable components and have eigenvalues close to or below unity, i.e., account for less variance than any single variable." and is certainly not a major result of the PCA presented in this paper.

8a. Page 25, Figure 4. (B) (component 2) vehicles emit aromatics and n-alkanes but component 2 did not in Table 5.

We interpret component 2 as being mainly due to mine fleet emissions as it is consistent with a sooty combustion source (strong correlations with rBC, pPAH, HOA as well as association with NO_y).

There is no doubt that non-road mining truck emit aromatics such as o-xylene and alkanes (Watson et al., 2013). However, one has to keep in mind that a PCA only gives insight into which components contribute to the variability of a specific variable's concentration with time. In this particular case, decane and undecane correlated with factor 2, alas poorly ($r=0.22$ and 0.27). However, these correlations were the second and third highest of all components. In other words, the results shown in Table 5 do not show the absence of n-alkanes (or xylenes) in component 2, but that another component (#1) that emitted higher concentrations of alkanes and xylenes dominated their variability at this measurement location.

This is not an unusual result at all for PCA. For example, Lan et al. (2014) observed 4 factors in Taiwan and found an association of n-alkanes with a vehicular traffic component, whereas the xylenes correlated with a different factor (labeled "industrial solvent").

We added the following to the discussion section on line 573:

"Furthermore, one would expect an association of non-road mining truck emissions with aromatics and alkanes. Component 2 exhibited only poor correlations with decane ($r = 0.22$) and undecane ($r = 0.27$) and negligible correlation with o-xylene ($r = 0.08$), suggesting that other components (i.e., component 1) explained most of the variability of their concentrations at this site."

8b. (D) (component 4) Upgrader facilities emitted TS and SO2 only? There was flare stack. Were there no VOC emissions (Table 5)?

As stated on line 683, we believe that we under sampled emissions from stacks. Flaring (combustion) would likely oxidize most VOCs, such it is doubtful that these emissions would or could be observed.

No changes were made to the manuscript in response to the reviewer's comment.

9a. Page 26, lines 382-385. Not true. $r=0.27$ only for Ox in component 5!

Our apologies - this was an error. We have made the following change:

"PM₁ and O₃ correlated strongly with the major IVOC component (component 5, $r = 0.80$), which also moderately associated with LO-OOA ($r=0.66$) and NO_3^- (p) ($r = 0.59$), as well as NH_4^+ (p) and SO_4^{2-} (p) ($r = 0.32$ and 0.33 , respectively)."

9b Moreover, why didn't O_x have high correlations with any variables in Table 7?

A discussion about odd oxygen budgets during this study is beyond the scope of this manuscript, but since the reviewer asked:

The communality for O_x was 0.91, suggesting that ~91% of the variability of O_x is accounted for. However, O_x is a complex variable whose concentration is affected by many processes, including air mass "age", i.e., extent of photochemical O₃ production, vertical entrainment of O₃ and NO₂, direct emission of NO₂, and dry deposition of O₃ and NO₂. Its mixing ratio also exhibits a strong diurnal cycle. As a result, no single component dominates its temporal variability. However, there are weak positive correlations of O_x with components 2 ($r = 0.36$) and 6 ($r = 0.33$) and sizeable negative correlations with components 3 ($r = -0.62$) and 7 ($r = -0.41$). These can be rationalized as follows:

Component 3 is associated with biogenic emissions; low ozone concentrations generally occurred when biogenics accumulated (i.e., low boundary layer height and low O₃ abundance at night) such that the anticorrelation is expected. The negative correlation of O_x with component 7 is consistent with the notion of it being a surface source. Component 6 is a factor associated with secondary production of aerosol, which goes hand-in-hand with photochemical O₃ production. Finally, the correlation of O_x with component 3 is likely a reflection of the diurnal cycle, since sulfur species were mainly observed during daytime.

No changes were made to the manuscript in response to the reviewer's comment.

10. Page 43, lines 718-720. Could any measurements be done downwind to verify this hypothesis?

The text on these lines reads: "Liggio et al. (2016) showed that these hydrocarbons constitute a group of IVOCs in the saturation vapor concentration (C*) range $10^5 \mu\text{g m}^{-3} < C^* < 10^7 \mu\text{g m}^{-3}$ that contribute significantly to secondary organic aerosol formation and growth downwind of the oil sands facilities."

Since this hypothesis was verified by Liggio et al. (2016), no changes were made to the manuscript in response to the reviewer's comment.

11. Page 44, lines 740-742. This also fits CO. But no discussion at all.

The text on these lines reads: "The PCA struggled most with the allocation of greenhouse gases. Mixing ratios of CO₂, in particular, were difficult to reconcile in this analysis due to a high background and large attenuation by biogenic activity and boundary layer meteorology."

Please see our response to major comment #2.

12. Page 44, lines 749-750. TAG-GC-ToF-MS technique has already been applied to identify and quantify many IVOC species. Many papers have been published in the society. In the "Supplement" document

Please see our response to minor comment #1e.

13a. Lines 54-55. Again, what are the selection criteria for these specific VOCs?

We are not sure what specific lines the reviewer is referring to. The selection criteria for specific VOC monitored as stated in our response to minor question #3.

13b. Can GC-ITMS measure more VOCs such as C2-C10 HCs and so on for better source identification?

In principle, yes. However, the GC-ITMS was on site to quantify monoterpenes and set up for measurements of C9 and higher hydrocarbons. Hydrocarbons up to an approximate volatility of toluene did not resolve on our column. It may be possible with column cooling, a different column and longer adsorption times that we might be able to see compounds as low as C2. However, this would be at the expense of C9 and higher time resolution and at the time of measurement was not feasible.

No changes were made to the manuscript in response to the reviewer's comment.

14. Line 330. No solid evidence for this.

We are not sure what the reviewer questions here, since the sentence that encompasses line 330 reads: "This is consistent with a recent study by Whaley et al. (2017) that estimated over half (~57%) of the near-surface NH₃ during the study period originated from NH₃ bi-directional exchange (i.e. re-emission of NH₃ from plants and soils), with the remainder being from a mix of anthropogenic sources (~20%) and forest fires (~23%)."

Whaley have published their results in Atmos. Chem. Phys., 18, 2011-2034, 10.5194/acp-18-2011-2018, 2017, and we have no reason to doubt their results.

No changes were made to the manuscript in response to the reviewer's comment.

15. Figs S2-S4, S7-S11 caption: Table 4 should be Table 5 in the text?

Thank you for noticing this. All captions have been corrected.

16. Figure S5 caption: Table 4 should be other Table in the text?

We believe the reviewer is referring to Table 7 in the main text. The following correction has been made:

"Bivariate polar plots associated with component 4 for the optimum secondary~~primary~~ pollutant solution (Table 74)"

17. Figure S6 caption: Table 4 should be Table 5 in the text?

We believe the reviewer is referring to Table 7 in the main text. The following correction has been made:

"Bivariate polar plots associated with component 5 for the optimum secondary~~primary~~ pollutant solution (Table 74)"

Anonymous Referee #2

This study investigates the sources of IVOCs in the Athabasca oil sands by applying PCA on air pollutants measured at a ground site. IVOCs have been indicated as an important class of SOA precursors. Identification of the major sources of IVOCs is needed in order to make effective measures to reduce their emissions. The objective of this study is interesting, but the data and presentation are too broad, lack of the focus on IVOCs given that the term of "IVOCs" is highlighted in the title.

Principal component analysis is a commonly used tool that allows characterization of major sources contributing to variability of pollutants at a particular measurement site. The AOS is an interesting region as there are many classes of pollutants emitted in high concentration (greenhouse gases, nitrogen oxides, flame retardants, heavy metals, etc.). This makes it necessary to focus the paper. The addition of "Sources of IVOCs" following "Principal component analysis of summertime ground site measurements in the Athabasca oil sands" in the title alerts the reader that the paper's discussion will focus primarily on factors that IVOCs are associated with. If "Sources of IVOCs" were omitted, the discussion ought to have been much broader and covered other (climate change advocates might argue more important) pollutants as well. However, many these other pollutants were measured close-up by aircraft, which provided more concise information (e.g., (Baray et al., 2018)). In contrast, IVOCs were not observed by the aircraft.

As it is, the observation IVOCs by GC-ITMS at this site was unexpected, as we were not aware a priori that these even existed let alone what processes or facilities would contribute to their release to the gas phase. The approach taken in this paper is to put the observed IVOC signature in context of other temporarily resolved measurements made concurrently, through PCA. We have therefore chosen to keep the title as is and have not altered the manuscript in response to the reviewer's comment.

1. Measurements of IVOCs were carried out using GC-ITMS. Atmospheric IVOCs are composed of both primary IVOCs, dominated by hydrocarbons, and oxygenated IVOCs, oxidation products of primary IVOCs and VOCs. The elution of oxygenated IVOCs from the GC column is likely incomplete. However, in this study, the split between hydrocarbon-IVOCs and oxygenated-IVOCs was neither performed nor discussed.

2. In addition, the collection efficiency and recovery of IVOCs was not described, either.

The reviewer makes two important points and is correct that oxygenated compounds (alcohols and acids) will likely not elute from the analytical column. They are, therefore, not included in the IVOC signature detected. For the second, we know that calibration curves for n-alkanes, which encompass the bulk of IVOCs observed, were linear, but we do not know what the collection efficiency and recovery of late eluting compounds would be, though we assumed it to be reproducible. We also observed minimal carry-over between chromatograms (see also our reply to comment #3 below).

We hadn't considered oxygenated compounds since bitumen contains very little oxygen (Yoon et al., 2009) and the extent of oxidative processing was assumed to be negligible. IVOCs, however, could have formed through chemical aging, though we'd expect them to be oxygenated (and hence not observed) and in relatively small abundance compared to primary IVOCs.

In response to these concerns, we have expanded section 2.2.1 (Analytically unresolved hydrocarbon signature) and added the following starting on line 142:

"This unresolved signal was integrated in all ambient air chromatograms from a retention time of 25 min to 45 min (gray area in Fig. 2). A qualitatively similar unresolved signal was observed in an offline analysis of the headspace above ground-up bitumen gave a similarly unresolved hydrocarbon signal (Fig. 2, black trace). In this particular case, the ambient air chromatogram also shows enhancements of lower molecular weight hydrocarbons (possibly from naphtha) that were not observed in the bitumen sample.

The major ions contributing to the unresolved signals in Figure 2 are associated with alkanes (i.e., m/z 55, 57, 67, 69, etc. – see Fig. S-1). In contrast, counts at masses associated with aromatics (i.e., m/z 115, $C_9H_7^+$, and m/z 91, $C_7H_7^+$) as reported by Cross et al. (2013) were negligible in both the bitumen head space and polluted day samples. The strong resemblance of the unresolved hydrocarbon feature in ambient air with the bitumen head space sample both in terms of volatility (i.e., elution time) and electron impact mass fragmentation is consistent with bitumen as the source of IVOCs at this site. In the interpretation of the integrated IVOC signal, it is assumed that it is of primary origin, i.e., emitted directly from point sources in the vicinity of the measurement site. For the PCA analysis, the unresolved signal was integrated from a retention time of 25 min to 45 min (gray area in Fig. 2) in all ambient air chromatograms.

The IVOCs observed in this work likely encompass a portion of the total that is emitted. For example, IVOCs generated by combustion processes, such as aircraft engine exhaust, are comprised of alkanes, aromatics and oxygenated compounds (Cross et al., 2013). The use of a chromatographic column in this work biases the IVOC signal towards hydrocarbon-IVOCs, since oxygenated compounds (i.e., alcohols and acids) will not elute from the analytical column. Furthermore, the recovery of VOCs from the pre-concentration unit, while reproducible and likely complete for n-alkanes which bracket the bulk of IVOC emitted and whose calibration curves were linear, is not known for late-eluting compounds, but is assumed to be sufficiently reproducible to yield a semi-quantitative signal. "

We also added the following to the S.I.:

"In the field, there was no noticeable carry-over (i.e., memory effects) of IVOCs, which was occasionally evaluated by flooding the inlet with purified, VOC-free air.

Matrices of ions plotted against retention times for the total ion chromatograms (shown in Figure 2 in the main manuscript) are shown in Fig. S-1. In both cases, the greatest intensity is with masses are associated with alkanes (i.e., m/z 55, 57, 67, 69, etc.).

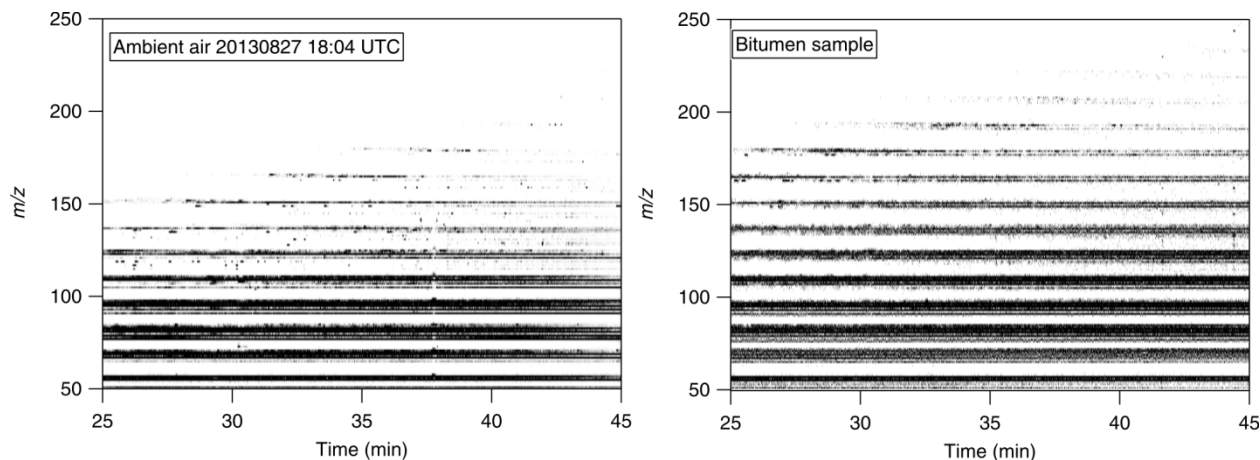


Figure S-1. Scatter of ions as a function of retention time for the total ion chromatograms shown in Figure 2 of the main manuscript. Darker pixels represent a higher intensity than lighter pixels."

3. In the light of the description of chemical analysis of IVOCs provided in this study, it is unclear whether the measurements capture the variability of atmospheric IVOCs, which is critical for PCA.

We agree with the reviewer that variability is critical for PCA. The integrated IVOCs vary in time and this is depicted in Figure 3A.

As we stated above, the IVOC signature does not encompass oxygenated compounds and captures mainly primary IVOCs; we hence agree that we are therefore not capturing the variability of all atmospheric IVOCs. However, it is still acceptable as an input parameter for PCA, and we have not changed the manuscript in response to this comment.

4. This manuscript mentioned that PCA is unable to determine the fractional contributions of sources to IVOCs in the section of "5. Summary and conclusions".

We believe the reviewer is referring to lines 758-760: "For instance, PCA does not provide insight into the magnitudes of emissions, though it does capture what conditions change ambient concentrations the most."

We changed the wording as follows:

"For instance, PCA does not provide insight into the magnitudes of emission factors of individual facilities, though it does capture what conditions change ambient concentrations the most."

5. Why is the PMF analysis not applied in this study? The number of samples is sufficient to provide a robust solution.

Both PMF and PCA are commonly used for source apportionment, and either receptor model could have been used in this work. In PMF (Paatero and Tapper, 1994), the experimental data is decomposed using non-negative constraints (instead of orthogonality constraints that are used for PCA). This aides in the physical interpretation (i.e., quantification of source contributions), since emissions are then non-negative by default. For this reason, PMF has become more popular than PCA in recent years. The PMF approach does, however, benefit from knowledge about the sources as the solution is not necessarily unique, and solutions are affected by the chosen dimensionality (Paatero and Tapper, 1994). Studies in which data sets were analyzed using both PCA and PMF (Marie et al., 2009; Cesari et al., 2016; Tauler et al., 2009) note that results are similar but not always yield the same number of factors.

We chose PCA with varimax rotation because the main goal of this work was the identification of (orthogonal) source types. Going in, we had little information as to what source or sources would contribute to the IVOC signature. PCA is attractive in this context as it gives a unique solution and is particularly suited as an exploratory tool for identification of components without *a priori* constraints (Jolliffe and Cadima, 2016).

We added the following on line 89:

"PCA was chosen over the more popular positive matrix factorization (PMF) method (Paatero and Tapper, 1994) because it yields a unique solution and is particularly suited as an exploratory tool for identification of components without *a priori* constraints (Jolliffe and Cadima, 2016)."

6. As mentioned above, ambient IVOCs includes oxygenated IVOCs, oxidation products of IVOCs and VOCs. However, the PCA in this study did not identify a component for oxygenated IVOCs.

Please see our response to comment #1 above.

7. Liggio et al. (2016) finds that the evaporation and atmospheric oxidation of low-volatility organic vapors from mined oil sands is directly responsible for the majority of observed SOA mass. Does this mean that the contribution of the component 2 to IVOCs shall be small given that this component is likely related to "Mine fleet and vehicle emissions". More discussion is needed.

The transformation of IVOCs to organic aerosol mass is outside the scope of this paper, considering that we were close to sources and oxygenated IVOCs were not quantified. The aircraft study, in contrast, focused on the atmospheric oxidation of IVOC emissions that were entrained aloft, transported several hours downwind, at which time emissions from different sources would have merged into a single plume. At our ground site, the extent of oxidative processing is less and more components are distinguishable. Our analysis indicates that IVOCs emitted in component 2 were qualitatively different from those emitted by components 1 and 5, in that they were less associated with the LO-OOA organic aerosol mass loading, but we do not have sufficient information to comment on how IVOCs from these compounds transform and add to aerosol mass downwind.

No changes were made to the manuscript in response to this comment.

Anonymous Referee #3

This paper describes principle component analysis (PCA) of ambient air quality data set collected in the Canadian oil sands region over a month or so in the summer of 2013. The data collection was part of a large field project to characterize the impact of oil sand operations on local air quality and climate. This is interesting question given the magnitude of the facilities. Recent work suggests dramatic secondary organic aerosol (SOA) formation downwind of these facilities. This SOA formation was attributed to emissions of low volatility organics, IVOCs. This was described in the Nature paper of Liggio et al. 2016.

This paper is focused on better understand the sources of IVOCs. This is an important question that is of interest to readers of ACP. They have done this by performing PCA on an ambient dataset of mainly traditional pollutants (a handful of anthropogenic and biogenic VOCs plus other species). They decompose the data into 10 or 11 factors (depending on if they are looking at secondary species). Three of the factors have some association with IVOCs. The paper contains some relatively qualitative description of the sources of the factors that generally make sense.

1. Although I am interested in this topic, after reading it I did not find the paper particularly interesting and did not feel like it made much of contribution to our understanding of the sources.

We are sorry that the reviewer did not find the paper particularly interesting, but appreciate the frank comment. We feel that we improved the understanding of the IVOC signature in the AOS region by identifying three components, all of which are associated with "the handling of raw bitumen, i.e., the unearthing, mining and transport of crude bitumen, and the disposal of processed material that contains residual bitumen in wet tailings ponds" (lines 744-746).

There has been a lot of emphasis in the literature on bitumen related pollution in tailings ponds (Small et al., 2015) and rivers (Kelly et al., 2010). In contrast, emissions of IVOCs from AOS operations to the gas-phase are understudied, in spite of their significant SOA formation potential (Liggio et al., 2016) and the very likely associated impact on human health. This data set and the analysis presented in this paper are important first steps, though we agree with the reviewer's sentiment that more needs to be done, as we indicated in the "Summary and conclusions" section of the manuscript.

No changes were made in response to this comment

2. I felt like going in the authors' attributed the IVOCs to bitumen. It was not clear that the paper did anything to support that hypothesis.

Figure 2 shows that the IVOC signature observed in ambient air is qualitatively similar to the bitumen head space vapor sample. We agree with the reviewer that there could have been other IVOC sources, which we don't believe to be significant at this site, however.

The following was added on lines 147-152:

"The major ions contributing to the unresolved signals in Figure 2 are associated with alkanes (i.e., m/z 55, 57, 67, 69, etc. – see Fig. S-1). In contrast, counts at masses associated with aromatics (i.e., m/z 115, $C_9H_7^+$, and m/z 91, $C_7H_7^+$) as reported by Cross et al. (2013) were negligible in both the bitumen

head space and polluted day samples. The strong resemblance of the unresolved hydrocarbon feature in ambient air with the bitumen head space sample both in terms of volatility (i.e., elution time) and electron impact mass fragmentation suggests that bitumen vapors dominate the IVOCs at this site."

We agree that the hypothesis that IVOCs originate from bitumen is supported mainly by a consistency argument and more studies are needed to pinpoint the exact sources. To do this, we would require access to the mining operation sites. However, this is not feasible at the present time since the AOS companies do not allow such measurements to take place for a variety of reasons, including safety.

4. There is nothing "wrong" with the paper, it is well written and has long descriptions.

We thank the reviewer for pointing out the absence of technical errors in this manuscript.

5. The paper would be much more interesting if it could quantitatively attribute IVOCs to sources (even the discussion of components seemed pretty speculative and qualitative).

We agree with the reviewer that a more quantitative approach would be beneficial, for example, by establishing concrete emission factors for each of the many components of AOS mining operations. As we noted above in comment 3, to accomplish this, we would require access to the mining operation sites.

We stated on lines 758-760, "The PCA analysis in this study suffered from ~~a~~ several limitations. For instance, PCA does not provide insight into ~~the magnitudes of~~ emission factors of individual facilities, though it does capture what conditions change ambient concentrations the most."

No changes were made in response to the reviewer's comment.

Larger comments

6. The paper uses a criteria of $r > 0.3$ to indicate moderate correlation. I view 0.3 as almost no correlation. I think the threshold should be much higher.

We agree. As reviewer #1 also expressed this concern, please see our response to major comment #3 of reviewer 1 and associated changes to the manuscript.

7. Presumably the GC-ITMS technique used to measure the VOCs and IVOCs could measure a much broader suite of compounds (or even break the chromatogram into subareas) that might yield more insight into what the sources of the IVOCs.

The GC-ITMS in its current configuration can quantify C9 and higher hydrocarbons. However, when IVOCs were observed, they did not resolve on the analytical column and produced many of the same ions (m/z 57, 71, 69, etc.). As a result, identification let alone quantification of individual IVOCs were unfortunately out of the question.

The suggestion to break up the chromatograms into subareas is an interesting idea. Prior to writing this paper, we had (qualitatively) examined the ambient air total ion chromatograms for differences and had found that IVOC volatility distributions were fairly consistent, i.e. varied collectively in area (by

more than 3 orders of magnitude) but not noticeably in the distribution of IVOCs into various volatility bins. In light of the reviewer's comment, we re-analyzed a subset of chromatograms (selected to encompass extreme events of the data set) and integrated the IVOC area prior to tridecane (an easily identified marker that was always present) and after tridecane. Unlike the total IVOC area, which varied by more than 3 orders of magnitude, the ratios of areas before tridecane to after tridecane varied by a relatively small amount, +/-50%. Changes in hydrocarbon volatility distributions are challenging to interpret as they will likely not only depend on the nature of IVOC sources but also on air mass "age" and chemical history (and possibly temperature for a source that outgasses IVOCs). We have therefore chosen not to differentiate between IVOC volatility bins to this manuscript, but have added the following to the conclusion section on line 784:

"Future studies should also investigate how IVOC volatility distributions vary with source type and chemical age."

Specific comments

1. Figure 1 – Including a wind rose for the study period as an inset panel on this figure would be very helpful.

We considered adding wind rose plots (in lieu of the bivariate plots such as those shown in Figure 5) but decided against it since local wind speeds can be misleading as explained on lines 245-249 "... implies a linear relationship between local wind conditions and air mass origin, which may not be always the case (for example, during or after stagnation periods). In addition, local topography, such as the Athabasca river valley, complicates regional air flow patterns and limit the interpretability of polar plots in general and in particular to the E of AMS 13, where the river valley is located."

No changes were made to the manuscript in response to the reviewer's comment.

2. Line 125 – Please add one or two sentences on calibration and QA procedures.

Details on how the instruments were operated are given in the supplemental information (lines 66-71). To make this clearer, we modified a sentence on lines 125-127.

"A detailed descriptions of these instruments and operational aspects such as calibrations are is given in the S.I. Sample observations of analytically unresolved hydrocarbons by GC-ITMS and how these data were used in the analysis are described in section 2.2.1 below."

3. Table 2. Who operated instruments is not that interesting. Time resolution would be more useful.

We modified the table as requested by the reviewer, but note that all the measurements were averaged to the 10 minute preconcentration time of the GC-ITMS (stated on lines 217-218).

4. Line 164 – What is the recovery and calibration of the IVOCs?

We do not know what fraction of IVOCs is recovered from the preconcentration trap. We do know, however, that there is limited carry-over (i.e., if the instrument was sampling purified air, the

chromatogram did not show IVOCs from preceding injections), and that calibration curves for the n-alkanes were linear (stated on line 97 of the S.I.), from which we deduce that the recovery (of alkanes) was reproducible and likely quantitative, i.e., not concentration dependent.

Since we do not know the identity of the individual compounds that make up the IVOCs, they were not calibrated for.

In response to the reviewer's question, we added the following to the S.I. on page 98:

"In the field, there was no noticeable carry-over (i.e., memory effects) of IVOCs, which was occasionally evaluated by flooding the inlet with purified, VOC-free air."

Please also see our response to question 2 of reviewer #2.

5. Line 198 – What fraction of the data are below LOD?

This value varied between species and instruments (see below).

<hr/> <hr/> % of data below LOD <hr/> <hr/>	
<u>Anthropogenic VOCs</u>	
o-xylene	10%
1,2,3 - TMB	27%
1,2,4 - TMB	8%
decane	44%
undecane	39%
<u>Biogenic VOCs</u>	
α -pinene	0%
β -pinene	0%
limonene	1%
<u>Combustion tracers</u>	
NO _y	0%
rBC	40%
CO	0%
CO ₂	0%
<u>Aerosol species</u>	
pPAH	39%
PM ₁₀₋₁	0%
HOA	N/A
LO-OOA	N/A
<u>Sulfur species</u>	
Total sulfur (TS)	35%
SO ₂	81%
Total reduced sulfur (TRS)	81%

<u>Other</u>	
IVOCs	N/A
CH ₄	0%
NH ₃	39%

This information has been added to Table 3.

6. Line 216 – I did not wade through the other solutions. Text on line 353 suggests they do not material change conclusions – maybe state that here.

We have added the following to line 238:

"Components 1 through 4 were consistent regardless of the number of components retained."

7. Line 345 – Moderately associated with IVOC ($r=0.31$) versus weakly associated with rBC ($r=0.3$). All these values seem very weak (to almost no) correlation.

Please see our response to major comment #3 by reviewer #1.

8. Figure 5. Add labels of directions to different facilities labeled in earlier table.

We chose to leave the Figure as is since association of specific facilities with pollutants is outside of the scope of this manuscript and would over-interpret the data - after all, air does not necessarily move in straight lines (see our response to minor comment #1).

9. Line 498 (and other locations) – diesel should not be capitalized.

Done.

10. Line 529 – This is not total PAH but particle bound PAH. Seems like surprising they are associated with combustion and not other components (e.g. 1 or 5).

It is. We stated and discussed potential reasons on lines 556-561.

"... Given this diversity of known sources, the associations of PAHs with only a single component is surprising, though indicates that emissions from the mining fleet (which would include diesel and, perhaps, wind-blown emissions from petcoke that is being transported) gave rise to most of the variability in surface-bound PAH concentrations in this data set. The petcoke emissions identified in the studies mentioned above are likely mainly associated with gas-phase molecules or larger, supermicron sized particles, whose PAH content would not be detected by the pPAH measurement in this data set."

No changes were made.

Line 544 – But diesel engines are not a major source of CO (gasoline engines are).

The reviewer is correct, of course. Wang et al. (2016a) give emission factors for CO and CO₂ by large caterpillar trucks, which show CO emissions from the big trucks to be minor. We have changed the sentences in question (on lines 570-573) as follows:

"There is little to no association of component 2 with ~~either CO or~~ CO₂ ($r = 0.18$ and 0.08 , respectively). This is somewhat unexpected as the trucks are expected to release ~~both CO₂~~ (Wang et al., 2016b) but could be due to significantly larger CO₂ sources in the area dominating the observed CO₂ variability at AMS 13 (e.g., components 3 and 6)."

Line 552 – Associating the IVOCs bitumen seemed to be the hypothesis going in. It is not clear how this analysis reinforces or tests that hypothesis. It seems pre-conceived and they are just interpreting the data that way.

Please see our response to major comment #2 above.

Line 695 – What is the evidence for this claim?

The sentence the reviewer is referring reads "The analysis indicates that the strongest IVOC source (Component 5) has the largest impact on PM₁ (Table 7)."

We rephrased this sentence as follows:

"The analysis indicates that the component with the strongest IVOC source-variability (Component 5) also has the ~~largest impact on~~ highest association with PM₁ ($r = 0.7$; Table 7)."

References

- Baray, S., Darlington, A., Gordon, M., Hayden, K. L., Leithead, A., Li, S. M., Liu, P. S. K., Mittermeier, R. L., Moussa, S. G., O'Brien, J., Staebler, R., Wolde, M., Worthy, D., and McLaren, R.: Quantification of methane sources in the Athabasca Oil Sands Region of Alberta by aircraft mass balance, *Atmos. Chem. Phys.*, 18, 7361-7378, 10.5194/acp-18-7361-2018, 2018.
- Cesari, D., Amato, F., Pandolfi, M., Alastuey, A., Querol, X., and Contini, D.: An inter-comparison of PM10 source apportionment using PCA and PMF receptor models in three European sites, *Environm. Sci. Poll. Res.*, 23, 15133-15148, 10.1007/s11356-016-6599-z, 2016.
- Cross, E. S., Hunter, J. F., Carrasquillo, A. J., Franklin, J. P., Herndon, S. C., Jayne, J. T., Worsnop, D. R., Miake-Lye, R. C., and Kroll, J. H.: Online measurements of the emissions of intermediate-volatility and semi-volatile organic compounds from aircraft, *Atmos. Chem. Phys.*, 13, 7845-7858, 10.5194/acp-13-7845-2013, 2013.
- Jolliffe, I. T., and Cadima, J.: Principal component analysis: a review and recent developments, *Philosophical Transactions of the Royal Society A: Mathematical, Physical and Engineering Sciences*, 374, 10.1098/rsta.2015.0202, 2016.
- Kelly, E. N., Schindler, D. W., Hodson, P. V., Short, J. W., Radmanovich, R., and Nielsen, C. C.: Oil sands development contributes elements toxic at low concentrations to the Athabasca River and its tributaries, *Proc. Natl. Acad. Sci. U.S.A.*, 107, 16178-16183, 10.1073/pnas.1008754107, 2010.

- Lan, C.-H., Huang, Y.-L., Ho, S.-H., and Peng, C.-Y.: Volatile organic compound identification and characterization by PCA and mapping at a high-technology science park, *Environ. Pollut.*, 193, 156-164, <https://doi.org/10.1016/j.envpol.2014.06.014>, 2014.
- Lee, A. K. Y., Adam, M. G., Liggio, J., Li, S.-M., Li, K., Willis, M. D., Abbatt, J. P. D., Tokarek, T. W., Odame-Ankrah, C. A., Huo, J. A., Osthoff, H. D., Strawbridge, K. B., and Brook, J. R.: A large contribution of anthropogenic organonitrate to secondary organic aerosol in Alberta oil sands, in prep., 2018.
- Liggio, J., Li, S.-M., Hayden, K., Taha, Y. M., Stroud, C., Darlington, A., Drollette, B. D., Gordon, M., Lee, P., Liu, P., Leithead, A., Moussa, S. G., Wang, D., O'Brien, J., Mittermeier, R. L., Brook, J., Lu, G., Staebler, R., Han, Y., Tokarek, T. W., Osthoff, H. D., Makar, P. A., Zhang, J., Plata, D., and Gentner, D. R.: Oil Sands Operations as a Large Source of Secondary Organic Aerosols, *Nature*, 534, 91-94, [10.1038/nature17646](https://doi.org/10.1038/nature17646), 2016.
- Marey, H. S., Hashisho, Z., Fu, L., and Gille, J.: Spatial and temporal variation in CO over Alberta using measurements from satellites, aircraft, and ground stations, *Atmos. Chem. Phys.*, 15, 3893-3908, [10.5194/acp-15-3893-2015](https://doi.org/10.5194/acp-15-3893-2015), 2015.
- Marie, C., Hervé, G., Vanessa, K., Brigitte, P., and Jérôme, S.: PCA- and PMF-based methodology for air pollution sources identification and apportionment, *Environmetrics*, 20, 928-942, [doi:10.1002/env.963](https://doi.org/10.1002/env.963), 2009.
- Paatero, P., and Tapper, U.: Positive matrix factorization: A non-negative factor model with optimal utilization of error estimates of data values, *Environmetrics*, 5, 111-126, [doi:10.1002/env.3170050203](https://doi.org/10.1002/env.3170050203), 1994.
- Small, C. C., Cho, S., Hashisho, Z., and Ulrich, A. C.: Emissions from oil sands tailings ponds: Review of tailings pond parameters and emission estimates, *J. Pet. Sci. Eng.*, 127, 490-501, [10.1016/j.petrol.2014.11.020](https://doi.org/10.1016/j.petrol.2014.11.020), 2015.
- Tauler, R., Viana, M., Querol, X., Alastuey, A., Flight, R. M., Wentzell, P. D., and Hopke, P. K.: Comparison of the results obtained by four receptor modelling methods in aerosol source apportionment studies, *Atmos. Environ.*, 43, 3989-3997, <https://doi.org/10.1016/j.atmosenv.2009.05.018>, 2009.
- Wang, X., Chow, J. C., Kohl, S. D., Percy, K. E., Legge, A. H., and Watson, J. G.: Real-world emission factors for Caterpillar 797B heavy haulers during mining operations, *Particuology*, 28, 22-30, [10.1016/j.partic.2015.07.001](https://doi.org/10.1016/j.partic.2015.07.001), 2016a.
- Wang, X. L., Chow, J. C., Kohl, S. D., Percy, K. E., Legge, A. H., and Watson, J. G.: Real-world emission factors for Caterpillar 797B heavy haulers during mining operations, *Particuology*, 28, 22-30, [10.1016/j.partic.2015.07.001](https://doi.org/10.1016/j.partic.2015.07.001), 2016b.
- Watson, J., Chow, J., Wang, X., Zielinska, B., Kohl, S., and Gronstal, S.: Characterization of real-world emissions from nonroad mining trucks in the Athabasca Oil Sands Region during September, 2009, 2013.
- Whaley, C., Makar, P. A., Shephard, M. W., Zhang, L., Zhang, J., Zheng, Q., Akingunola, A., Wentworth, G. R., Murphy, J. G., Kharol, S. K., and Cady-Pereira, K. E.: Contributions of natural and anthropogenic sources to ambient ammonia in the Athabasca Oil Sands and north-western Canada, *Atmos. Chem. Phys.*, 18, 2011-2034, [10.5194/acp-18-2011-2018](https://doi.org/10.5194/acp-18-2011-2018), 2017.
- Williams, B. J., Goldstein, A. H., Kreisberg, N. M., and Hering, S. V.: An in-situ instrument for speciated organic composition of atmospheric aerosols: Thermal Desorption Aerosol GC/MS-FID (TAG), *Aerosol Sci. Technol.*, 40, 627-638, [10.1080/02786820600754631](https://doi.org/10.1080/02786820600754631), 2006.
- Yoon, S., Bhatt, S. D., Lee, W., Lee, H. Y., Jeong, S. Y., Baeg, J.-O., and Lee, C. W.: Separation and characterization of bitumen from Athabasca oil sand, *Korean Journal of Chemical Engineering*, 26, 64-71, [10.1007/s11814-009-0011-3](https://doi.org/10.1007/s11814-009-0011-3), 2009.

1 **Principal component analysis of summertime ground site measurements in the Athabasca oil sands:**

2 **Sources of IVOCs**

3
4 Travis W. Tokarek¹, Charles A. Odame-Ankrah¹, Jennifer A. Huo¹, Robert McLaren², Alex K. Y. Lee^{3, 4},
5 Max G. Adam⁴, Megan D. Willis⁵, Jonathan P. D. Abbatt⁵, Cristian Mihele⁶, Andrea Darlington⁶,
6 Richard L. Mittermeier⁶, Kevin Strawbridge⁶, Katherine L. Hayden⁶, Jason S. Olfert⁷, Elijah G. Schnitzler⁸,
7 Duncan K. Brownsey¹, Faisal V. Assad¹, Gregory R. Wentworth^{5, a}, Alex G. Tevlin⁵, Douglas E. J. Worthy⁶,
8 Shao-Meng Li⁶, John Liggi⁶, Jeffrey R. Brook⁶, and Hans D. Osthoff^{1*}

9
10 [1] Department of Chemistry, University of Calgary, Calgary, Alberta, T2N 1N4, Canada

11 [2] Centre for Atmospheric Chemistry, York University, Toronto, Ontario, M3J 1P3, Canada

12 [3] Department of Civil and Environmental Engineering, National University of Singapore, Singapore
13 117576, Singapore

14 [4] NUS Environmental Research Institute, National University of Singapore, Singapore

15 [5] Department of Chemistry, University of Toronto, Toronto, Ontario, M5S 3H6, Canada

16 [6] Air Quality Research Division, Environment and Climate Change Canada, Toronto, Ontario, M3H 5T4,
17 Canada

18 [7] Department of Mechanical Engineering, University of Alberta, Edmonton, Alberta, T6G 1H9, Canada

19 [8] Department of Chemistry, University of Alberta, Edmonton, Alberta, T6G 2G2, Canada

20 [a] Now at: Environmental Monitoring and Science Division, Alberta Environment and Parks, Edmonton,
21 Alberta, T5J 5C6, Canada

22 * Corresponding author

23

24 *for Atmos. Chem. Phys.*

25 **Abstract**

26 In this paper, measurements of air pollutants made at a ground site near Fort McKay in the Athabasca
27 oil sands region as part of a multi-platform campaign in the summer of 2013 are presented. The
28 observations included measurements of selected volatile organic compounds (VOCs) by a gas
29 chromatograph – ion trap mass spectrometer (GC-ITMS). This instrument observed a large, analytically
30 unresolved hydrocarbon peak (with retention index between 1100 and 1700) associated with
31 intermediate volatility organic compounds (IVOCs). However, the activities or processes that contribute
32 to the release of these IVOCs in the oil sands region remain unclear.

33 Principal component analysis (PCA) with Varimax rotation was applied to elucidate major source types
34 impacting the sampling site in the summer of 2013. The analysis included 28 variables, including
35 concentrations of total odd nitrogen (NO_y), carbon dioxide (CO_2), methane (CH_4), ammonia (NH_3), carbon
36 monoxide (CO), sulfur dioxide (SO_2), total reduced sulfur compounds (TRS), speciated monoterpenes
37 (including α - and β -pinene and limonene), particle volume calculated from measured size distributions
38 of particles less than $10\ \mu\text{m}$ and $1\ \mu\text{m}$ in diameter (PM_{10-1} and PM_1), particle-surface bound polycyclic
39 aromatic hydrocarbons (pPAH), and aerosol mass spectrometer composition measurements, including
40 refractory black carbon (rBC) and organic aerosol components. The PCA was complemented by bivariate
41 polar plots showing the joint wind speed and direction dependence of air pollutant concentrations to
42 illustrate the spatial distribution of sources in the area. Using the 95% cumulative percentage of
43 variance criterion, ten components were identified and categorized by source type. These included
44 emissions by wet tailings ponds, vegetation, open pit mining operations, upgrader facilities, and surface
45 dust. Three components correlated with IVOCs, with the largest associated with surface mining and is
46 likely caused by the unearthing and processing of raw bitumen.

47 1. Introduction

48 The Athabasca oil sands region of Northern Alberta, Canada, has seen extraordinary expansion of its oil
49 sands production and processing facilities (CAPP, 2016) and associated emissions of air pollutants over
50 the last several decades (Englander et al., 2013; Bari and Kindzierski, 2015). Air emissions from these
51 facilities have been impacting surrounding communities, including the city of Ft. McMurray and the
52 community of Ft. McKay (WBEA, 2013). To assess the impact of these emissions on human health,
53 visibility ~~and~~ climate, and the ecosystems downwind, it is critical to obtain an understanding of the
54 source types from all activities associated with oil sands operations (ECCC, 2016).

55 Prior to 2013, there had been only a single industry-independent study of trace gas emissions from the
56 Athabasca oil sands mining operations (Simpson et al., 2010; Howell et al., 2014). The data showed
57 elevated concentrations in n-alkanes (30% of the total quantified hydrocarbon emissions), cycloalkanes
58 (49%), and aromatics (15%) in plumes from an oil sands surface mining facility intercepted from a single
59 aircraft flight. These compounds are associated with oil and gas developments including mining,
60 upgrading, and transportation of bitumen (Siddique et al., 2006). Specifically, these activities involve the
61 use of naphtha, a complex mixture of aliphatic and aromatic hydrocarbons in the range of C₃ to C₁₄
62 containing n-alkanes (e.g., n-heptane, n-octane, and n-nonane) and benzene, toluene, ethylbenzene,
63 and xylenes (BTEX).

64 In August 2013, a comprehensive air quality study as a part of the Joint Oil Sands Monitoring (JOSM)
65 plan (JOSM, 2012), referred to here as the 2013 JOSM intensive study was conducted. This study was
66 performed in northern Alberta at two ground sites in and near Fort McKay and from a National Research
67 Council of Canada (NRC) Convair 580 research aircraft to characterize oil sands emissions and their
68 downwind physical and chemical transformations (Gordon et al., 2015; Liggio et al., 2016; Li et al., 2017).
69 One ground site, located at the Wood Buffalo Environmental Association (WBEA) air monitoring station

70 (AMS) 13 (Fig. 1), was equipped with a comprehensive set of instrumentation to measure
71 concentrations of trace gases and aerosols (Table 1). As part of this effort, a gas chromatograph
72 equipped with an ion trap mass spectrometer (GC-ITMS) was deployed at AMS 13. When air masses
73 passing over regions with industrial activities were observed (as judged from a combination of local wind
74 direction and tracer measurements), the total ion chromatogram showed an analytically unresolved
75 hydrocarbon signal associated with intermediate volatile organic compounds (IVOCs) with saturation
76 concentration (C^*) in the range $10^5 \mu\text{g m}^{-3} < C^* < 10^7 \mu\text{g m}^{-3}$ (Liggio et al., 2016).

77 Emission estimates for analytically unresolved hydrocarbons range from $5 \times 10^6 \text{ kg year}^{-1}$ to $14 \times 10^6 \text{ kg}$
78 year^{-1} for the two facilities that reported such emissions (Li et al., 2017). Using aircraft measurements
79 during the 2013 study, Liggio et al. (2016) showed that IVOCs contributed to the majority of the
80 observed secondary organic aerosol (SOA) mass production in a similar fashion as anthropogenic VOCs
81 contributed to SOA production during the Deepwater Horizon oil spill (de Gouw et al., 2011) and rivaling
82 the magnitude of SOA formation observed downwind of megacities (Liggio et al., 2016), though
83 ultimately it has remained unclear which activities are associated with IVOC emissions.

84 In this paper, concurrent measurements of air pollutants at the AMS 13 ground site during the 2013
85 JOSM intensive study are presented and analyzed using principal component analysis (PCA) to elucidate
86 the origin of the IVOCs in the Athabasca oil sands. The analysis presented here is a receptor analysis
87 focusing on the normalized variability of pollutants impacting the AMS 13 ground site and hence does
88 not constitute a comprehensive emission profile analysis of the oil sands facilities as a whole, for which
89 aircraft-based measurements and/or direct plume or stack measurements are more suitable. PCA was
90 chosen over the more popular positive matrix factorization (PMF) method (Paatero and Tapper, 1994)
91 because it yields a unique solution and is particularly suited as an exploratory tool for identification of
92 components without *a priori* constraints (Jolliffe and Cadima, 2016). The PCA was complemented by
93 bivariate polar plots (Carslaw and Ropkins, 2012; Carslaw and Beevers, 2013) to show the spatial

94 distribution of sources in the region as a function of locally measured wind direction and speed. A
95 second PCA was performed to investigate which components correlate with (and generate) secondary
96 pollutants, i.e., pollutants that are formed by atmospheric processes. Potential sources and processes
97 contributing to each of the components identified by PCA are discussed.

98

99 **2. Experimental**

100 **2.1 Measurement location**

101 Measurements of air pollutants were made at AMS 13 routine air monitoring station (Fig. 1), which is
102 operated by WBEA. The site is located at 111.6423° W longitude and 57.1492° N latitude about 3 km
103 from the southern edge of the community of Fort McKay, 300 m west from a public road, and 1 km west
104 of the Athabasca river. The immediate vicinity of the site consisted of mixed-leaf boreal forest with a
105 variety of tree species, including poplar, aspen, pine and spruce trees (Smreciu et al., 2013). The site was
106 accessible via a gravel road; traffic on this road was restricted during the study period (August -
107 September, 2013).

108 The site is impacted by emissions from nearby oil sands facilities (Table 1 and Fig. 1), including a large
109 surface mining site operated by Syncrude Canada whose northeastern corner is located 3.5 km to the
110 south of AMS 13 (and which is adjacent to the 5 km long Syncrude – Mildred Lake (SML) tailings pond)
111 and from a large upgrader stack facility operated by Suncor Energy Inc. located to the Southeast. There
112 are additional oil sands facilities operated (during the study period) by Canadian Natural Resources
113 Limited, Imperial Oil, and Shell Canada to the North and Northeast.

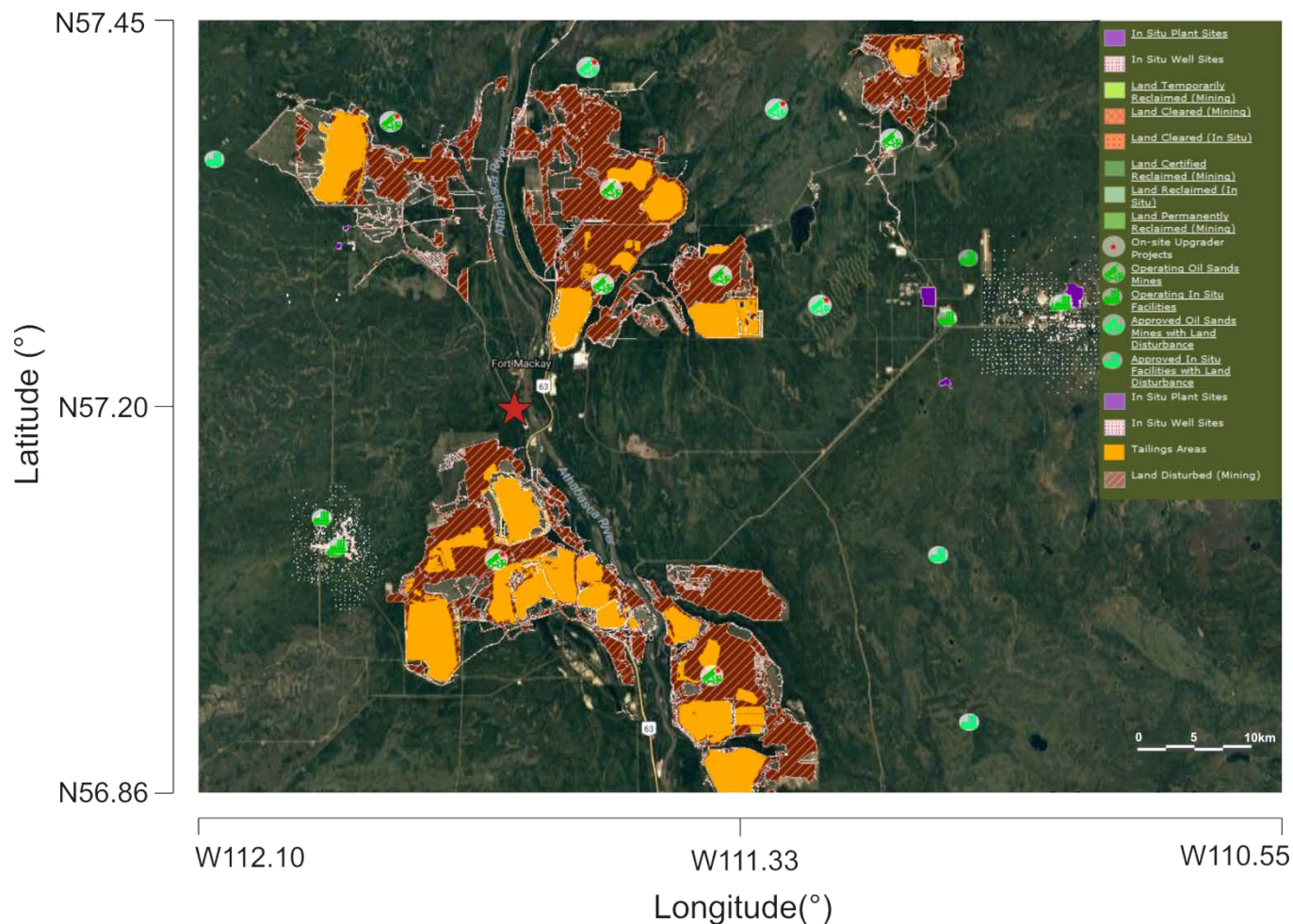
114 **Table 1.** Oil sands facilities located within 30 km of AMS 13. Distances were estimated using coordinates
 115 provided in the National Pollutant Release Inventory (NPRI, 2013) and do not account for the size of
 116 each facility whose boundaries may be considerably closer to (or further away from) AMS 13. PACPRM =
 117 Petroleum and coal products refining and manufacturing; OGPS = Oil and gas pipelines and storage.

Company	Name	Type	Direction	Distance (km)
Syncrude Canada Ltd.	Mildred Lake Plant Site	PACPRM	S	12.2
Athabasca Minerals Inc.	Susan Lake Gravel Pit	Mining and Quarrying	N	15.5
Syncrude Canada Ltd.	Aurora North Mine Site	PACPRM	NE	18.7
Suncor Energy	Suncor Energy Inc. Oil Sands	PACPRM	SE	19.4
Enbridge Pipelines Inc.	Mackay River Terminal	OGPS	WSW	19.7
Suncor Energy	Mackay River, In-Situ, Oil Sands Plant	PACPRM	WSW	19.9
Enbridge Pipelines Inc.	Athabasca Terminal	OGPS	SE	21.2
Williams Energy	Fort McMurray Hydrocarbon Liquids Extraction Facility	Conventional oil and gas extraction	SE	21.6
Canadian Natural Resources Limited	Horizon Oil Sands Processing Plant and Mine	PACPRM	NNW	21.8
Shell Canada Energy	Muskeg River Mine and Jackpine Mine	PACPRM	NNE	23.7

118

119

120 **Figure 1.** Map of oil sands facilities showing locations of surface mines and tailings ponds, downloaded
121 from the Oil Sands Information Portal (Alberta, 2017). The red star indicates the location of AMS 13.



122

123 2.2 Instrumentation

124 A large number of instruments was deployed for this study; a partial list whose data were utilized in this
125 manuscript is given in Table 2. A-detailed descriptions of these instruments and operational aspects
126 such as calibrations ~~is~~are given in the S.I. Sample observations of analytically unresolved hydrocarbons
127 by GC-ITMS and how these data were used in the analysis are described in section 2.2.1 below.

128 **Table 2.** Instruments used to measure ambient gas-phase and aerosol species during the 2013 JOSM

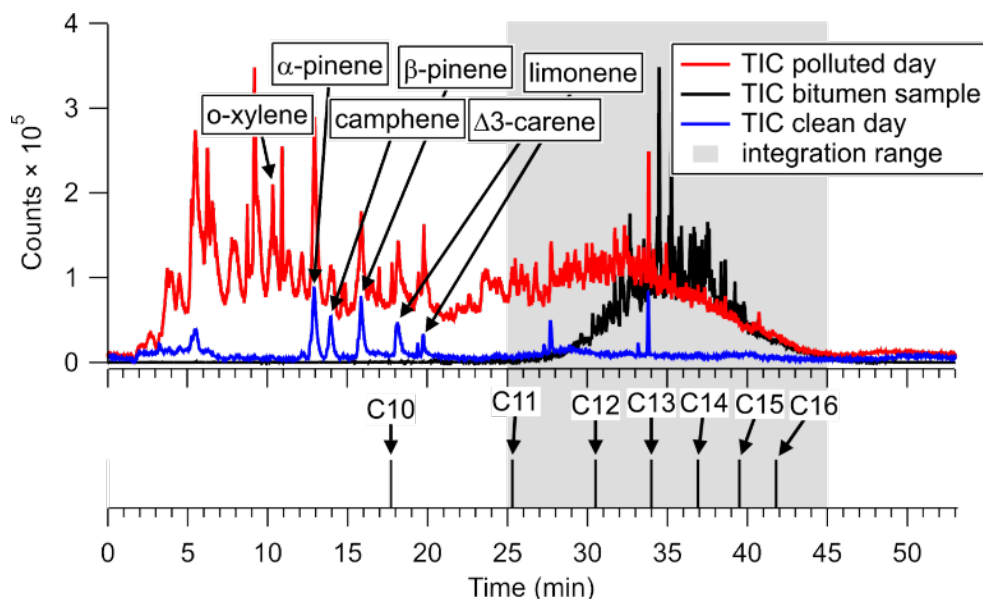
129 intensive study at AMS 13.

Instrument and Model	Species measured	Operated by Time resolution	Reference
Picarro CRDS G2401	CO, CO ₂ , CH ₄	York University and ECCC 1 min	(Chen et al., 2013; Nara et al., 2012)
Thermo Scientific, Model 42i	NO _y	University of Calgary 10 s	(Tokarek et al., 2014; Odame-Ankrah, 2015)
Blue diode cavity ring-down spectroscopy	NO ₂	University of Calgary 1 s	(Paul and Osthoff, 2010; Odame-Ankrah, 2015)
Thermo Scientific Model 49i	O ₃	University of Calgary 10 s	(Tokarek et al., 2014; Odame-Ankrah, 2015)
Griffin/FLIR, model 450 GC-ITMS	VOCs	University of Calgary 1 hr	(Tokarek et al., 2017; Liggio et al., 2016)
Thermo Scientific CON101	TS	ECCC 1 min	n/a
Thermo Scientific 43iTLE	SO ₂	ECCC 1 min	n/a
AIM-IC	NH _{3(g)} , NH _{4⁺(p)}	University of Toronto 1 hr	(Markovic et al., 2012)
Aerodyne SP-AMS	rBC, NH _{4⁺(p)} , SO _{4²⁻(p)} , NO _{3⁻(p)} , Cl ⁻ (p), organics	University of Toronto and ECCC 1-5 min (variable)	(Onasch et al., 2012)
TSI APS 3321	PM ₁₀₋₁ size distribution	University of Calgary 5-6 min (variable)	(Peters and Leith, 2003)
TSI SMPS (3081 DMA, 3776 CPC)	PM ₁ size distribution	University of Alberta 6 min	(Wang and Flagan, 1990)
EcoChem Analytics PAS 2000CE	pPAH	ECCC 1 min	(Wilson et al., 1994; Burtscher et al., 1982)

130

131 **2.2.1 Analytically unresolved hydrocarbon signature**

132 As previously reported (Liggio et al., 2016), the total ion chromatogram of the GC-ITMS occasionally
133 showed elevated and analytically unresolved hydrocarbons in the volatility range of C₁₁ – C₁₇ with
134 saturation vapor concentration (C*) from 10⁵ µg m⁻³ < C* < 10⁷ µg m⁻³. An example is shown in Fig. 2.



135
136 **Figure 2. (Top)** Total ion chromatograms of air samples collected on August 27, 2013 from 18:04 to
137 18:14 UTC (red) and on August 28, 2013 from 13:43 to 13:53 UTC (blue). The TIC of a head space sample
138 of ground-up bitumen collected post-campaign is superimposed (black). The gray area indicates the
139 range over which IVOC signal was integrated. **(Bottom)** Retention times of n-alkanes, determined after
140 the measurement intensive by sampling a VOC mixture containing a C₁₀ – C₁₆ n-alkane ladder.

141
142 This unresolved signal was integrated in all ambient air chromatograms from a retention time of 25 min
143 to 45 min (gray area in Fig. 2). A qualitatively similar unresolved signal was observed in an offline
144 analysis of the headspace above ground-up bitumen gave a similarly unresolved hydrocarbon signal (Fig.
145 2, black trace). In this particular case, the ambient air chromatogram also shows enhancements of lower

146 molecular weight hydrocarbons (possibly from naphtha) that were not observed in the bitumen sample.

147 The major ions contributing to the unresolved signals in Figure 2 are associated with alkanes (i.e., m/z
148 55, 57, 67, 69, etc. – see Fig. S-1). In contrast, counts at masses associated with aromatics (i.e., m/z 115,
149 $C_9H_7^+$, and m/z 91, $C_7H_7^+$) as reported by Cross et al. (2013) were negligible in both the bitumen head
150 space and polluted day samples. The strong resemblance of the unresolved hydrocarbon feature in
151 ambient air with the bitumen head space sample both in terms of volatility (i.e., elution time) and
152 electron impact mass fragmentation is consistent with bitumen as the source of IVOCs at this site.

153 In the interpretation of the integrated IVOC signal, it is assumed that it is of primary origin, i.e., emitted
154 directly from point sources in the vicinity of the measurement site. For the PCA analysis, the unresolved
155 signal was integrated from a retention time of 25 min to 45 min (gray area in Fig. 2) in all ambient air
156 chromatograms.

157 The IVOCs observed in this work likely encompass a portion of the total that is emitted. For example,
158 IVOCs generated by combustion processes, such as aircraft engine exhaust, are comprised of alkanes,
159 aromatics and oxygenated compounds (Cross et al., 2013). The use of a chromatographic column in this
160 work biases the IVOC signal towards hydrocarbon-IVOCs, since oxygenated compounds (i.e., alcohols
161 and acids) will not elute from the analytical column. Furthermore, the recovery of VOCs from the pre-
162 concentration unit, while reproducible and likely complete for n-alkanes which bracket the bulk of IVOC
163 emitted and whose calibration curves were linear, is not known for late-eluting compounds, but is
164 assumed to be sufficiently reproducible to yield a semi-quantitative signal.

165

166 **2.3 Principal Component Analysis**

167 The PCA was carried out using the "Statistical Analysis System" (SAS™) Studio 3.4 software (SAS, 2015)

168 using a method similar to that described by Thurston et al. (2011; 1985). The source-related
169 components and their associated profiles are derived from the correlation matrix of the input trace
170 constituents. This approach assumes that the total concentration of each "observable" (i.e., input
171 variable) is made up of the sum of contributions from each of a smaller number of pollution sources and
172 that variables are conserved between the points of emission and observation.

173

174 **2.3.1 Selection of variables**

175 22 variables whose ambient concentrations are dominated by primary emissions or which are formed
176 very shortly after emission (such as the less oxidized oxygenated organic aerosol (LO-OOA) factor
177 observed by the SP-AMS, see below) were included in the PCA (Table 3). These variables included CO₂,
178 CH₄, NO_y, CO, and SO₂, which are known to be emitted in the oil sands region from stacks, the mine fleet
179 and faces, tailings ponds, and by fugitive emissions (Percy, 2013). The median NO_x (= NO + NO₂) to NO_y
180 ratio was 0.85, consistent with the close proximity of the measurement site to emission sources and
181 limited chemical processing. Because NO_x constituted a large fraction of NO_y, its temporal variation was
182 captured by the latter, and it was not included as a separate variable in the PCA analysis.

183 For this work, mixing ratios of all non-methane hydrocarbons (NMHCs) that were quantified (i.e., o-
184 xylene, the n-alkanes decane and undecane, the aromatics 1, 2, 3- and 1, 2, 4-TMB, as well as limonene
185 and α- and β-pinene) were included as variables. In addition, the aforementioned unresolved signal
186 associated with IVOCs was included as a variable by integrating total GC-ITMS ion counts (*m/z* 50–425)
187 over a retention time range of 25-45 min (retention index range of 1100 to 1700).

188 Gas-phase ammonia was included as a variable because elevated reduced nitrogen concentrations have
189 been observed in the region and were linked to the use of ammonia on an industrial scale, for example
190 as a floating agent and for hydrotreating (Bytnerowicz et al., 2010). Total sulfur and total reduced sulfur

191 were added as tracers of upgrader stack SO₂ emissions and of "odours", believed to be emitted from oil
192 sands tailings ponds which continue to be of concern in surrounding communities (Small et al., 2015;
193 Percy, 2013; Holowenko et al., 2000).

194 Refractory black carbon was added as a variable since it is present in ~~Diesel~~diesel truck exhaust and in
195 biomass burning plumes and, hence, a combustion tracer (Wang et al., 2016; Briggs and Long). pPAHs
196 were included because of their association with facility stack emissions and combustion particles in the
197 area (Allen, 2008; Grimmer et al., 1987). Hydrocarbon-like organic aerosol (HOA) was included as a
198 surrogate for fossil fuel combustion by vehicles (Jimenez et al., 2009). The LO-OOA factor was included
199 as it is unique to the Alberta oil sands and appears to form rapidly after emission of precursors (Lee et
200 al., 2018). Supermicron aerosol volume (PM₁₀₋₁, i.e., the volume of particles between PM₁₀ and PM₁) was
201 also included as a tracer of coarse particles from primary sources, which are expected to be dominated
202 by dust emissions.

203

204 **Table 3.** Variables observed at the AMS 13 ground site during the 2013 JOSM campaign used for PCA.

Variable	Unit	Median ^a	Average ^{a,b}	Standard deviation ^{a,b}	LOD ^e	Min. ^a	Max. ^a	Fraction <u><LOD</u>
<u>Anthropogenic VOCs</u>								
o-xylene	pptv ^f	5	30	69	1	< LOD	635	<u>10%</u>
1,2,3 - TMB	pptv	1.7	4.3	7.9	0.2	< LOD	67	<u>27%</u>
1,2,4 - TMB	pptv	2.1	7.7	14.7	0.2	< LOD	107	<u>8%</u>
decane	pptv	0.5	8.5	18.2	0.1	< LOD	125	<u>44%</u>
undecane	pptv	0.4	3.0	6.3	0.1	< LOD	37	<u>39%</u>
<u>Biogenic VOCs</u>								
α-pinene	pptv	477	542	401	1	19	1916	<u>0%</u>
β-pinene	pptv	390	467	334	1	18	1594	<u>0%</u>
limonene	pptv	150	179	158	2	< LOD	711	<u>1%</u>
<u>Combustion tracers</u>								
NO _y	ppbv	1.79	4.00	5.44	0.01	0.13	41.6	<u>0%</u>
rBC	μg m ⁻³	0.13	0.20	0.10	0.02	< LOD	0.90	<u>40%</u>
CO	ppbv	117.6	120.0	18.2	5.7 ^h	90.9	241.2	<u>0%</u>
CO ₂	ppmv	420.2	433.2	39.5	0.4 ^h	386.0	577.7	<u>0%</u>
<u>Aerosol species</u>								
pPAH	ng m ⁻³	1	2	2	1 ^c	< LOD	14	<u>39%</u>
PM ₁₀₋₁	μm ³ cm ⁻³	11.2	14.4	12.9	0.003	1.0	79.5	<u>0%</u>
HOA	μg m ⁻³	0.31	0.43	0.35	N/A ^g	0.04	2.32	<u>N/A</u>
LO-OOA	μg m ⁻³	1.19	2.00	2.26	N/A ^g	0.11	15.6	<u>N/A</u>
<u>Sulfur species</u>								
Total sulfur (TS)	ppbv	0.22	1.41	4.27	0.13	< LOD	33.3	<u>35%</u>
SO ₂	ppbv	< LOD	1.0	4.0	0.2	< LOD	33.5	<u>81%</u>
Total reduced sulfur (TRS)	ppbv	0.26	0.38	1.05	0.2	< LOD	14.8	<u>81%</u>
<u>Other</u>								
IVOCs	Counts × min	1.8×10 ⁷	3.4×10 ⁷	4.2×10 ⁷	N/A ^g	1.4×10 ⁶	2.5×10 ⁸	<u>N/A</u>
CH ₄	ppbv	1999.2	2065.5	169.6	1.8 ^h	1880	2959	<u>0%</u>
NH ₃	μg m ⁻³	0.79	1.10	1.03	0.05	0.06	5.75	<u>39%</u>

^a Values were determined only from data points included in PCA analysis, not from entire campaign.

^b Average and standard deviation were calculated before zeros were replaced with 0.5×LOD.

^c Estimated.

^e LOD = limit of detection.

^f parts-per-trillion by volume (10⁻¹²)

^g N/A = data not available

^h calculated using 3 × standard deviation at ambient background levels

206 To assess which components have the greatest impact on secondary product formation, a second PCA
 207 was performed which included variables mainly formed through atmospheric chemical processes and
 208 whose concentrations more strongly depend on air mass chemical age than those variables selected
 209 initially. In this PCA, odd oxygen ($O_x = O_3 + NO_2$), submicron aerosol $SO_4^{2-}(p)$, $NO_3^-(p)$, $NH_4^+(p)$, a second,
 210 more-oxidized OOA factor (MO-OOA), and PM_{10} volume were included, increasing the total number of
 211 variables to 28 (Table 4).

212

213 **Table 4.** Variables added in the second PCA. Particle-phase concentrations, i.e., $SO_4^{2-}(p)$, $NO_3^-(p)$, $NH_4^+(p)$
 214 and MO-OOA were made by aerosol mass spectrometry and account for PM_{10} only.

Variable	Unit	Median	Average	Standard deviation	LOD	Min.	Max.
O_x	ppbv	7.35	11.1	10.6	1	<LOD	41.1
$SO_4^{2-}(p)$	$\mu g m^{-3}$	0.3	0.8	1.1	0.1	<LOD	6.6
$NO_3^-(p)$	$\mu g m^{-3}$	0.08	0.13	0.13	0.01	0.01	0.72
$NH_4^+(p)$	$\mu g m^{-3}$	0.13	0.28	0.37	0.05	<LOD	2.21
MO-OOA	$\mu g m^{-3}$	1.65	1.83	0.960	N/A	1.41×10^{-6}	4.65
PM_{10} volume	$\mu m^3 cm^{-3}$	2.48	3.77	3.72	N/A	0.35	20.9

215

216 2.3.2 Treatment of input data

217 Data used in the PCA analysis were averaged to match the time resolution of the GC-ITMS VOC and IVOC
218 measurements, i.e. over 10 minute long periods (spaced ~ 1 hr apart) set by the start and stop times of
219 the GC-ITMS pre-concentration period. When concentrations were below their respective limit of
220 detection (LOD; values are given in Table 3), half the reported LOD was used to minimize bias (Harrison
221 et al., 1996; Buhamra et al., 1998). Prior to PCA, input variables were standardized to eliminate unit
222 differences by subtracting the mean concentration \bar{C}_i of pollutant i from the concentration of sample k
223 ($C_{i,k}$) and dividing by the standard deviation (s_i) of all samples included in the PCA analysis.

$$224 \quad Z_{i,k} = \frac{C_{i,k} - \bar{C}_i}{s_i} \quad (1)$$

225 Here, $Z_{i,k}$ is the standardized pollutant concentration. In total, 218 data points from all identified species
226 over the period of the campaign were used for the main PCA analysis.

227

228 2.3.3 PCA solutions

229 In this work, the Varimax method (Kaiser, 1958) was used to rotate the loading matrix. This method is an
230 orthogonal rotation (i.e., components are not expected to correlate) which minimizes the impact of high
231 loadings, making the results easier to interpret (Kaiser, 1958). Several criteria (Table S-10) were
232 considered for component selection: the latent root criterion, i.e., on the basis that rotated eigenvalues
233 must be greater than unity, the (cumulative) percentage of variance criterion, where the extracted
234 components accounts for >95% of the variance, and the Scree test (Fig. S-12) (Thurston and Spengler,
235 1985; Guo et al., 2004; Hair et al., 1998; Cattell, 1966). For the optimal solution presented in the main
236 manuscript, the 95% variance criterion was chosen, providing a 10-component solution for the PCA with

237 only primary variables and an 11-component solution for the PCA with both primary and secondary
238 variables. [Components 1 through 4 were consistent regardless of the number of components retained.](#)
239 Solutions with fewer and more components are presented in the supplemental material section.
240 Time series of each of the components were calculated by multiplying the original standardized matrix
241 by the rotated loading matrix and were used to generate bivariate polar plots (section 2.4).

242

243 **2.4 Bivariate polar plots**

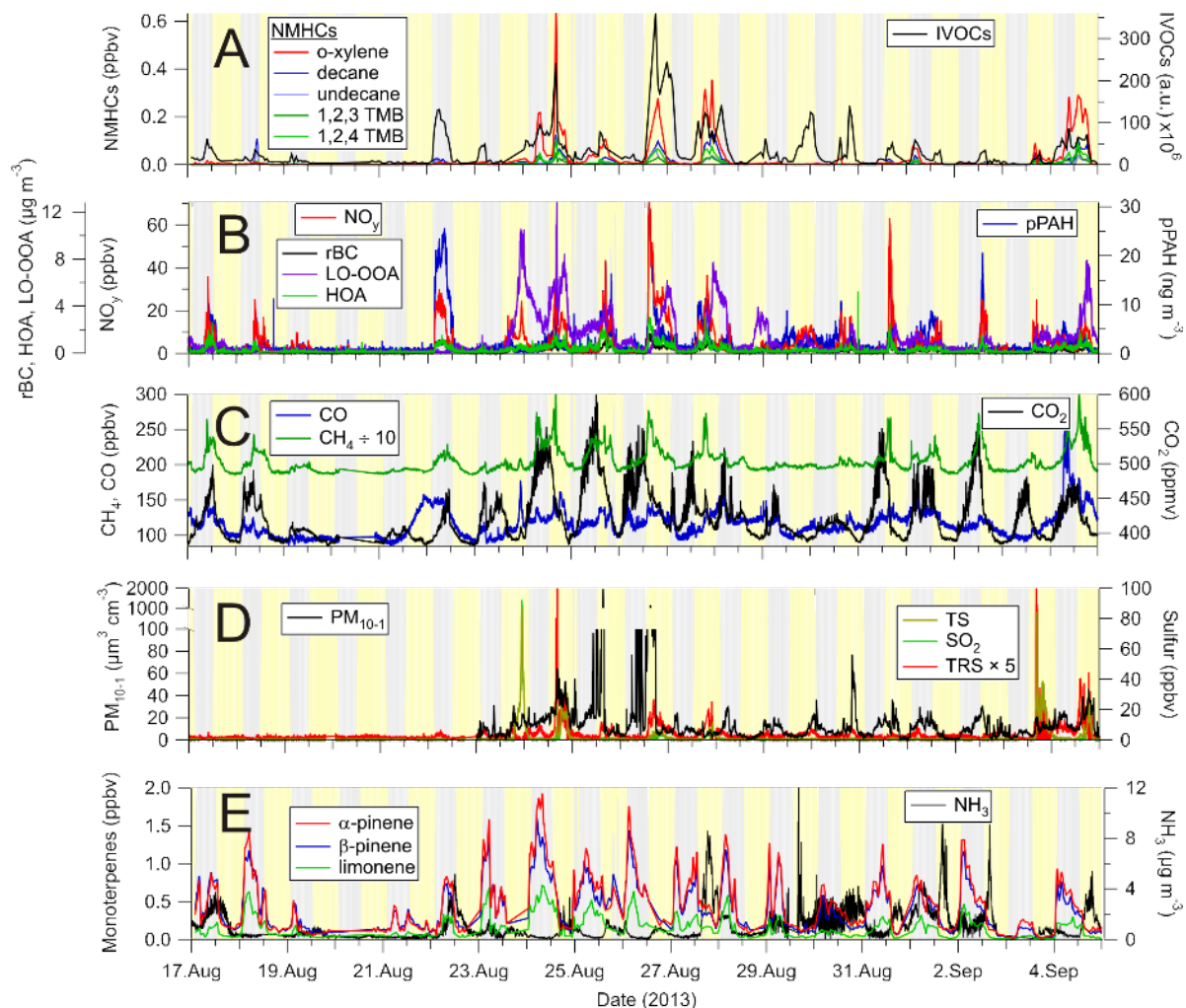
244 The PCA was complemented by bivariate polar plots showing the wind speed and direction dependence
245 of air pollutant concentrations. The use of these representations implies a linear relationship between
246 local wind conditions and air mass origin, which may not be always the case (for example, during or after
247 stagnation periods). In addition, local topography, such as the Athabasca river valley, complicates
248 regional air flow patterns and limit the interpretability of polar plots in general and in particular to the E
249 of AMS 13, where the river valley is located. The plots were generated with the Openair software
250 package (Carslaw and Ropkins, 2012; Carslaw and Beevers, 2013) using the R programming language and
251 the open-source software "RStudio: Integrated development environment for R" (RStudio Boston,
252 2017). The default setting (100) was used as the smoothing function.

253 **3. Results**

254 **3.1. Overview of the data set**

255 Time series of the 22 pollution tracers chosen for PCA analysis are presented in Fig. 2, grouped
256 approximately by source type. Statistics of the data (i.e., median, average, maxima, minima, etc.) are
257 summarized in Table 3.

258



259

260 **Figure 3.** Time series of selected pollution tracers observed at the AMS 13 ground site in the Athabasca
 261 oil sands during the 2013 JOSM measurement intensive. The gray and yellow backgrounds represent
 262 night and day, respectively. **(A)** Selected non-methane hydrocarbons (NMHCs) and IVOCs. **(B)**
 263 Combustion product tracers: refractory black carbon (rBC), total odd nitrogen (NO_y) and particle surface
 264 bound polycyclic aromatic hydrocarbons (pPAH), and organic aerosol components: hydrocarbon-like
 265 organic aerosol (HOA) and less oxidized oxygenated organic aerosol (LO-OOA). **(C)** Methane (CH_4),
 266 carbon dioxide (CO_2) and monoxide (CO). **(D)** Total sulfur (TS), sulfur dioxide (SO_2), and total reduced
 267 sulfur (TRS) and PM_{10-1} particle volume. **(E)** Biogenic VOCs (α -pinene, β -pinene and limonene) and
 268 ammonia (NH_3).

269 Time series of VOCs of primarily anthropogenic origin (i.e., o-xylene, 1, 2, 3- and 1, 2, 4-TMB, etc.) as
270 well as the IVOC signature are shown in Fig. 3A. The abundances of these species, as well as the other
271 compounds, were highly variable and varied as a function of time of day (i.e., boundary layer mixing
272 height) and air mass origin, with higher VOC concentrations generally observed during daytime. The VOC
273 concentrations varied between nearly pristine, remote conditions, with concentrations below
274 detectable limits, to mixing ratios of aromatic species exceeding 100 pptv. The concentration range of o-
275 xylene is within the extremes reported by WBEA in their 2013 annual report (WBEA, 2013), exemplifying
276 that the data set is representative of typical pollutant levels in this region.

277 While there is some obvious covariance between variables (i.e., when the mixing ratios of one particular
278 VOC increases, so do others), the ratios of hydrocarbons varied considerably. For example, on August
279 18, 10:50 UTC, the n-decane to o-xylene ratio was ~22:1, whereas on August 24, 07:40 UTC it was ~1:5.7.
280 The IVOC magnitude also varied greatly and often increased and decreased in tandem with the other
281 VOCs (e.g., on Aug 24, 16:30 UTC) but also increased independently from the other VOC abundances
282 (e.g., on Aug 30, 01:20 UTC, and on the night of Aug 22). This behaviour suggests the presence of
283 multiple sources with distinct signatures that are being sampled to a varying extent at different times.
284 This, coupled with the intermittency of the highly elevated signals, presents an analysis problem
285 frequently encountered in environmental analysis that is usually investigated through a factor or
286 principal component analysis (Thurston et al., 2011; Guo et al., 2004).

287 Presented in Fig. 3B are the time series of NO_y, rBC and pPAH abundances, all of which are combustion
288 byproducts. For example, rBC is emitted from combustion of fossil fuels, biofuels, open biomass burning,
289 and burning of urban waste (Bond et al., 2004). Similar to the VOCs, the abundances of these species
290 varied greatly, from very low, continental background levels (i.e., <100 pptv of NO_y, < LOD for rBC and
291 pPAHs) to polluted concentrations (i.e., > 60 ppbv of NO_y, > 1 µg m⁻³ rBC, > 10 ng m⁻³ pPAHs)
292 characteristic of polluted urban and industrial areas. When high concentrations of NO_y were observed,

293 its main component was NO_x (data not shown), which is a combustion byproduct usually associated with
294 automobile exhaust. In the Alberta oil sands, emissions from off-road mining trucks as well as the
295 upgrading processes are the main contributors to the NO_y burden (Percy, 2013; Watson et al., 2013).

296 Shown in Fig. 3C are the mixing ratios of the greenhouse gases CH₄ and CO₂ along with CO. Abundances
297 of CO₂ were clearly attenuated by photosynthesis and respiration of the vegetation near the
298 measurement site, as judged from the strong diurnal cycle in its concentration (not shown). Maxima
299 typically occurred shortly after sunrise, coincident with the expected break-up of the nocturnal
300 boundary layer. In addition to biogenic emissions from vegetation and soil, CO₂ originates from a variety
301 of point and mobile sources in this region, including off-road mining trucks (Watson et al., 2013) and the
302 extraction, upgrading, and refining of bitumen and on-road vehicle sources in the area (Nimana et al.,
303 2015a, b). Concentrations of CO₂ spiked whenever these emissions were transported to the
304 measurement site.

305 Concentrations of CH₄ also exhibit a diurnal cycle, with higher concentrations generally observed at
306 night and peaking in the early morning hours. While CH₄ and CO₂ mixing ratios frequently correlated in
307 plumes, their ratios were variable overall, suggesting they [often](#) originated from distinct sources.

308 Potential methane point sources in the region include microbial production in tailings ponds (Siddique et
309 al., 2012) and fugitive emissions associated with the mining and processing of bitumen (Johnson et al.,
310 2016). Indeed, a recent analysis shows tailings ponds and open pit mining sources to be the largest
311 sources of CH₄ in the region (Baray et al., 2018).

312 Similar to the anthropogenic VOCs, the abundances of CH₄ and CO₂ were highly variable and ranged
313 from minima of 1.88 and 384 ppmv to maxima of 2.96 and 578 ppmv, corresponding to maximum
314 enhancements of 1.63 and 1.47 relative to tropospheric global monthly means of 1.806±0.001 and
315 394.3±0.1 ppmv for July, 2013 (Dlugokencky, 2017b, a), respectively.

316 Mixing ratios of CO also varied with time but generally were not elevated greatly (median 118 ppbv)
317 above background levels (minimum 91 ppbv), except for occasional spikes in concentration (Fig. 3C).
318 Carbon monoxide is a tracer of biomass burning and fossil fuel combustion, in particular in automobiles
319 with poorly performing or absent catalytic converters, but is also a byproduct of the oxidation of VOCs,
320 in particular of methane and isoprene which are oxidized over a wide area upwind of AMS 13 (Miller et
321 al., 2008).

322 Time series of sulfur species and PM₁₀₋₁ volume are shown in Fig. 3D. The TS and SO₂ data are dominated
323 by intermittent plumes containing SO₂ mixing ratios exceeding 5 ppbv. The highest mixing ratio
324 observed was 92.5 ppbv (in between the preconcentration periods of the GC-ITMS). Mixing ratios of SO₂
325 exhibited the most variability of all pollutants, as judged from the standard deviation of each of the
326 measurements (Table 3). TRS levels were generally small (< 1 ppbv) and variable, except for plumes; TRS
327 abundances in plumes, however, are more uncertain since they were calculated by subtraction of two
328 large numbers. When TS and SO₂ abundances were low (< 1 ppbv), TRS abundances were variable and
329 occasionally exhibited spikes that did not show any obvious correlation with other variables, suggesting
330 the presence of one or more distinct TRS sources. PM₁₀ volume concentrations varied a lot as well and,
331 just like TRS, did not show an obvious correlation with other variables. Fugitive dust emissions likely
332 contributed to much of the PM₁₀ volume in the Athabasca oil sands region (Wang et al., 2015).

333 Time series of monoterpene mixing ratios are shown in Fig. 3E. α -Pinene was generally the most
334 abundant monoterpene, followed by β -pinene. Their ratio, averaged over the entire campaign was
335 1:0.85, though occasionally the α - to β -pinene ratio was below 1:2 (e.g., on Aug 28, 14:50 UTC and Sept
336 5, 12:40 UTC). Terpene mixing ratios were generally higher at night than during the day, with maxima of
337 1.9 and 1.6 ppbv, respectively, a diurnal pattern consistent with what has been observed at other forest
338 locations (Fuentes et al., 1996). Monoterpenes are emitted by plants via both photosynthetic and non-
339 photosynthetic pathways (Fares et al., 2013; Guenther et al., 2012); at night, their emissions accumulate

340 in a shallow nocturnal boundary layer, whereas during daytime, they are entrained aloft (above the
341 canopy) and oxidized by the hydroxyl radical (OH) and O₃, which are more abundant during the day than
342 at night (Fuentes et al., 1996). α- and β-pinene mixing ratios were lowest mid-day (median values at
343 noon of 140 and 133 pptv, respectively). The largest daytime concentrations were observed on Aug 25, a
344 cloudy day (as judged from spectral radiometer measurements of the NO₂ photolysis frequency): on this
345 particular day, mixing ratios at noon were 687 and 850 pptv, respectively.

346 Also shown in Fig. 3E is the time series of ammonia. These data were dominated by spikes which were
347 observed sporadically and did not correlate with other variables, suggesting the presence of nearby
348 ammonia point sources. Ammonia was not as variable as some of the other pollutants (e.g., the
349 anthropogenic VOCs, sulfur species) as judged from its standard deviation (Table 3), which suggests a
350 geographically more disperse source or sources similar to CO or CH₄, which have a "background". This is
351 consistent with a recent study by Whaley et al. (2017) that estimated over half (~57%) of the near-
352 surface NH₃ during the study period originated from NH₃ bi-directional exchange (i.e. re-emission of NH₃
353 from plants and soils), with the remainder being from a mix of anthropogenic sources (~20%) and forest
354 fires (~23%).

355

356 **3.2. Principal component analysis**

357 **3.2.1. PCA analysis with primary variables**

358 The loadings of the optimum solution are presented in Table 5. The 10-component solution accounts for
359 a cumulative variance of 95.5%. The communalities for the analysis, i.e., the fraction of total pollutant
360 observations accounted for by the PCA are all greater than 85%, with the lowest communality obtained
361 for the IVOCs (0.86).

362 In the following, an overview of the observed components is presented. Associations with $r > 0.7$, $r > 0.3$,

363 and $r > 0.1$ are referred to as "strong", "~~moderate~~weak", and "~~weak~~poor", respectively. Hypothesized
364 identifications are given in section 4 and are summarized in Table 6 and Fig. 4.

365 The component accounting for most of the variance of the data, component 1, is strongly associated
366 with the anthropogenic VOCs ($r > 0.87$), ~~moderate~~weakly associated with CH₄ ($r = 0.59$), TRS ($r = 0.59$),
367 HOA ($r = 0.40$), LO-OOA ($r = 0.45$), CO ($r = 0.41$), and the IVOCs ($r = 0.31$), and ~~weakly~~poorly associated
368 with NO_y ($r = 0.27$) and rBC ($r = 0.30$). Component 2 is strongly associated with the combustion tracers
369 NO_y ($r = 0.82$), rBC ($r = 0.77$), HOA ($r = 0.74$), and pPAH ($r = 0.94$), ~~moderate~~weakly associated with CH₄ (r
370 $= 0.39$) and IVOCs ($r = 0.39$), and ~~weak~~poorly associated with ammonia ($r = 0.20$), CO ($r = 0.18$) and
371 undecane and decane ($r = 0.27$ and 0.22 , respectively). Component 3 is strongly associated ($r > 0.9$) with
372 the biogenic VOCs and ~~moderate~~weakly associated with CO₂ ($r = 0.48$) and shows ~~weak~~poor negative
373 correlations with NO_y ($r = -0.26$), ammonia ($r = -0.24$), and SO₂ ($r = -0.15$). Component 4 is strongly
374 associated with SO₂ and TS ($r = 0.97$ and 0.93 , respectively) and ~~weak~~poorly with NO_y ($r = 0.21$) and LO-
375 OOA ($r = 0.28$).

376 Components 1 through 4 emerged regardless of the number of components used to represent the data,
377 whereas the structure of components 5 through 10 only fully emerged in the 10-component solution
378 (see S.I.). Hence, components 6 through 10 are somewhat tentative as many (i.e., 7 – 9) are single
379 variable components and have eigenvalues close to or below unity, i.e., account for less variance than
380 any single variable. [As a result, the interpretations of these components are subject to more uncertainty
381 and are more speculative but are presented in the S.I. for the sake of completeness and transparency.](#)
382 For the purpose of this manuscript, this is inconsequential as components 6 – 10 are not associated with
383 IVOCs.

384

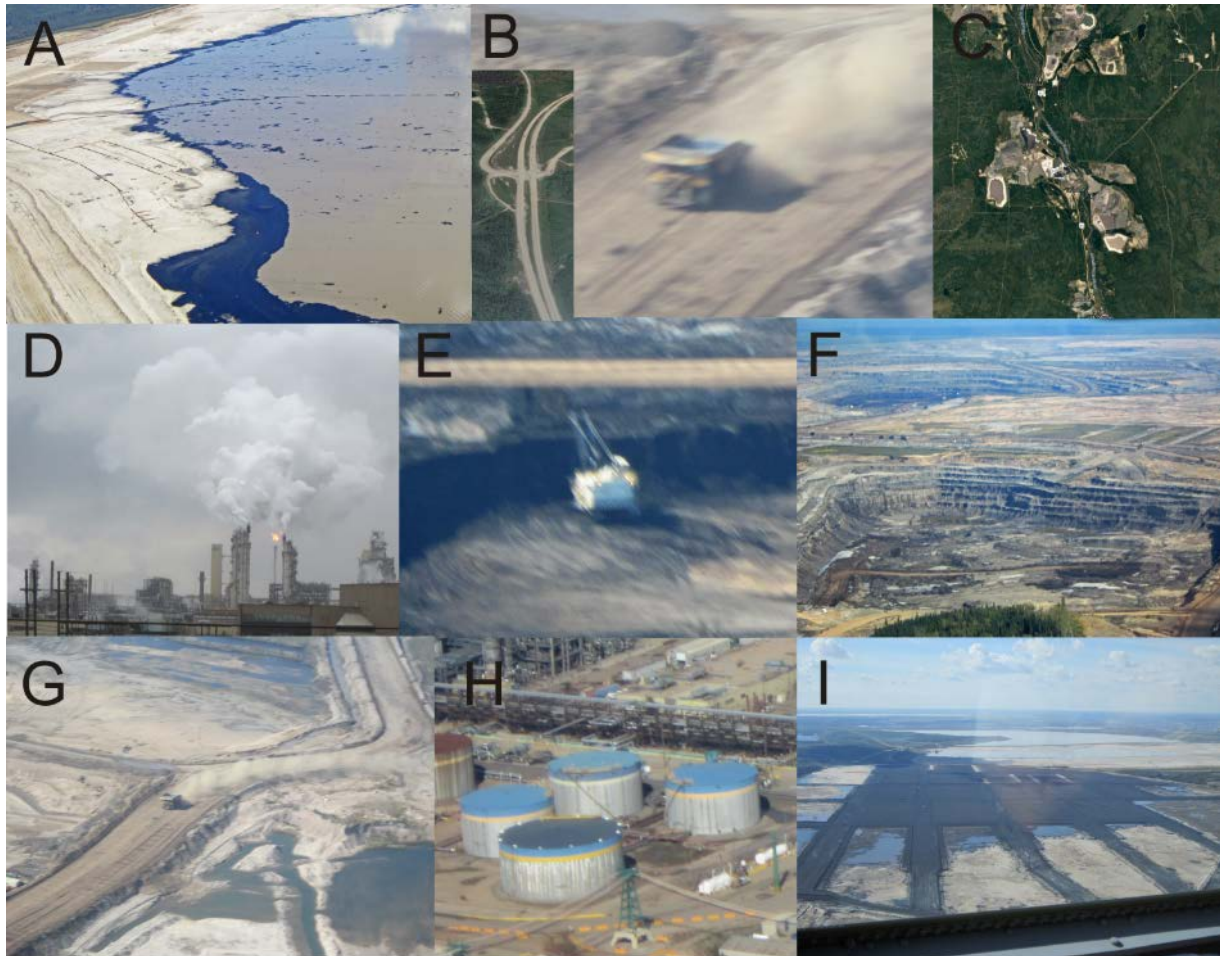
385 **Table 5.** Loadings for the 10-factor, optimal solution (primary variables only). Coefficients with Pearson
 386 correlation coefficients $r > 0.3$ are ~~interpreted as being moderately or strongly associated with a~~
 387 ~~component and are~~ shown in bold font.

	1	2	3	4	5	6	7	8	9	10	Communalities
<u>Anthropogenic VOCs</u>											
o-xylene	0.88	0.08	0.02	0.10	0.14	0.13	0.07	-0.04	0.16	0.32	0.95
1,2,3 - TMB	0.93	0.16	0.07	0.05	0.05	0.11	0.04	-0.02	0.18	-0.01	0.95
1,2,4 - TMB	0.94	0.14	0.01	0.10	0.11	0.08	0.07	-0.03	0.18	0.13	0.98
decane	0.92	0.22	-0.02	0.15	0.23	0.01	0.05	0.04	0.04	0.03	0.97
undecane	0.87	0.27	-0.08	0.23	0.20	-0.06	0.12	0.07	-0.04	-0.10	0.96
<u>Biogenic VOCs</u>											
α -pinene	-0.03	-0.08	0.98	-0.11	0.02	0.04	0.01	-0.08	0.02	0.01	0.98
β -pinene	-0.02	-0.08	0.98	-0.12	0.02	0.03	0.02	-0.07	0.00	0.01	0.98
limonene	0.07	-0.03	0.92	-0.08	0.12	0.24	0.05	-0.11	0.03	-0.05	0.95
<u>Combustion tracers</u>											
NO _y	0.27	0.82	-0.26	0.21	0.22	-0.04	0.02	0.10	-0.08	0.01	0.92
rBC	0.30	0.77	0.03	0.05	0.44	0.10	0.09	0.13	0.12	-0.10	0.94
CO	0.41	0.18	0.04	0.02	0.09	0.09	0.08	0.06	0.87	-0.01	0.99
CO ₂	0.09	0.08	0.48	-0.12	-0.03	0.77	0.25	-0.14	0.05	-0.08	0.95
<u>Aerosol species</u>											
pPAH	0.06	0.94	-0.07	-0.13	-0.11	0.07	0.01	0.13	0.10	0.04	0.95
PM ₁₀₋₁	0.18	0.14	0.08	0.09	0.11	0.17	0.93	-0.03	0.07	0.08	0.98
HOA	0.40	0.74	0.02	0.12	0.25	0.15	0.23	-0.06	0.16	0.09	0.90
LO-OOA	0.45	0.11	0.12	0.28	0.72	0.05	0.25	0.00	0.10	0.04	0.91
<u>Sulfur</u>											
TS	0.25	0.04	-0.16	0.93	0.08	-0.05	0.07	-0.02	0.01	0.12	1.00
SO ₂	0.12	0.03	-0.15	0.97	0.02	-0.04	0.03	-0.03	0.01	-0.05	0.99
TRS	0.59	0.04	-0.08	0.11	0.26	-0.04	0.16	0.04	-0.04	0.71	0.96
<u>Other</u>											
IVOCs	0.31	0.39	0.12	-0.08	0.74	-0.02	-0.02	-0.06	0.02	0.20	0.86
NH ₃	0.01	0.20	-0.24	-0.05	-0.02	-0.08	-0.03	0.94	0.04	0.02	0.99
CH ₄	0.59	0.39	0.10	-0.05	0.12	0.59	0.11	0.00	0.17	0.14	0.93
Eigenvalues	5.72	3.32	3.23	2.16	1.64	1.13	1.13	0.99	0.96	0.74	
% of variance	25.99	15.08	14.69	9.80	7.46	5.14	5.13	4.51	4.36	3.35	
Cumulative variance	25.99	41.07	55.76	65.56	73.02	78.16	83.30	87.81	92.17	95.52	

388

389 **Table 6.** Hypothesized identification_s of principal components.

Component	Key observations	Possible source(s)	Relevant references
1	Enhancements of aromatics, n-alkanes, TRS, NO _y , rBC, HOA, LO-OOA, CO and CH ₄	Wet tailings ponds and associated facilities	(Simpson et al., 2010; Small et al., 2015; Percy, 2013; Holowenko et al., 2000; Howell et al., 2014)
2	Enhancements of NO _y , rBC, pPAH and HOA due to engine exhaust	Mine fleet and operations	(Wang et al., 2016; Grimmer et al., 1987; Allen, 2008; Briggs and Long, 2016)
3	Enhancements of monoterpenes and CO ₂ , weak/poor anticorrelation with NO _y and absence of anthropogenic VOCs	Biogenic emission and respiration	(Guenther et al., 2012; Helmig et al., 1999)
4	Enhancements of SO ₂ and TS, weak/poor correlation with NO _y and LO-OOA	Upgrader facilities	(Simpson et al., 2010; Kindziarski and Ranganathan, 2006)
5	Enhancements of IVOCs, rBC, LO-OOA, NO _y , and TRS	Surface exposed bitumen and hot-water based bitumen extraction	this work
6	Enhancements of CO ₂ and CH ₄ , absence of combustion tracers	Mine face and soil	(Johnson et al., 2016; Rooney et al., 2012)
7	Enhancement of PM ₁₀₋₁	Wind-blown dust	(Wang et al., 2015)
8	Enhancement of ammonia	Fugitive emissions from storage tanks and natural soil/plant emissions	(Bytnerowicz et al., 2010; Whaley et al., 2017)
9	Enhancement of CO	Incomplete VOC hydrocarbon oxidation	(Marey et al., 2015)
10	Enhancements of TRS and o-xylene, weak/poor association with CH ₄	Composite tailings	(Small et al., 2015; Warren et al., 2016)



391

392 **Figure 4.** Images of likely sources associated with each of the principal components. From top left to
 393 bottom: **(A)** Wet tailings ponds (component 1). **(B)** Mine truck fleet and highway traffic emissions
 394 (component 2). **(C)** Biogenic emissions from vegetation (component 3). **(D)** Upgrader facilities
 395 (component 4). **(E)** Exposed bitumen on mined surfaces (component 5). **(F)** Fugitive greenhouse gas
 396 emissions from mine faces (component 6). **(G)** Wind-blown dust from exposed sand (component 7). **(H)**
 397 Fugitive emissions of ammonia from storage tanks (Component 8). **(I)** Composite (dry) tailings
 398 (component 10). No image is shown for production CO from oxidation of VOCs (component 9).

399

400 3.2.2. Extended PCA analysis with added secondary variables

401 The loadings of the optimum solution that includes primary and secondary variables are shown in Table
402 7. In this 11-component solution, the 10 components originally identified were preserved, though their
403 relative order was changed, with the upgrader component moving from the 4th to 2nd position. There
404 was one new component (#6), which encompassed only secondary species, including MO-OOA (r =
405 0.92), O_x (r = 0.33), NO₃⁻(p) (r = 0.36), PM₁ (r = 0.31) and LO-OOA (r = 0.31).

406 NH₄⁺(p), SO₄²⁻(p), and NO₃⁻(p) are associated with the stack emissions component (#2, with r = 0.84, 0.84
407 and 0.44, respectively), which also moderateweakly correlated with PM₁ (r = 0.44) and O_x (r = 0.36). The
408 association of secondary variables with the primary components suggests rapid formation of these
409 secondary products on a time scale that is similar to the transit time of the pollutants to the
410 measurement site. PM₁ and O_x correlated strongly with the major IVOC component (component 5, r =
411 0.80), which also moderateweakly associated with LO-OOA (r=0.66) and NO₃⁻(p) (r = 0.59), as well as
412 NH₄⁺(p) and SO₄²⁻(p) (r = 0.32 and 0.33, respectively).

413

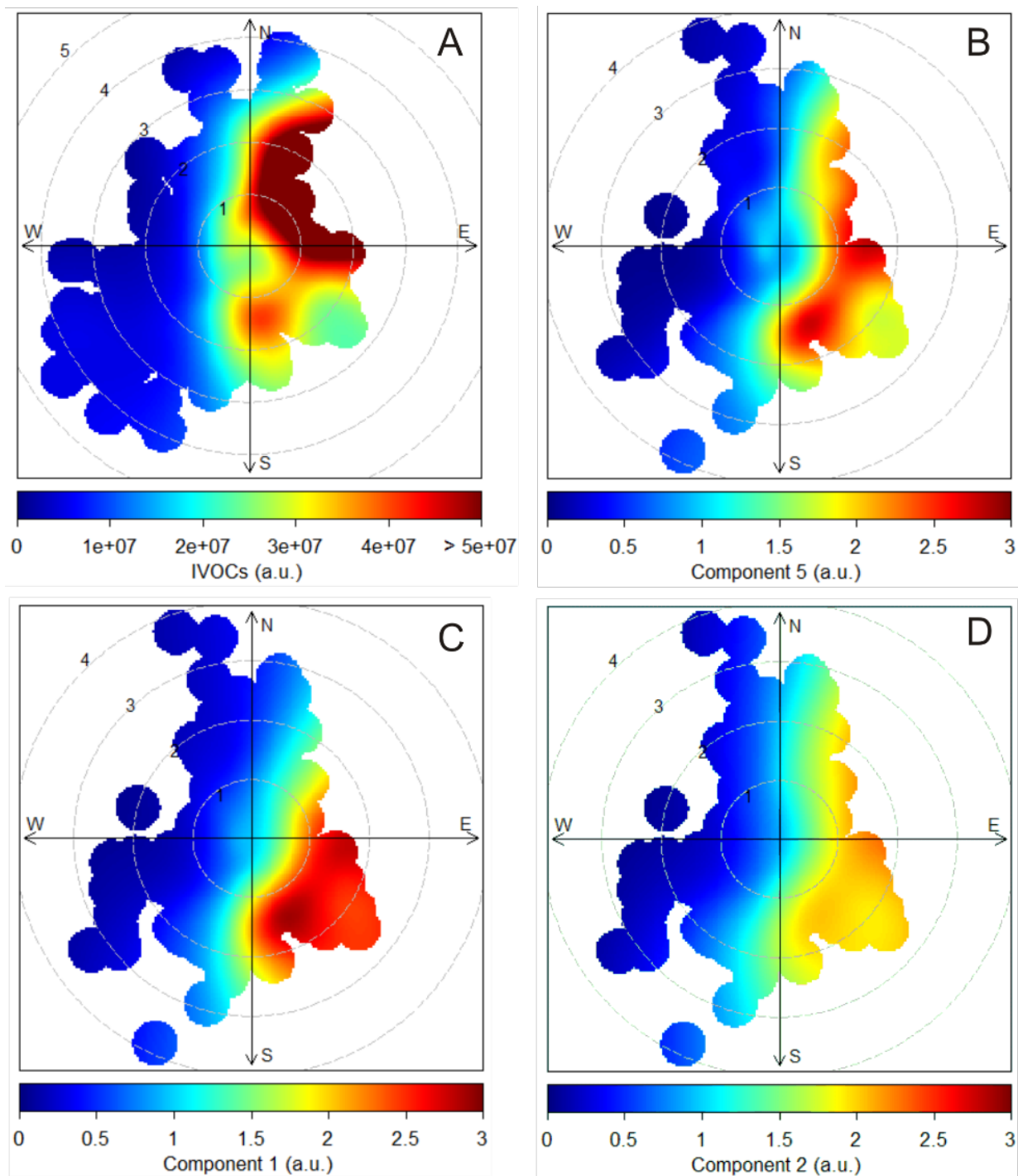
414 **Table 7.** Loadings for the 11-component solution with the inclusion of variables associated with
 415 secondary processes.

	1	2	3	4	5	6	7	8	9	10	11	Communalities
Anthropogenic VOCs												
o-xylene	0.89	0.16	0.04	0.04	0.15	0.00	0.10	0.07	-0.04	0.17	0.24	0.94
1,2,3 - TMB	0.91	0.13	0.10	0.16	0.09	0.07	0.11	0.03	-0.03	0.16	-0.08	0.95
1,2,4 - TMB	0.93	0.19	0.02	0.13	0.13	0.05	0.06	0.07	-0.03	0.17	0.06	0.99
decane	0.89	0.25	0.00	0.22	0.26	0.05	-0.01	0.05	0.01	0.00	0.01	0.98
undecane	0.81	0.35	-0.08	0.27	0.21	0.15	-0.07	0.08	0.04	-0.12	-0.10	0.96
Biogenic VOCs												
α-pinene	0.00	-0.08	0.98	-0.07	0.05	0.03	0.01	0.01	-0.07	0.02	0.01	0.98
β-pinene	0.01	-0.08	0.98	-0.08	0.05	0.05	0.01	0.03	-0.06	0.01	0.02	0.98
limonene	0.11	-0.02	0.92	-0.02	0.14	0.09	0.21	0.02	-0.10	0.02	-0.03	0.95
Combustion tracers												
NO _y	0.23	0.20	-0.27	0.82	0.21	-0.06	-0.07	0.03	0.10	-0.10	0.01	0.92
rBC	0.22	0.15	0.05	0.80	0.43	0.15	0.10	0.05	0.09	0.07	0.00	0.95
CO	0.40	0.09	0.08	0.20	0.09	0.22	0.08	0.06	0.03	0.83	-0.02	0.97
CO ₂	0.12	-0.07	0.50	0.08	-0.03	0.09	0.75	0.28	-0.12	0.03	-0.08	0.95
Aerosol species												
pPAH	0.06	-0.10	-0.06	0.93	-0.07	-0.06	0.07	0.03	0.15	0.13	-0.05	0.94
PM ₁₀₋₁	0.19	0.16	0.08	0.16	0.13	0.08	0.18	0.91	-0.03	0.05	0.07	0.99
PM ₁	0.24	0.44	0.00	0.17	0.70	0.31	-0.06	0.11	-0.04	0.07	-0.14	0.90
NH ₄ ⁺ _(p)	0.28	0.84	0.02	0.12	0.32	0.22	0.06	0.07	-0.04	0.14	-0.04	0.97
SO ₄ ²⁻ _(p)	0.29	0.84	0.03	0.12	0.33	0.19	0.06	0.06	-0.05	0.12	-0.05	0.97
NO ₃ ⁻ _(p)	0.30	0.44	0.09	0.23	0.59	0.36	0.08	0.15	-0.13	0.02	0.24	0.92
HOA	0.37	0.18	0.02	0.77	0.25	0.10	0.10	0.18	-0.08	0.13	0.14	0.93
LO-OOA	0.37	0.40	0.12	0.16	0.66	0.31	0.03	0.12	-0.06	0.00	0.27	0.97
MO-OOA	0.10	0.15	0.09	0.00	0.10	0.92	0.05	0.07	0.10	0.16	-0.03	0.95
Sulfur												
TS	0.27	0.90	-0.20	0.03	0.04	-0.04	-0.09	0.07	0.00	-0.04	0.18	0.98
SO ₂	0.09	0.96	-0.19	0.02	-0.03	-0.01	-0.08	0.03	-0.02	-0.03	0.00	0.98
TRS	0.65	0.14	-0.10	0.05	0.23	-0.08	-0.07	0.17	0.06	-0.04	0.63	0.95
Other												
IVOCs	0.34	-0.01	0.12	0.33	0.80	-0.23	-0.02	0.02	0.02	0.06	0.06	0.94
NH ₃	-0.03	-0.08	-0.22	0.21	-0.04	0.09	-0.07	-0.03	0.93	0.02	0.02	0.99
O _x	0.07	0.36	-0.62	0.01	0.27	0.33	-0.41	-0.07	-0.03	-0.14	0.12	0.91
CH ₄	0.60	0.00	0.14	0.42	0.10	0.08	0.57	0.08	-0.04	0.13	0.16	0.94
Eigenvalues	5.85	4.30	3.71	3.51	2.78	1.58	1.24	1.09	1.01	0.94	0.75	
% of variance	20.90	15.34	13.25	12.52	9.92	5.65	4.43	3.88	3.59	3.37	2.66	
Cumulative variance	20.90	36.24	49.49	62.02	71.94	77.59	82.03	85.90	89.50	92.87	95.53	

416 **3.3 Spatial distribution of IVOC sources**

417 Bivariate polar plots were generated for all components and their dominant, associated variables and
418 are shown in the supplemental material section (Figs. S2-S11). Winds were predominantly from the SW
419 but were also observed often from the S and N. Fig. 5A shows the plot for IVOCs. The highest
420 concentrations were observed when the local wind direction was from the NE, where several facilities
421 including the Aurora North, Musket River and Jackpine mines and large swaths of disturbed and cleared
422 land are located in close proximity to each other (Table 1 and Fig. 1). The second highest IVOC signal
423 intensity was observed when local wind direction was from the SSE.

424 The bivariate polar plots of the 3 components associated with IVOCs are shown in Fig. 5B-D. These
425 components are associated with winds from the NE, E, SE and S at low to moderate speeds ($1-3 \text{ m s}^{-1}$).
426 Component 5 (Fig. 5B) was the most strongly correlated with IVOCs and shows the most spatial overlap
427 with the distribution of the IVOC source; however, the intensities differ owing to the association of
428 component 5 with other variables such rBC and LO-OOA.



429

430 **Figure 5.** Bivariate polar plots related to IVOCs: **(A)** IVOCs from the complete data set. **(B)** Component 5
 431 extracted from the main PCA (Table 5). **(C)** Component 1 extracted from the main PCA. **(D)** Component 2
 432 extracted from the main PCA analysis. Wind direction is binned into 10° intervals and wind direction into
 433 30° intervals. The polar axis indicates wind speed (m s⁻¹). a.u. = arbitrary units.

434 4. Discussion

435 The main objective of this work is to elucidate the origin of the IVOC signature observed at the AMS 13
436 ground site downwind from the AB oil sands mining operations (Fig. 2) through a principal component
437 analysis. The optimum PCA solution identified 10 components, of which three were associated with the
438 IVOC signature: 1, 2, and 5 (Table 5). The assignments of these components to source types in the oil
439 sands are given in Table 6 and are discussed below.

440 Emission inventories show that the facilities that process the mined bitumen are by far the largest
441 anthropogenic point sources in the oil sands region (NPRI, 2013), consistent with recent aircraft
442 measurements (Baray et al., 2018; Howell et al., 2014; Li et al., 2017; Simpson et al., 2010) which have
443 shown substantial emissions of NO_y, SO₂, CO, VOCs, CO₂, and CH₄, from these facilities and associated
444 mining activities. No single component correlates with all of these variables, suggesting that the PCA is
445 able to distinguish between source types within the facilities such as tailings ponds (component 1), stack
446 emissions (component 4), and mining (component 2).

447 Close-up overflights (Howell et al., 2014; Li et al., 2017; Baray et al., 2018) were able to spatially resolve
448 various oil sands facility emission sources (i.e., tailings ponds from upgraders, fluid coking reactors,
449 hydrocrackers and –treaters); the PCA presented in this manuscript is not expected to do this in all cases
450 because some emissions would have frequently merged into a single plume by the time of observation
451 at AMS 13; unless their emissions vary considerably in time, these sources could be interpreted as
452 originating from a single source in the PCA.

453 The discussion below focuses on components that are associated with IVOCs (section 4.1), followed by
454 those that are not (section 4.2). The PCA analysis that included 6 secondary products is discussed in
455 section 4.3. Components which are not associated with IVOCs and have only tentatively been identified
456 (i.e., components 6 – 10) are discussed in the S.I.

457 4.1 Sources associated with IVOCs

458 4.1.1. Component 1: Tailings ponds (wet tailings)

459 Component 1 is strongly associated with anthropogenic VOCs ($r > 0.87$) and ~~moderate~~weakly with TRS (r
460 $= 0.59$), and CH_4 ($r = 0.59$). These pollutants originate from tailings ponds (Small et al., 2015), though it is
461 unclear from this analysis how large a source tailings ponds are compared to fugitive emissions of these
462 pollutants from the nearby processing (e.g., bitumen separation and mining) facilities.

463 Tailings ponds cover large areas of land and are used to slowly (on a time scale of years to decades)
464 separate solid components, or tailings, from water used in bitumen extraction. Residual bitumen often
465 floats to the top of the settling basins. Most tailings ponds are "wet" (as they contain residual naphtha
466 that is used as a diluent during the transfer of tailings to the ponds) and emit VOCs, CH_4 , and CO_2 (Small
467 et al., 2015). The presence of o-xylene, TMB and the n-alkanes in component 1 is consistent with the
468 fugitive release of VOCs from residual naphtha, which contains these compounds (Siddique et al., 2008;
469 Siddique et al., 2011; Small et al., 2015). Furthermore, the observation of TRS and CH_4 from this source is
470 consistent with the presence of anaerobic sulfur reducing bacteria and methanogens within the ponds,
471 which degrade not only the residual bitumen (Holowenko et al., 2000; Percy, 2013; Quagraine et al.,
472 2005) but also the various components of naphtha (Shahimin and Siddique, 2017; Small et al., 2015).
473 Overall, tailings ponds emissions explain much of the TRS and CH_4 concentration variability in this data
474 set (Table 5) and in a recent aircraft study (Baray et al., 2018).

475 While component 1 correlates with CH_4 ($r = 0.59$), it does not correlate with CO_2 ($r = 0.09$). Emissions of
476 CH_4 from tailings ponds due to methanogenic bacterial activity are well-documented (Small et al., 2015;
477 Yeh et al., 2010) and hence the correlation with CH_4 is not unexpected. On the other hand, the lack of
478 correlation with CO_2 seems inconsistent with emission inventories that generally present tailings ponds
479 as large CO_2 sources (Small et al., 2015). One plausible explanation is that tailings ponds are a relatively

480 small CO₂ source overall in the region and that other, larger CO₂ sources and sinks (such as
481 photosynthesis and respiration by the vegetation surrounding the site) dominate the variance impacting
482 the PCA results. It may also indicate that, at least on aggregate and for the particular ponds detected in
483 this work, the emissions are in a regime where the release of CH₄ dominates over CO₂, i.e., the ponds
484 have, perhaps, become more anoxic than believed to be the case in previous studies and hence emit
485 more CH₄ (Holowenko et al., 2000). For example, Small et al. (2015) showed that older tailings ponds
486 (those without the addition of fresh froth or thickening treatments) tended to emit more CH₄, while
487 newer ponds are associated with higher VOC emissions. It is likely that component 1 is dominated by the
488 nearest pond (the Mildred Lake settling basin, 6 – 11 km SSE of AMS 13) and other tailings in the SE
489 where the majority of air samples originated from. The Mildred Lake settling basin is one of the oldest in
490 the region and is still actively being used; the correlation with CH₄ and VOC emissions is hence expected.

491 Component 1 is also associated with NO_y, rBC, CO, and HOA, though these correlations are relatively
492 modest ($r = 0.27, 0.30, 0.41, \text{ and } 0.40$, respectively). These species typically originate from combustion
493 sources, such as generators, motor vehicles, including ~~Diesel~~diesel powered engines powering
494 generators or pumps; it is not obvious if and to what extent these are operated on or near tailings
495 ponds, though. Satellite observations have shown elevated concentrations of NO₂ above on-site
496 upgrader facilities, likely a result of emissions from extraction and transport sources (McLinden et al.,
497 2012). In addition, one of the major highways of the region is located adjacent to the Mildred Lake
498 settling basin and other major ponds in the region; highway traffic emissions (of CO, NO_y, rBC, and HOA)
499 may hence also be partially included in component 1.

500 The bivariate polar plot shows that component 1 was observed when local wind speeds were from the
501 SE and E of the measurement site (Fig. 5C), which is consistent with the notion that the Mildred Lake
502 settling basin and emissions along Highway 63 and, potentially, more distant facilities are sources
503 contributing to this component.

504 Component 1 is associated with the IVOC signature, though to a lesser degree than components 2 and 5.
505 The association of the IVOC signal with component 1 is slightly weaker ($r = 0.31$) than the
506 association with component 2 ($r = 0.39$), but significantly weaker than component 5 ($r = 0.74$). The
507 association of IVOCs with tailings ponds vapor can be explained by the presence of bitumen in the ponds
508 that was not separated from the sand during the separation stage (Holowenko et al., 2000). Tailings
509 ponds contain anywhere from 0.5% - 5% residual bitumen by weight (Chalaturnyk et al., 2002;
510 Holowenko et al., 2000; Penner and Foght, 2010). As illustrated in Fig. 4A, some of this material floats on
511 the ponds' surfaces, where IVOCs can partition to the air. Emission of IVOCs from bitumen floating on
512 tailings ponds would be a function of many variables (e.g., diluent composition, extraction methodology,
513 settling rate, temperature, etc.) and is thus not expected to be as persistent as CH_4 partitioning from the
514 ponds to the above air or from exposed bitumen on the mine surface, leading to a lower overall
515 correlation.

516 Component 1 is also weakly associated with the less oxidized oxygenated organic aerosol factor, LO-
517 OOA ($r = 0.45$). Liggio et al. (2016) found that the observed secondary organic aerosol is dominated by
518 an OOA factor whose mass spectrum was similar to those of aerosols formed from oxidized bitumen
519 vapours. The organic aerosol budget in this study was also dominated by an OOA factor, the LO-OOA
520 (Lee et al., 2018). The association of LO-OOA with component 1 is thus consistent with its association
521 with IVOCs.

522 **4.1.2. Component 2: Mine fleet and vehicle emissions**

523 Component 2 strongly correlates with NO_y ($r = 0.82$), rBC ($r = 0.77$), pPAH ($r = 0.94$), and HOA ($r = 0.74$),
524 which suggests a combustion source such as Diesel engines. In the AB oil sands, there is a sizeable
525 off-road mining truck fleet consisting of heavy aggregate haulers. In addition, there are Diesel
526 engine sources associated with generators, pumps and land moving equipment, i.e., graders, dozers,

527 hydraulic excavators, and electric rope shovels (Watson et al., 2013; Wang et al., 2016). Most of these
528 non-road applications have been exempt from highway fuel taxes, on-road fuel formulation
529 requirements and after-engine exhaust treatment (Watson et al., 2013). Emissions from the hauler fleet
530 and the stationary sources would fit the profile of component 2. Other ~~Diesel~~diesel engines operated in
531 the region include a commuter bus fleet, pickup and delivery trucks, tractor-trailers, and privately
532 owned ~~Diesel~~diesel powered automobiles used to commute from the work sites to the major residential
533 areas around Fort McMurray, whose emissions are likely captured by component 2 as well, though the
534 magnitude of these relative to the mining truck fleet is not known. Consistent with component 2 being
535 associated with an anthropogenic source is its weakpoor correlation with undecane ($r = 0.27$), likely
536 arising from fugitive fuel emissions.

537 The bivariate polar plot (Fig. 5D) for component 2 and NO_y in particular (Fig. S-~~3A4A~~) match the location
538 of Highway 63 which crosses the river to the SE of AMS 13 and bends to the E and is indicative of a line
539 source. At the same time, some of the largest mining operations in the region, the Susan Lake Gravel Pit,
540 Aurora North, Muskeg river, and Millennium mines are located to the NE and SE of AMS 13 as well. NO_y ,
541 rBC, and HOA (Fig. S-~~3A4A~~, B and D) all appear to have dominating point sources to the S and E when
542 wind speeds are $1\text{-}2 \text{ m s}^{-1}$. These directions are the same as the Fort McKay industrial park to the E and
543 the Syncrude Mildred Lake facility parking lot to the S which would have a higher concentration of
544 vehicles emitting these pollutants in a smaller area, whose emissions would be in addition to those from
545 industrial activities.

546 Component 2 is associated with the IVOCs signature and CH_4 (both $r = 0.39$). The mining activities bring
547 bitumen to the surface; similar to what we had observed in lab experiments (Fig. 2, black trace), the
548 surface exposure of bitumen during mining and on-site processing is expected to be associated with
549 fugitive emissions of CH_4 (Johnson et al., 2016) and IVOCs.

550 Fine-fraction particle-surface bound PAHs (pPAH) are associated strongly with component 2, but no
551 other components. Measurements of individual PAHs in snow and moss downwind from the oil sands
552 facilities have identified multiple sources of PAHs in the Athabasca oil sands, which include wind-blown
553 petroleum coke dust (also referred to as petcoke for short), a carbonaceous residual product from the
554 upgrading of crude petroleum that is stockpiled on mine sites, and emissions from fine tailings, oil sands
555 ore, and naturally exposed bitumen (Zhang et al., 2016; Jautzy et al., 2015; Parajulee and Wania, 2014).
556 Given this diversity of known sources, the associations of PAHs with only a single component is
557 surprising, though indicates that emissions from the mining fleet (which would include ~~Dieseldiesel~~ and,
558 perhaps, wind-blown emissions from petcoke that is being transported) gave rise to most of the
559 variability in surface-bound PAH concentrations in this data set. The petcoke emissions identified in the
560 studies mentioned above are likely mainly associated with larger, supermicron sized particles, whose
561 PAH content would not be detected by the pPAH measurement in this data set.

562 Component 2 is not significantly associated with LO-OOA ($r = 0.11$), even though IVOCs are associated
563 with this component. This feature may indicate that the IVOCs emitted in component 2 are qualitatively
564 different from those emitted by components 1 and 5, in that they are less likely to yield organic aerosol
565 on the time scale of transport from emission to observation. One reason for the difference could be that
566 the bitumen that is transported by the mining fleet is relatively freshly exposed, whereas the IVOCs
567 released by bitumen in tailings ponds has been processed by microbes and that released by mine faces
568 (component 5) may have been photochemically oxidized to a greater extent and hence more prone to
569 rapid aerosol formation.

570 There is little to no association of component 2 with ~~either CO or CO₂~~ ($r = 0.18$ and 0.08 , respectively).
571 This is somewhat unexpected as the trucks are expected to release CO₂ both (Wang et al., 2016) but
572 could be due to significantly larger CO₂ sources in the area dominating the observed CO₂ variability at
573 AMS 13 (e.g., components 3 and 6). Furthermore, one would expect an association of non-road mining

574 truck emissions with aromatics and alkanes. Component 2 exhibited only poor correlations with decane
575 ($r = 0.22$) and undecane ($r = 0.27$) and negligible correlation with o-xylene ($r = 0.08$), suggesting that
576 other components (i.e., component 1) explained most of the variability of their concentrations at this
577 site.

578

579 **4.1.3. Component 5: Surface-exposed bitumen and hot-water bitumen extraction**

580 Component 5 correlates more strongly with the IVOCs ($r = 0.74$) than with any other component and
581 correlates strongly with LO-OOA ($r = 0.72$), moderateweakly with rBC ($r = 0.44$), and weakpoorly with
582 HOA ($r = 0.25$), NO_y ($r = 0.22$), decane ($r = 0.23$), undecane ($r = 0.20$), and TRS ($r = 0.26$). We interpret this
583 profile as emissions from surface-exposed bitumen which outgases IVOCs.

584 One possibility is that these emissions occur on mine faces, where previously unexposed bitumen is
585 brought to the surface as a result of mining. Only a relatively small portion of the mine faces is actively
586 mined; those parts give rise to rBC and NO_y emissions from combustion engines in heavy haulers or
587 generators powering equipment. The weakpoor association of component 5 with TRS could be due to
588 sulfur reducing bacteria found on the surface of bitumen. However, most of the variability of TRS at AMS
589 13 is attributed to composite or "dry" tailings ponds given their more conducive environment to
590 microbial activity.

591 Component 5 does not correlate with CO_2 ($r = -0.03$) and only weakpoorly with CH_4 ($r = 0.12$), which is
592 somewhat at odds with the notion of mine faces as the main source of IVOCs. The mine faces give rise to
593 substantial fugitive emissions of CO_2 and CH_4 (Johnson et al., 2016) – these emissions are likely captured
594 by component 6 in this analysis (see S.I.). It is unclear to what extent these greenhouse gases are
595 released relatively quickly from "hot spots" (i.e., from a small number of locations) through surface
596 cracks and fissures or by slow release from new material that is exposed and then releases greenhouse

597 gases during material handling, transport and processing (Johnson et al., 2016). IVOCs from surface-
598 exposed bitumen are likely released by the latter mechanism and are temperature-dependent. If the
599 mine faces are indeed the main IVOC source, the analysis results presented here suggest that the IVOCs
600 emissions from surface-exposed bitumen on mine faces are decoupled from CH₄ emissions in time and
601 appear as a distinct component and hence corroborate the "hot spots" or fast release hypothesis,
602 though clearly, more work is needed to characterize greenhouse gas emissions from oil sands mine
603 faces.

604 The association of IVOCs with component 5 may also be a result of fugitive emissions during the hot
605 water-based extraction of bitumen sand slurries during the separation phase of bitumen treatment.
606 Generally, bitumen is extracted in a weak alkaline environment by aeration of the solution to optimize
607 the separation of sand and bitumen (Masliyah et al., 2004). Unrecovered bitumen and naphtha then end
608 up in tailings. The recovered bitumen and naphtha are moved to upgrader facilities where they undergo
609 further treatment (such as coking or hydrotreatment). The magnitude of fugitive emissions during these
610 downstream extraction processes could be large, considering the bitumen is heated and actively
611 aerated. Future work should investigate IVOC fluxes near extraction plants and on mine faces.

612 Finally, it is conceivable that a "natural" background of IVOCs exists in the region (since bitumen can be
613 found at or near the surface in many parts of the region); such a natural background would also be
614 included in component 5. However, this "natural" bitumen would have been exposed at the surface for
615 geological time scales and, unlike unexposed, buried bitumen, likely would have lost most of its volatile
616 content over that period. Furthermore, the mine faces occupy large swaths of land in the region (as
617 evident from satellite imagery). Thus, the IVOCs emissions are more likely due to anthropogenic activity
618 than due to a natural phenomenon.

619

620 4.2. Sources not associated with IVOCs

621 4.2.1. Component 3: Biogenic emissions and respiration

622 Component 3 is strongly correlated with the monoterpenes α -pinene ($r = 0.98$), β -pinene ($r = 0.98$) and
623 limonene ($r = 0.92$) and is hence identified as a biogenic emissions source. This component is also
624 ~~moderate~~weakly associated with CO_2 ($r = 0.48$).

625 At AMS 13, CO_2 and the monoterpenes exhibit a very similar diurnal cycle: they are present in higher
626 concentrations during the night than during the day (Fig. 3) due to a decrease in the boundary layer
627 height (BLH) at night coupled with plant respiration of CO_2 and non-photochemical emission of
628 monoterpenes (Fares et al., 2013; Guenther et al., 2012). During the day, mixing ratios of CO_2 are lower
629 due to plant uptake and photosynthesis, and mixing ratios of terpenes are lower due to higher mixing
630 heights and vertical entrainment and due to oxidation by O_3 and OH (Fuentes et al., 1996). Hence, the
631 PCA gives a *positive* correlation of monoterpenes with CO_2 even though the physical processes,
632 photosynthesis and respiration, work in opposite direction.

633 The bivariate polar plots (Fig. S-45A-C) show that the monoterpenes and CO_2 were observed in highest
634 concentrations when the wind speeds were low ($< 1 \text{ m s}^{-1}$), consistent with formation of a stable
635 nocturnal boundary layer.

636 To corroborate this interpretation, the PCA was repeated with BLH estimated by a light detection and
637 ranging (LIDAR) instrument (Strawbridge et al., in prep.) added as a variable (Table S-9 in the S.I.). Since
638 BLH is not "emitted" by any source, it appears as a single variable component ($r = 0.90$). The only other
639 component that BLH (anti)correlates with is the biogenic component 3 ($r = -0.35$).

640 The dominant monoterpene species observed was α -pinene, followed by β -pinene and limonene,
641 though occasionally there was twice as much β -pinene than α -pinene in the sampled air. Some

642 variability of this ratio is expected since emission factors vary considerably between tree species (Geron
643 et al., 2000) which are not homogeneously distributed throughout the region (e.g., Fig. S1 of Rooney et
644 al. (2012)).

645 Simpson et al. (2010) observed enhancements of α -pinene and, to a greater extent, β -pinene over the
646 oil sands (up to 217 pptv and 610 pptv) compared to background levels of 20 ± 7 and 84 ± 24 pptv,
647 respectively, during mid-day overflights (which occurred between 11:00 and 13:00 local time). Similar
648 enhancements were also reported by Li et al. (2017) who observed emissions of biogenic hydrocarbons
649 in the four facilities sampled, three of which showed a higher β - than α -pinene concentration. The PCA
650 analysis (Table 5) showed no significant correlation of α - and β -pinene with any of the anthropogenic
651 sources, which implies that the biogenic source strength is simply too large for any anthropogenic
652 emissions of terpenes to be picked up in the analysis, especially considering that terpenes are relatively
653 short-lived.

654 The biogenic source shows weakpoor anticorrelations with NO_y ($r = -0.26$), NH_3 ($r = -0.24$), and SO_2 (r
655 $= -0.15$). Many NO_y species (i.e., NO_2 , HONO, peroxy-carboxylic nitric anhydrides or PAN, and HNO_3) and
656 SO_2 deposit to the forest canopy (Hsu et al., 2016; Min et al., 2014; Fenn et al., 2015); at night, when
657 mixing heights are lower, their concentrations are expected to decrease faster than during the day and
658 are thus out of phase with the CO_2 and terpene concentrations. In addition, there is a time-of-day
659 observation bias for SO_2 and, to lesser extent, NO_y , which are found in upgrader plumes (see 4.2.2.). The
660 weakpoor anticorrelation with NH_3 likely arises because the NH_3 emissions from plants are mainly
661 stomatal and scale with temperature and are hence larger during the day than at night, anticorrelated
662 with the terpene source (Whaley et al., 2017).

663 **4.2.2 Component 4: Upgrader emissions**

664 Component 4 is strongly correlated with SO_2 ($r = 0.97$) and total sulfur ($r = 0.93$). By far the largest

665 source of SO₂ in the region are upgrader facilities, which emit as much as 6×10⁷ kg annually according to
666 emission inventories (ECCC, 2013). Significant SO₂ emissions from upgrader facilities have recently been
667 confirmed by aircraft studies (Simpson et al., 2010; Howell et al., 2014; Liggio et al., 2016). Component 4
668 is also weakpoorly correlated with NO_y (r = 0.21) but not with rBC (r = 0.05), consistent with a non-sooty
669 (i.e., lean) combustion source such as upgrader stacks. Strong enhancements in SO₂ were only observed
670 intermittently as "spikes", which is expected when sampling emissions from relatively few and discrete
671 point sources.

672 Component 4 is weakpoorly anticorrelated with CO₂ (r = -0.12), even though inventories indicate that
673 the upgrading facilities are the largest CO₂ source in the region (Furimsky, 2003; Englander et al., 2013;
674 Yeh et al., 2010). In this data set, the lack of correlation of component 4 with CO₂ (and to some extent
675 with PM₁₀₋₁ as well) likely arises mainly from a sampling bias as stack emissions were only observed
676 during daytime, likely due to diurnal variability of the atmospheric boundary layer structure as explained
677 below.

678 Most of the variability in CO₂ concentration at AMS 13 is due to surface-based sources that originate
679 from large areas, especially biogenic processes (photosynthesis during the day and respiration at night,
680 component 3) and anthropogenic surface sources such as those captured by component 6 (section
681 4.2.3). Other anthropogenic pollutants, such as SO₂, NO_y, and CH₄, are not subject to large biogenically
682 driven processes and are less affected than CO₂.

683 In contrast to surface sources, emissions from the > 100 m tall stacks are comparatively under-sampled
684 and observed mainly during daytime, when vertical mixing brings elevated plumes to the surface, yet
685 CO₂ concentrations are generally much lower than during the night due to uptake by vegetation. At
686 night, pollutants emitted from stacks are injected above the likely very shallow nocturnal surface layer
687 and were hence not observed at the surface. Vertical profile measurements of SO₂ stack plumes by a

688 Pandora spectral sun photometer at Fort McKay during daytime have shown considerable vertical
689 gradients and only occasional transport of SO₂ all the way to the surface (Fioletov et al., 2016).

690 The association of component 4 with CO₂ is negative because the stack emission source is observed only
691 during the day when the large biogenic sink dominates and effectively masks the relatively small
692 increase due to anthropogenic CO₂. In contrast, background concentrations of SO₂ are comparatively
693 low, and the increase in SO₂ concentrations is readily picked up the PCA.

694 It would be interesting to conduct a future study in winter when biogenic activities decrease; a
695 wintertime PCA analysis of surface measurements might be able to associate CO₂ enhancements with
696 upgraders, though boundary layer mixing heights would decrease as well, which would make a PCA
697 analysis using surface data even more challenging.

698 Component 4 does not correlate with PM₁₀₋₁ volume ($r = 0.09$). It is clear that the emitted SO₂ will
699 contribute to secondary aerosol formation downwind, such that a correlation of stack emissions with
700 PM₁₀₋₁ volume might be expected. However, these secondary contributions will likely mostly be in the
701 submicron aerosol fraction, which adds relatively little to PM₁₀₋₁ volume. Further, PM₁₀₋₁ volume is
702 dominated by coarse particles from other primary sources, mostly wind-blown emission of sand from
703 the mine surfaces, roadways and, perhaps, bioaerosol (component 7, see S.I.). These effects make PM₁₀₋₁
704 volume from stacks appear comparatively small, such that the variability of the larger, surface-based
705 sources likely masks the contribution of stacks emissions to PM₁₀₋₁ variability.

706 The bivariate polar plot of component 4 (Fig. S-~~5D6D~~) shows that the largest magnitudes were observed
707 when local winds were from the SE. The corresponding plot of SO₂ (Fig. S-~~5A6A~~) reveals two more
708 distinct sources: a larger one from the E and a smaller one from the SSE. However, only two facilities
709 (Sunrise and Firebag) are located to the E at relatively large distances of 37 km and 47 km respectively.
710 The largest known upgraders and SO₂ sources in the area (i.e., upgraders located at the Mildred Lake

711 and Suncor base plants) are located to the S and SE of AMS 13. Considering that the stack emissions are
712 only observed intermittently, we speculate that there exists a mesoscale transport pattern in the
713 Athabasca river valley which channel emissions, such that the local wind direction and speed may be
714 misleading as to the true location of these sources. For more extensive data sets, such phenomena may
715 very well average out but perhaps did not in this case.

716 **4.3. Extended PCA with added secondary variables**

717 The extended analysis (Table 7) qualitatively preserves the structure (with the exception of an added
718 “Aged” component, # 6) of the original 10-component solution but allows an assessment of which
719 components most result in formation of secondary products such as SOA, which has implications for
720 health (Bernstein, 2004) and climate (Charlson et al., 1992). Secondary products vary considerably as a
721 function of air mass chemical age (which depends, amongst other components, on time of day and
722 synoptic conditions, including wind speed) and are hence expected to add considerable noise and
723 scatter to the results leading to lower correlations. On the other hand, the distance between the
724 measurement site and sources is fixed, such that this variability should average out over time. This
725 indeed appears to have happened in this data set in spite of the relatively low sample size.

726 The analysis indicates that the component with the strongest IVOC source (Component 5) also has the
727 largest impact on-highest association with PM_1 ($r = 0.7$; Table 7). Aircraft measurements combined with
728 a modelling study have required a group of IVOC hydrocarbons to explain the significant SOA formation
729 and growth downwind of the oil sands region (Liggio et al., 2016). The association of IVOCs with PM_1
730 volume is consistent with the hypothesis that oxidation of IVOCs observed at AMS 13 leads to SOA
731 generation and appears to have a significant impact on the variation in PM_1 mass.

732 The second component influencing PM_1 is that from stack emissions (Component 4 in the primary PCA;
733 Component 2 in the secondary PCA) (Tables 5 and 7). It is well established that the oxidation of SO_2 to

734 sulfate will lead to formation of fine particulate matter. This apparently occurs, at least partially, on the
735 time scale between the point of emission and the AMS 13 site (assuming a wind speed of 3 m/s and a
736 distance of 11 km, the transit time is 1 hour), though some fraction of $\text{SO}_4^{2-}(\text{p})$ is likely directly emitted.

737

738 **5. Summary and conclusions**

739 A PCA was applied to continuous measurements of 22 primary pollutant tracers at the AMS 13 ground
740 site in the Athabasca oil sands during the 2013 JOSM intensive study to elucidate the origins of airborne
741 analytically unresolved hydrocarbons that were observed by GC-ITMS. The analysis identified 10
742 components. Three components correlated with the IVOC signature and were assigned to mine faces
743 and, potentially, hot-water bitumen extraction facilities, the mine hauler fleet, and wet tailings ponds
744 emissions. All three are anthropogenic activities that involve the handling of raw bitumen, i.e., the
745 unearthing, mining and transport of crude bitumen, and the disposal of processed material that contains
746 residual bitumen in wet tailings ponds. The PCA results are consistent with our previous interpretation
747 that the unresolved hydrocarbons originate from bitumen, which was based on the similarity of the
748 chromatograms with those obtained in a head space vapor analysis of ground-up bitumen in the
749 laboratory.

750 Liggio et al. (2016) showed that these hydrocarbons constitute a group of IVOCs in the saturation vapor
751 concentration (C^*) range $10^5 \mu\text{g m}^{-3} < C^* < 10^7 \mu\text{g m}^{-3}$ that contribute significantly to secondary organic
752 aerosol formation and growth downwind of the oil sands facilities. The correlation of LO-OOA with 2-two
753 of the three3 IVOC components in the main PCA analysis and with PM_1 in the extended analysis
754 corroborates the high SOA formation potential of IVOCs and suggests that further differentiation may be
755 needed and stresses the need for IVOCs to be routinely monitored. In particular, direct measurements
756 of emissions throughout the processing of raw bitumen are needed to pinpoint source contributions

757 more accurately and aid in the development of potential mitigation strategies.

758 The PCA analysis in this study suffered from a several limitations. For instance, PCA does not provide
759 insight into ~~the magnitudes of emission~~ factors of individual facilities, though it does capture what
760 conditions change ambient concentrations the most. Further, the receptor nature of PCA did not always
761 discern between large source areas that may have many individual point sources coming together at the
762 point of observation. For example, component 1 contains an obvious tailings pond signature because of
763 its high correlations with anthropogenic VOCs, methane and TRS, but also includes several combustion
764 sources, making interpretation of this IVOC source location more challenging. A longer continuous data
765 set with a greater number of variables would have perhaps been able to resolve these different sources,
766 including the various tailings ponds, of which there are 19 in the region, all with slightly different
767 emission profiles (Small et al., 2015) .

768 Another limitation is the bias of this (and most) ground site data set towards surface-based emissions
769 and the undersampling of stack emissions. Facility stacks were only observed in the daytime because at
770 night the mixing height is so low that the stacks are emitting directly into the residual layer. These
771 emissions could be quantified using aircraft based platforms (Howell et al., 2014; Li et al., 2017; Baray et
772 al., 2018). The PCA struggled most with the allocation of greenhouse gases. Mixing ratios of CO₂, in
773 particular, were difficult to reconcile in this analysis due to a high background and large attenuation by
774 biogenic activity and boundary layer meteorology. Forests greatly affected CO₂ levels in the region
775 because it is taken up during the day when plants are photosynthetically active and emitted at night
776 when plants undergo cellular respiration. This CO₂ source and sink appears to dominate the PCA,
777 effectively masking relatively small emissions from tailings ponds, facilities, and tail pipes in particular
778 from the mine hauling fleet.

779 Finally, there is a need for improved monitoring methods for IVOCs. For instance, future studies should

780 focus on characterizing the VOCs in the above mentioned volatility range using a greater mass and time
781 resolution instrument, such as a time-of-flight mass spectrometer (TOF-MS) or higher resolution
782 separation methods (e.g., multi-dimensional gas chromatography), and also include measurement of
783 speciated aerosol organic composition by, for example, thermal desorption aerosol GC (TAG) analysis
784 (Williams et al., 2006). Future studies should also investigate how IVOC volatility distributions vary with
785 source type and chemical age.

786 **Acknowledgments**

787 Funding for this study was provided by Environment and Climate Change Canada and the Canada-
788 Alberta Oil Sands Monitoring program. The GC-ITMS used in this work was purchased using funds
789 provided by the Canada Foundation for Innovation and matching funds by the Alberta government.
790 TWT, JAH, DKB, FVA and GRW acknowledge financial support from the Natural Sciences and Engineering
791 Research Council of Canada (NSERC) Collaborative Research and Training Experience Program (CREATE)
792 program Integrating Atmospheric Chemistry and Physics from Earth to Space (IACPES).

793 **6. References**

- 794 Government of Alberta, oil sands information portal: <http://osip.alberta.ca>, access: 23-FEB-2017, 2017.
- 795 Allen, E. W.: Process water treatment in Canada's oil sands industry: II. A review of emerging
796 technologies, *J. Environ. Eng. Sci.*, 7, 499-524, 10.1139/s08-020, 2008.
- 797 Baray, S., Darlington, A., Gordon, M., Hayden, K. L., Leithead, A., Li, S. M., Liu, P. S. K., Mittermeier, R. L.,
798 Moussa, S. G., O'Brien, J., Staebler, R., Wolde, M., Worthy, D., and McLaren, R.: Quantification of
799 methane sources in the Athabasca Oil Sands Region of Alberta by aircraft mass balance, *Atmos.*
800 *Chem. Phys.*, 18, 7361-7378, 10.5194/acp-18-7361-2018, 2018.
- 801 Bari, M., and Kindzierski, W. B.: Fifteen-year trends in criteria air pollutants in oil sands communities of
802 Alberta, Canada, *Environ. Int.*, 74, 200-208, 10.1016/j.envint.2014.10.009, 2015.
- 803 Bernstein, D. M.: Increased mortality in COPD among construction workers exposed to inorganic dust,
804 *Eur. Resp. J.*, 24, 512-512, 10.1183/09031936.04.00044504, 2004.
- 805 Bond, T. C., Streets, D. G., Yarber, K. F., Nelson, S. M., Woo, J. H., and Klimont, Z.: A technology-based
806 global inventory of black and organic carbon emissions from combustion, *J. Geophys. Res.*, 109,
807 D14203, 10.1029/2003JD003697, 2004.
- 808 Briggs, N. L., and Long, C. M.: Critical review of black carbon and elemental carbon source
809 apportionment in Europe and the United States, *Atmos. Environ.*, 144, 409-427,
810 10.1016/j.atmosenv.2016.09.002, 2016.
- 811 Buhamra, S. S., Bouhamra, W. S., and Elkilani, A. S.: Assessment of air quality in ninety-nine residences of
812 Kuwait, *Environ. Technol.*, 19, 357-367, 10.1080/09593331908616691, 1998.
- 813 Burtscher, H., Scherrer, L., Siegmann, H. C., Schmidtott, A., and Federer, B.: Probing aerosols by
814 photoelectric charging, *J. Appl. Phys.*, 53, 3787-3791, 10.1063/1.331120, 1982.
- 815 Bytnerowicz, A., Fraczek, W., Schilling, S., and Alexander, D.: Spatial and temporal distribution of
816 ambient nitric acid and ammonia in the Athabasca Oil Sands Region, Alberta, *J. Limnol.*, 69, 11-21,
817 10.3274/jl10-69-s1-03, 2010.
- 818 The facts on Canada's oil sands: <http://www.capp.ca/publications-and-statistics/publications/296225>,
819 access: April 20, 2017, 2016.
- 820 Carslaw, D. C., and Ropkins, K.: openair - An R package for air quality data analysis, *Environ. Modell.*
821 *Softw.*, 27-28, 52-61, 10.1016/j.envsoft.2011.09.008, 2012.
- 822 Carslaw, D. C., and Beevers, S. D.: Characterising and understanding emission sources using bivariate
823 polar plots and k-means clustering, *Environ. Modell. Softw.*, 40, 325-329,
824 10.1016/j.envsoft.2012.09.005, 2013.
- 825 Cattell, R. B.: The Scree Test For The Number Of Factors, *Multivariate Behavioral Research*, 1, 245-276,
826 10.1207/s15327906mbr0102_10, 1966.
- 827 Chalaturnyk, R. J., Don Scott, J., and Ozum, B.: Management of oil sands tailings, *Petroleum Science and*
828 *Technology*, 20, 1025-1046, 10.1081/lft-120003695, 2002.
- 829 Charlson, R. J., Schwartz, S. E., Hales, J. M., Cess, R. D., Coakley, J. A., Hansen, J. E., and Hofmann, D. J.:
830 Climate forcing by anthropogenic aerosols, *Science*, 255, 423-430, 10.1126/science.255.5043.423
831 1992.
- 832 Chen, H., Karion, A., Rella, C. W., Winderlich, J., Gerbig, C., Filges, A., Newberger, T., Sweeney, C., and
833 Tans, P. P.: Accurate measurements of carbon monoxide in humid air using the cavity ring-down
834 spectroscopy (CRDS) technique, *Atmos. Meas. Tech.*, 6, 1031-1040, 10.5194/amt-6-1031-2013, 2013.
- 835 Cross, E. S., Hunter, J. F., Carrasquillo, A. J., Franklin, J. P., Herndon, S. C., Jayne, J. T., Worsnop, D. R.,
836 Miake-Lye, R. C., and Kroll, J. H.: Online measurements of the emissions of intermediate-volatility and
837 semi-volatile organic compounds from aircraft, *Atmos. Chem. Phys.*, 13, 7845-7858, 10.5194/acp-13-
838 7845-2013, 2013.

839 de Gouw, J. A., Middlebrook, A. M., Warneke, C., Ahmadov, R., Atlas, E. L., Bahreini, R., Blake, D. R.,
840 Brock, C. A., Brioude, J., Fahey, D. W., Fehsenfeld, F. C., Holloway, J. S., Le Henaff, M., Lueb, R. A.,
841 McKeen, S. A., Meagher, J. F., Murphy, D. M., Paris, C., Parrish, D. D., Perring, A. E., Pollack, I. B.,
842 Ravishankara, A. R., Robinson, A. L., Ryerson, T. B., Schwarz, J. P., Spackman, J. R., Srinivasan, A., and
843 Watts, L. A.: Organic Aerosol Formation Downwind from the Deepwater Horizon Oil Spill, *Science*,
844 331, 1295-1299, 10.1126/science.1200320, 2011.

845 Trends in atmospheric methane: www.esrl.noaa.gov/gmd/ccgg/trends_ch4/, access: April 11, 2017,
846 2017a.

847 Trends in atmospheric carbon dioxide: www.esrl.noaa.gov/gmd/ccgg/trends/, access: April 11, 2017,
848 2017b.

849 National pollutant release inventory (NPRI): [http://open.canada.ca/data/en/dataset/e40099ae-b116-](http://open.canada.ca/data/en/dataset/e40099ae-b116-4c48-9475-f3806fe5a6a6)
850 [4c48-9475-f3806fe5a6a6](http://open.canada.ca/data/en/dataset/e40099ae-b116-4c48-9475-f3806fe5a6a6), access: October 5, 2016, 2013.

851 ECCC: Joint oil sands monitoring program emissions inventory compilation report, Environment and
852 Climate Change Canada, Downsview, 2016.

853 Englander, J. G., Bharadwaj, S., and Brandt, A. R.: Historical trends in greenhouse gas emissions of the
854 Alberta oil sands (1970-2010), *Environm. Res. Lett.*, 8, 044036, 10.1088/1748-9326/8/4/044036,
855 2013.

856 Fares, S., Schnitzhofer, R., Jiang, X., Guenther, A., Hansel, A., and Loreto, F.: Observations of Diurnal to
857 Weekly Variations of Monoterpene-Dominated Fluxes of Volatile Organic Compounds from
858 Mediterranean Forests: Implications for Regional Modeling, *Environm. Sci. Technol.*, 47, 11073-
859 11082, 10.1021/es4022156, 2013.

860 Fenn, M. E., Bytnerowicz, A., Schilling, S. L., and Ross, C. S.: Atmospheric deposition of nitrogen, sulfur
861 and base cations in jack pine stands in the Athabasca Oil Sands Region, Alberta, Canada, *Environ.*
862 *Pollut.*, 196, 497-510, 10.1016/j.envpol.2014.08.023, 2015.

863 Fioletov, V. E., McLinden, C. A., Cede, A., Davies, J., Mihele, C., Netcheva, S., Li, S. M., and O'Brien, J.:
864 Sulfur dioxide (SO₂) vertical column density measurements by Pandora spectrometer over the
865 Canadian oil sands, *Atmospheric Measurement Techniques*, 9, 2961-2976, 10.5194/amt-9-2961-
866 2016, 2016.

867 Fuentes, J. D., Wang, D., Neumann, H. H., Gillespie, T. J., DenHartog, G., and Dann, T. F.: Ambient
868 biogenic hydrocarbons and isoprene emissions from a mixed deciduous forest, *J. Atmos. Chem.*, 25,
869 67-95, 10.1007/BF00053286, 1996.

870 Furimsky, E.: Emissions of carbon dioxide from tar sands plants in Canada, *Energy Fuels*, 17, 1541-1548,
871 10.1021/ef0301102, 2003.

872 Geron, C., Rasmussen, R., Arnts, R. R., and Guenther, A.: A review and synthesis of monoterpene
873 speciation from forests in the United States, *Atmos. Environm.*, 34, 1761-1781, 10.1016/S1352-
874 2310(99)00364-7, 2000.

875 Gordon, M., Li, S. M., Staebler, R., Darlington, A., Hayden, K., O'Brien, J., and Wolde, M.: Determining air
876 pollutant emission rates based on mass balance using airborne measurement data over the Alberta
877 oil sands operations, *Atmos. Meas. Tech.*, 8, 3745-3765, 10.5194/amt-8-3745-2015, 2015.

878 Grimmer, G., Brune, H., Deutschwenzel, R., Dettbarn, G., Jacob, J., Naujack, K. W., Mohr, U., and Ernst,
879 H.: Contribution of polycyclic aromatic-hydrocarbons and nitro-derivatives to the carcinogenic impact
880 of diesel-engine exhaust condensate evaluated by implantation into the lungs of rats, *Cancer Lett.*,
881 37, 173-180, 10.1016/0304-3835(87)90160-1, 1987.

882 Guenther, A. B., Jiang, X., Heald, C. L., Sakulyanontvittaya, T., Duhl, T., Emmons, L. K., and Wang, X.: The
883 Model of Emissions of Gases and Aerosols from Nature version 2.1 (MEGAN2.1): an extended and
884 updated framework for modeling biogenic emissions, *Geosci. Model Dev.*, 5, 1471-1492,
885 10.5194/gmd-5-1471-2012, 2012.

886 Guo, H., Wang, T., and Louie, P. K. K.: Source apportionment of ambient non-methane hydrocarbons in
887 Hong Kong: Application of a principal component analysis/absolute principal component scores
888 (PCA/APCS) receptor model, *Environ. Pollut.*, 129, 489-498, 10.1016/j.envpol.2003.11.006, 2004.

889 Hair, J. F., Anderson, R. E., Tatham, R. L., and Black, W. C.: *Multivariate data analysis*, in, 7th edition ed.,
890 Prentice-Hall, Upper Saddle River, NJ, pp. 108 -110, 1998.

891 Harrison, R. M., Smith, D. J. T., and Luhana, L.: Source apportionment of atmospheric polycyclic aromatic
892 hydrocarbons collected from an urban location in Birmingham, UK, *Environ. Sci. Technol.*, 30, 825-
893 832, 10.1021/es950252d, 1996.

894 Helmig, D., Klinger, L. F., Guenther, A., Vierling, L., Geron, C., and Zimmerman, P.: Biogenic volatile
895 organic compound emissions (BVOCs) I. Identifications from three continental sites in the U.S,
896 *Chemosphere*, 38, 2163-2187, 10.1016/S0045-6535(98)00425-1, 1999.

897 Holowenko, F. M., MacKinnon, M. D., and Fedorak, P. M.: Methanogens and sulfate-reducing bacteria in
898 oil sands fine tailings waste, *Canadian Journal of Microbiology*, 46, 927-937, 10.1139/cjm-46-10-927,
899 2000.

900 Howell, S. G., Clarke, A. D., Freitag, S., McNaughton, C. S., Kapustin, V., Brekovskikh, V., Jimenez, J. L.,
901 and Cubison, M. J.: An airborne assessment of atmospheric particulate emissions from the processing
902 of Athabasca oil sands, *Atmos. Chem. Phys.*, 14, 5073-5087, 10.5194/acp-14-5073-2014, 2014.

903 Hsu, Y. M., Bytnerowicz, A., Fenn, M. E., and Percy, K. E.: Atmospheric dry deposition of sulfur and
904 nitrogen in the Athabasca Oil Sands Region, Alberta, Canada, *Sci. Tot. Environm.*, 568, 285-295,
905 10.1016/j.scitotenv.2016.05.205, 2016.

906 Jautzy, J. J., Ahad, J. M. E., Gobeil, C., Smirnoff, A., Barst, B. D., and Savard, M. M.: Isotopic Evidence for
907 Oil Sands Petroleum Coke in the Peace-Athabasca Delta, *Environm. Sci. Technol.*, 49, 12062-12070,
908 10.1021/acs.est.5b03232, 2015.

909 Jimenez, J. L., Canagaratna, M. R., Donahue, N. M., Prevot, A. S. H., Zhang, Q., Kroll, J. H., DeCarlo, P. F.,
910 Allan, J. D., Coe, H., Ng, N. L., Aiken, A. C., Docherty, K. S., Ulbrich, I. M., Grieshop, A. P., Robinson, A.
911 L., Duplissy, J., Smith, J. D., Wilson, K. R., Lanz, V. A., Hueglin, C., Sun, Y. L., Tian, J., Laaksonen, A.,
912 Raatikainen, T., Rautiainen, J., Vaattovaara, P., Ehn, M., Kulmala, M., Tomlinson, J. M., Collins, D. R.,
913 Cubison, M. J., E., Dunlea, J., Huffman, J. A., Onasch, T. B., Alfarra, M. R., Williams, P. I., Bower, K.,
914 Kondo, Y., Schneider, J., Drewnick, F., Borrmann, S., Weimer, S., Demerjian, K., Salcedo, D., Cottrell,
915 L., Griffin, R., Takami, A., Miyoshi, T., Hatakeyama, S., Shimono, A., Sun, J. Y., Zhang, Y. M., Dzepina,
916 K., Kimmel, J. R., Sueper, D., Jayne, J. T., Herndon, S. C., Trimborn, A. M., Williams, L. R., Wood, E. C.,
917 Middlebrook, A. M., Kolb, C. E., Baltensperger, U., and Worsnop, D. R.: Evolution of Organic Aerosols
918 in the Atmosphere, *Science*, 326, 1525-1529, 10.1126/science.1180353, 2009.

919 Johnson, M. R., Crosland, B. M., McEwen, J. D., Hager, D. B., Armitage, J. R., Karimi-Golpayegani, M., and
920 Picard, D. J.: Estimating fugitive methane emissions from oil sands mining using extractive core
921 samples, *Atmos. Environm.*, 144, 111-123, 10.1016/j.atmosenv.2016.08.073, 2016.

922 Jolliffe, I. T., and Cadima, J.: Principal component analysis: a review and recent developments,
923 *Philosophical Transactions of the Royal Society A: Mathematical, Physical and Engineering Sciences*,
924 374, 10.1098/rsta.2015.0202, 2016.

925 Kaiser, H. F.: The varimax criterion for analytic rotation in factor-analysis, *Psychometrika*, 23, 187-200,
926 10.1007/bf02289233, 1958.

927 Kindzierski, W. B., and Ranganathan, H. K. S.: Indoor and outdoor SO₂ in a community near oil sand
928 extraction and production facilities in northern Alberta, *J. Environ. Eng. Sci.*, 5, S121-S129,
929 10.1139/s06-022, 2006.

930 Lee, A. K. Y., Adam, M. G., Liggio, J., Li, S.-M., Li, K., Willis, M. D., Abbatt, J. P. D., Tokarek, T. W., Odame-
931 Ankrah, C. A., Huo, J. A., Osthoff, H. D., Strawbridge, K. B., and Brook, J. R.: A large contribution of
932 anthropogenic organonitrate to secondary organic aerosol in Alberta oil sands, in prep., 2018.

933 Li, S.-M., Leithead, A., Moussa, S. G., Liggio, J., Moran, M. D., Wang, D., Hayden, K., Darlington, A.,
934 Gordon, M., Staebler, R., Makar, P. A., Stroud, C. A., McLaren, R., Liu, P. S. K., O'Brien, J.,
935 Mittermeier, R. L., Zhang, J., Marson, G., Cober, S. G., Wolde, M., and Wentzell, J. J. B.: Differences
936 between measured and reported volatile organic compound emissions from oil sands facilities in
937 Alberta, Canada, *Proceedings of the National Academy of Sciences*, 114, E3756-E3765,
938 10.1073/pnas.1617862114, 2017.

939 Liggio, J., Li, S.-M., Hayden, K., Taha, Y. M., Stroud, C., Darlington, A., Drollette, B. D., Gordon, M., Lee, P.,
940 Liu, P., Leithead, A., Moussa, S. G., Wang, D., O'Brien, J., Mittermeier, R. L., Brook, J., Lu, G., Staebler,
941 R., Han, Y., Tokarek, T. W., Osthoff, H. D., Makar, P. A., Zhang, J., Plata, D., and Gentner, D. R.: Oil
942 Sands Operations as a Large Source of Secondary Organic Aerosols, *Nature*, 534, 91-94,
943 10.1038/nature17646, 2016.

944 Marey, H. S., Hashisho, Z., Fu, L., and Gille, J.: Spatial and temporal variation in CO over Alberta using
945 measurements from satellites, aircraft, and ground stations, *Atmos. Chem. Phys.*, 15, 3893-3908,
946 10.5194/acp-15-3893-2015, 2015.

947 Markovic, M. Z., VandenBoer, T. C., and Murphy, J. G.: Characterization and optimization of an online
948 system for the simultaneous measurement of atmospheric water-soluble constituents in the gas and
949 particle phases, *J. Environ. Monit.*, 14, 1872-1884, 10.1039/C2EM00004K, 2012.

950 Masliyah, J., Zhou, Z. J., Xu, Z. H., Czarnecki, J., and Hamza, H.: Understanding water-based bitumen
951 extraction from athabasca oil sands, *Can. J. Chem. Eng.*, 82, 628-654, 10.1002/cjce.5450820403,
952 2004.

953 McLinden, C. A., Fioletov, V., Boersma, K. F., Krotkov, N., Sioris, C. E., Veefkind, J. P., and Yang, K.: Air
954 quality over the Canadian oil sands: A first assessment using satellite observations, *Geophys. Res.
955 Lett.*, 39, 8, 10.1029/2011gl050273, 2012.

956 Miller, S. M., Matross, D. M., Andrews, A. E., Millet, D. B., Longo, M., Gottlieb, E. W., Hirsch, A. I., Gerbig,
957 C., Lin, J. C., Daube, B. C., Hudman, R. C., Dias, P. L. S., Chow, V. Y., and Wofsy, S. C.: Sources of carbon
958 monoxide and formaldehyde in North America determined from high-resolution atmospheric data,
959 *Atmos. Chem. Phys.*, 8, 7673-7696, 10.5194/acp-8-7673-2008, 2008.

960 Min, K. E., Pusede, S. E., Browne, E. C., LaFranchi, B. W., and Cohen, R. C.: Eddy covariance fluxes and
961 vertical concentration gradient measurements of NO and NO₂ over a ponderosa pine ecosystem:
962 observational evidence for within-canopy chemical removal of NO_x, *Atmos. Chem. Phys.*, 14, 5495-
963 5512, 10.5194/acp-14-5495-2014, 2014.

964 Nara, H., Tanimoto, H., Tohjima, Y., Mukai, H., Nojiri, Y., Katsumata, K., and Rella, C. W.: Effect of air
965 composition (N₂, O₂, Ar, and H₂O) on CO₂ and CH₄ measurement by wavelength-scanned cavity ring-
966 down spectroscopy: calibration and measurement strategy, *Atmos. Meas. Tech.*, 5, 2689-2701,
967 10.5194/amt-5-2689-2012, 2012.

968 Nimana, B., Canter, C., and Kumar, A.: Energy consumption and greenhouse gas emissions in the
969 recovery and extraction of crude bitumen from Canada's oil sands, *Appl. Energy*, 143, 189-199,
970 10.1016/j.apenergy.2015.01.024, 2015a.

971 Nimana, B., Canter, C., and Kumar, A.: Energy consumption and greenhouse gas emissions in upgrading
972 and refining of Canada's oil sands products, *Energy*, 83, 65-79, 10.1016/j.energy.2015.01.085, 2015b.

973 Detailed facility information: [http://www.ec.gc.ca/inrp-npri/donnees-](http://www.ec.gc.ca/inrp-npri/donnees-data/index.cfm?do=facility_information&lang=En&opt_npri_id=0000002274&opt_report_year=2013)
974 [data/index.cfm?do=facility_information&lang=En&opt_npri_id=0000002274&opt_report_year=2013](http://www.ec.gc.ca/inrp-npri/donnees-data/index.cfm?do=facility_information&lang=En&opt_npri_id=0000002274&opt_report_year=2013)
975 , access: April 13, 2017, 2013.

976 Odame-Ankrah, C. A.: Improved detection instrument for nitrogen oxide species, Ph.D., Chemistry,
977 University of Calgary, <http://hdl.handle.net/11023/2006>, Calgary, 2015.

978 Onasch, T. B., Trimborn, A., Fortner, E. C., Jayne, J. T., Kok, G. L., Williams, L. R., Davidovits, P., and
979 Worsnop, D. R.: Soot Particle Aerosol Mass Spectrometer: Development, Validation, and Initial
980 Application, *Aerosol Sci. Technol.*, 46, 804-817, 10.1080/02786826.2012.663948, 2012.

981 Paatero, P., and Tapper, U.: Positive matrix factorization: A non-negative factor model with optimal
982 utilization of error estimates of data values, *Environmetrics*, 5, 111-126,
983 doi:10.1002/env.3170050203, 1994.

984 Parajulee, A., and Wania, F.: Evaluating officially reported polycyclic aromatic hydrocarbon emissions in
985 the Athabasca oil sands region with a multimedia fate model, *Proceedings of the National Academy
986 of Sciences*, 111, 3344-3349, 10.1073/pnas.1319780111, 2014.

987 Paul, D., and Osthoff, H. D.: Absolute Measurements of Total Peroxy Nitrate Mixing Ratios by Thermal
988 Dissociation Blue Diode Laser Cavity Ring-Down Spectroscopy, *Anal. Chem.*, 82, 6695-6703,
989 10.1021/ac101441z, 2010.

990 Penner, T. J., and Foght, J. M.: Mature fine tailings from oil sands processing harbour diverse
991 methanogenic communities, *Canadian Journal of Microbiology*, 56, 459-470, 10.1139/w10-029, 2010.

992 Percy, K. E.: Ambient Air Quality and Linkage to Ecosystems in the Athabasca Oil Sands, Alberta, *Geosci.
993 Can.*, 40, 182-201, 10.12789/geocanj.2013.40.014, 2013.

994 Peters, T. M., and Leith, D.: Concentration measurement and counting efficiency of the aerodynamic
995 particle sizer 3321, *J. Aerosol Sci.*, 34, 627-634, 10.1016/s0021-8502(03)00030-2, 2003.

996 Quagraine, E. K., Headley, J. V., and Peterson, H. G.: Is biodegradation of bitumen a source of recalcitrant
997 naphthenic acid mixtures in oil sands tailing pond waters?, *J. Environ. Sci. Health Part A-Toxic/Hazard.
998 Subst. Environ. Eng.*, 40, 671-684, 10.1081/ese-200046637, 2005.

999 Rooney, R. C., Bayley, S. E., and Schindler, D. W.: Oil sands mining and reclamation cause massive loss of
1000 peatland and stored carbon, *Proc. Natl. Acad. Sci. U.S.A.*, 109, 4933-4937, 10.1073/pnas.1117693108,
1001 2012.

1002 RStudio Boston, M.: Integrated development environment for R, 2017.

1003 Shahimin, M. F. M., and Siddique, T.: Sequential biodegradation of complex naphtha hydrocarbons
1004 under methanogenic conditions in two different oil sands tailings, *Environ. Pollut.*, 221, 398-406,
1005 10.1016/j.envpol.2016.12.002, 2017.

1006 Siddique, T., Fedorak, P. M., and Foght, J. M.: Biodegradation of short-chain n-alkanes in oil sands
1007 tailings under methanogenic conditions, *Environ. Sci. Technol.*, 40, 5459-5464, 10.1021/es060993m,
1008 2006.

1009 Siddique, T., Gupta, R., Fedorak, P. M., MacKinnon, M. D., and Foght, J. M.: A first approximation kinetic
1010 model to predict methane generation from an oil sands tailings settling basin, *Chemosphere*, 72,
1011 1573-1580, 10.1016/j.chemosphere.2008.04.036, 2008.

1012 Siddique, T., Penner, T., Semple, K., and Foght, J. M.: Anaerobic Biodegradation of Longer-Chain n-
1013 Alkanes Coupled to Methane Production in Oil Sands Tailings, *Environm. Sci. Technol.*, 45, 5892-5899,
1014 10.1021/es200649t, 2011.

1015 Siddique, T., Penner, T., Klassen, J., Nesbo, C., and Foght, J. M.: Microbial Communities Involved in
1016 Methane Production from Hydrocarbons in Oil Sands Tailings, *Environ. Sci. Technol.*, 46, 9802-9810,
1017 10.1021/e53022024, 2012.

1018 Simpson, I. J., Blake, N. J., Barletta, B., Diskin, G. S., Fuelberg, H. E., Gorham, K., Huey, L. G., Meinardi, S.,
1019 Rowland, F. S., Vay, S. A., Weinheimer, A. J., Yang, M., and Blake, D. R.: Characterization of trace
1020 gases measured over Alberta oil sands mining operations: 76 speciated C₂-C₁₀ volatile organic
1021 compounds (VOCs), CO₂, CH₄, CO, NO, NO₂, NO_y, O₃ and SO₂, *Atmos. Chem. Phys.*, 10, 11931-11954,
1022 10.5194/acp-10-11931-2010, 2010.

1023 Small, C. C., Cho, S., Hashisho, Z., and Ulrich, A. C.: Emissions from oil sands tailings ponds: Review of
1024 tailings pond parameters and emission estimates, *Journal of Petroleum Science and Engineering*, 127,
1025 490-501, 10.1016/j.petrol.2014.11.020, 2015.

1026 Thurston, G. D., and Spengler, J. D.: A quantitative assessment of source contributions to inhalable
1027 particulate matter pollution in metropolitan Boston, *Atmos. Environ.*, 19, 9-25, 10.1016/0004-
1028 6981(85)90132-5, 1985.

1029 Thurston, G. D., Ito, K., and Lall, R.: A source apportionment of U.S. fine particulate matter air pollution,
1030 Atmos. Environ., 45, 3924-3936, 10.1016/j.atmosenv.2011.04.070, 2011.

1031 Tokarek, T. W., Huo, J. A., Odame-Ankrah, C. A., Hammoud, D., Taha, Y. M., and Osthoff, H. D.: A gas
1032 chromatograph for quantification of peroxy-carboxylic nitric anhydrides calibrated by thermal
1033 dissociation cavity ring-down spectroscopy, Atmos. Meas. Tech., 7, 3263-3283, 10.5194/amt-7-3263-
1034 2014, 2014.

1035 Tokarek, T. W., Brownsey, D. K., Jordan, N., Garner, N. M., Ye, C. Z., Assad, F. V., Peace, A., Schiller, C. L.,
1036 Mason, R. H., Vingarzan, R., and Osthoff, H. D.: Biogenic Emissions and Nocturnal Ozone Depletion
1037 Events at the Amphitrite Point Observatory on Vancouver Island, Atmosphere-Ocean, 1-12,
1038 10.1080/07055900.2017.1306687, 2017.

1039 Wang, S. C., and Flagan, R. C.: Scanning electrical mobility spectrometer, Aerosol Sci. Technol., 13, 230-
1040 240, 10.1080/02786829008959441, 1990.

1041 Wang, X. L., Chow, J. C., Kohl, S. D., Percy, K. E., Legge, A. H., and Watson, J. G.: Characterization of
1042 PM_{2.5} and PM₁₀ fugitive dust source profiles in the Athabasca Oil Sands Region, J. Air Waste Manag.
1043 Assoc., 65, 1421-1433, 10.1080/10962247.2015.1100693, 2015.

1044 Wang, X. L., Chow, J. C., Kohl, S. D., Percy, K. E., Legge, A. H., and Watson, J. G.: Real-world emission
1045 factors for Caterpillar 797B heavy haulers during mining operations, Particuology, 28, 22-30,
1046 10.1016/j.partic.2015.07.001, 2016.

1047 Warren, L. A., Kendra, K. E., Brady, A. L., and Slater, G. F.: Sulfur Biogeochemistry of an Oil Sands
1048 Composite Tailings Deposit, Front. Microbiol., 6, 14, 10.3389/fmicb.2015.01533, 2016.

1049 Watson, J., Chow, J., Wang, X., Zielinska, B., Kohl, S., and Gronstal, S.: Characterization of real-world
1050 emissions from nonroad mining trucks in the Athabasca Oil Sands Region during September, 2009,
1051 2013.

1052 WBEA: WBEA annual report 2013, Wood Buffalo Environmental Association, 2013.

1053 Whaley, C., Makar, P. A., Shephard, M. W., Zhang, L., Zhang, J., Zheng, Q., Akingunola, A., Wentworth, G.
1054 R., Murphy, J. G., Kharol, S. K., and Cady-Pereira, K. E.: Contributions of natural and anthropogenic
1055 sources to ambient ammonia in the Athabasca Oil Sands and north-western Canada, Atmos. Chem.
1056 Phys., 18, 2011-2034, 10.5194/acp-18-2011-2018, 2017.

1057 Williams, B. J., Goldstein, A. H., Kreisberg, N. M., and Hering, S. V.: An in-situ instrument for speciated
1058 organic composition of atmospheric aerosols: Thermal Desorption Aerosol GC/MS-FID (TAG), Aerosol
1059 Sci. Technol., 40, 627-638, 10.1080/02786820600754631, 2006.

1060 Wilson, N. K., Barbour, R. K., Chuang, J. C., and Mukund, R.: Evaluation of a real-time monitor for fine
1061 particle-bound PAH in air, Polycycl. Aromat. Compd., 5, 167-174, 10.1080/10406639408015168,
1062 1994.

1063 Yeh, S., Jordaan, S. M., Brandt, A. R., Turetsky, M. R., Spatari, S., and Keith, D. W.: Land Use Greenhouse
1064 Gas Emissions from Conventional Oil Production and Oil Sands, Environm. Sci. Technol., 44, 8766-
1065 8772, 10.1021/es1013278, 2010.

1066 Zhang, Y., Wang, Y., Chen, G., Smeltzer, C., Crawford, J., Olson, J., Szykman, J., Weinheimer, A. J., Knapp,
1067 D. J., Montzka, D. D., Wisthaler, A., Mikoviny, T., Fried, A., and Diskin, G.: Large vertical gradient of
1068 reactive nitrogen oxides in the boundary layer: Modeling analysis of DISCOVER-AQ 2011
1069 observations, J. Geophys. Res.-Atmos., 121, 1922-1934, 10.1002/2015jd024203, 2016.

1070

1071

1 **Supplementary information for**
2 **Principal component analysis of summertime ground site measurements in the Athabasca oil sands:**
3 **Sources of IVOCs**
4

5 Travis W. Tokarek¹, Charles A. Odame-Ankrah¹, Jennifer A. Huo¹, Robert McLaren², Alex K. Y. Lee^{3, 4},
6 Max G. Adam⁴, Megan D. Willis⁵, Jonathan P. D. Abbatt⁵, Cristian Mihele⁶, Andrea Darlington⁶,
7 Richard L. Mittermeier⁶, Kevin Strawbridge⁶, Katherine L. Hayden⁶, Jason S. Olfert⁷, Elijah. G. Schnitzler⁸,
8 Duncan K. Brownsey¹, Faisal V. Assad¹, Gregory R. Wentworth^{5, a}, Alex G. Tevlin⁵, Douglas E. J. Worthy⁶,
9 Shao-Meng Li⁶, John Liggio⁶, Jeffrey R. Brook⁶, and Hans D. Osthoff^{1*}

10
11 [1] Department of Chemistry, University of Calgary, Calgary, Alberta, T2N 1N4, Canada
12 [2] Centre for Atmospheric Chemistry, York University, Toronto, Ontario M3J 1P3, Canada
13 [3] Department of Civil and Environmental Engineering, National University of Singapore, Singapore
14 117576, Singapore.
15 [4] NUS Environmental Research Institute, National University of Singapore, Singapore
16 [5] Department of Chemistry, University of Toronto, Toronto, Ontario, M5S 3H6, Canada
17 [6] Air Quality Research Division, Environment and Climate Change Canada, Toronto, Ontario, M3H 5T4,
18 Canada
19 [7] Department of Mechanical Engineering, University of Alberta, Edmonton, Alberta, T6G 1H9, Canada
20 [8] Department of Chemistry, University of Alberta, Edmonton, Alberta, T6G 2G2, Canada
21 [a] Now at: Environmental Monitoring and Science Division, Alberta Environment and Parks, Edmonton,
22 Alberta, T5J 5C6, Canada
23 * Corresponding author

24

Table of contents

25 Descriptions of instrumentation used..... pp. 3 -

26 [56](#)

27 [Figure S-1. Scatter of ions as a function of retention time for bitumen and ambient air..... pg. 4](#)

28 Determination of optimum PCA solution..... pp. ~~6~~[7](#) -

29 ~~11~~[12](#)

30 Discussion of low eigenvalue components..... pp. ~~10~~[13](#) -

31 ~~16~~[17](#)

32 Bivariate polar plots..... pp. ~~18~~[7](#) -

33 ~~19~~[18](#)

34 Figure S-~~21~~[21](#). Scree plot..... pg.

35 ~~19~~[18](#)

36 Table S-1. Ionimed Analytical GCU standard..... pg.

37 ~~19~~[20](#)

38 Table S-2. The component pattern after Varimax rotation pg.

39 ~~20~~[21](#)

40 Table S-3. The pattern after Varimax rotation with 5 components selected pg.

41 ~~21~~[22](#)

42 Table S-4. The pattern after Varimax rotation with 6 components selected..... pg.

43 ~~22~~[23](#)

44 Table S-5. The pattern after Varimax rotation with 7 components selected..... pg.

45 ~~23~~[24](#)

46 Table S-6. The pattern after Varimax rotation with 8 components selected..... pg.

47 ~~24~~[25](#)

48 Table S-7. The pattern after Varimax rotation with 9 components selected..... pg.

49 ~~25~~[26](#)

50 Table S-8. The pattern after Varimax rotation with 11 components selected..... pg.

51 ~~26~~[27](#)

52 Table S-9. The pattern with mixing height included after Varimax rotation with 10 components ... pg.

53 ~~27~~[28](#)

54 Table S-10. Criteria for number of components extracted by PCA..... pg. ~~28~~[29](#)

55 Table S-11. Association of IVOCs with relevant components..... pg.

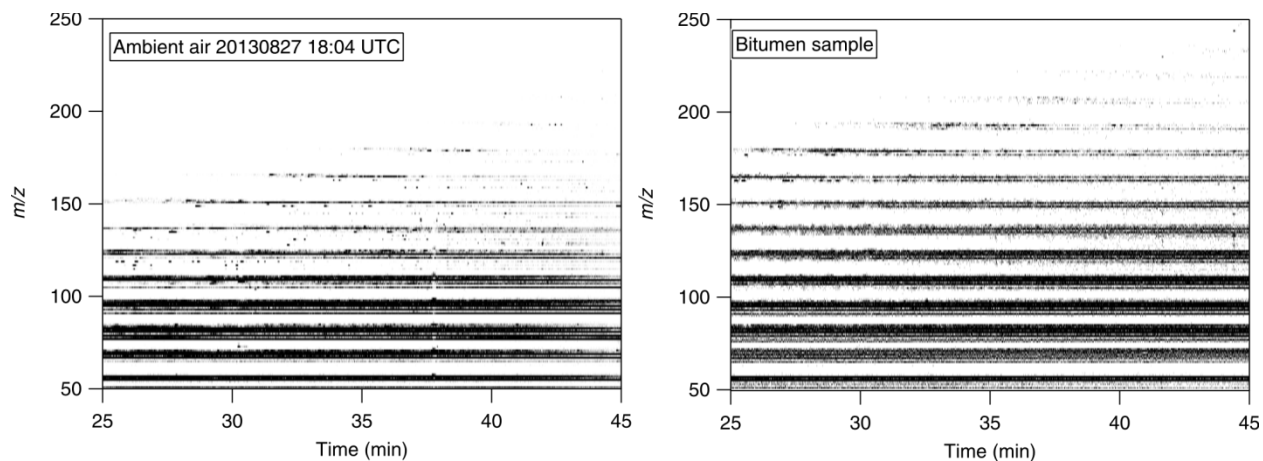
56	2829	
57	Figure S- 32 . Bivariate polar plots associated with component 1.....	pg.
58	2930	
59	Figure S- 43 . Bivariate polar plots associated with component 2.....	pg.
60	3031	
61	Figure S- 54 . Bivariate polar plots associated with component 3.....	pg.
62	3132	
63	Figure S- 65 . Bivariate polar plots associated with component 4.....	pg.
64	3233	
65	Figure S- 76 . Bivariate polar plots associated with component 5.....	pg.
66	3334	
67	Figure S- 87 . Bivariate polar plots associated with component 6.....	pg.
68	3435	
69	Figure S- 89 . Bivariate polar plots associated with component 7.....	pg.
70	3435	
71	Figure S- 910 . Bivariate polar plots associated with component 8.....	pg.
72	3536	
73	Figure S- 1011 . Bivariate polar plots associated with component 9.....	pg.
74	3536	
75	Figure S- 1112 . Bivariate polar plots associated with component 10.....	pg.
76	3637	
77	References.....	pp. 3638 -
78	3940	

79 Descriptions of instrumentation used

80 A Griffin 450 gas chromatograph equipped with a cylindrical ion trap mass spectrometer and electron
81 impact ionization (GC-ITMS) was used to quantify selected VOCs including o-xylene, decane, undecane,
82 1,2,3- and 1,2,4-trimethylbenzene (TMB), and several monoterpenes (i.e., α -pinene, β -pinene and
83 limonene). Operation, calibration and performance of this instrument have been described elsewhere
84 (Tokarek et al., 2017; Liggio et al., 2016). The GC-ITMS sampled from a 3.6 m long stainless steel inlet
85 with an o.d. of 0.635 cm from a height of 5 m above ground. A 1 m long section of the inlet was heated
86 to 110 °C and optimized to remove interference due to O₃ while avoiding decomposition of alkenes
87 (Tokarek et al., 2017). The GC oven was programmed as follows: hold at 40 °C for 3.00 min, heat at 1.5 °
88 C min⁻¹ to 70 °C (reached at 23.00 min), heat at 5 °C min⁻¹ to 200 °C (reached at 49.00 min) and hold for 4
89 min (total 53.00 min). This was followed by a 5 min recovery time to allow the oven and pre-
90 concentration trap to cool back to 40 °C. The ion trap mass spectrometer was set to an m/z range of 50-
91 425. After data reduction, the GC-ITMS generated 10-minute average concentrations of each VOC
92 quantified every hour.

93 During the campaign, the GC-ITMS was calibrated in the field using an IONICON VOC standard (Table S-
94 1) containing (in addition to VOCs that the GC-ITMS did not detect) α -pinene and o-xylene at mixing
95 ratios of ~ 1 ppmv and an uncertainty of 5% and 6%, respectively. A commercial calibrator assembly
96 (IONICON, GCU Standard) was used to deliver diluted calibration mixtures. The instrument responses to
97 the VOC standards were highly linear ($R^2 > 0.99$). The GC-ITMS was calibrated for other VOCs offline
98 relative to α -pinene. In the field, there was no noticeable carry-over (i.e., memory effects) of IVOCs,
99 which was occasionally evaluated by flooding the inlet with purified, VOC-free air.

100 Matrices of ions plotted against retention times for the total ion chromatograms (shown in Figure 2 in
101 the main manuscript) are shown in Fig. S-1. In both cases, the greatest intensity is with masses are
102 associated with alkanes (i.e., m/z 55, 57, 67, 69, etc.).



103 Figure S-1. Scatter of ions as a function of retention time for the total ion chromatograms shown in
 104 Figure 2 of the main manuscript. Darker pixels represent a higher intensity than lighter pixels.

106
 107 Mixing ratios of carbon monoxide (CO), carbon dioxide (CO₂) and methane (CH₄) in ambient air were
 108 quantified using a commercial cavity ring-down spectrometer (Picarro G2401) (Chen et al., 2013; Nara et
 109 al., 2012). Ambient air was sampled from a height of 10 m through 0.635 cm outer diameter (o.d.)
 110 perfluoroalkoxyalkane (PFA) Teflon™ tubing and a 47 mm diameter, 1 μm pore filter at a flow rate of
 111 ~0.5 L min⁻¹. A scrubber (MgClO₄) was installed at the base of the sample line to remove water from the
 112 air. Operating procedures developed for Canada's greenhouse gas network of monitors across all
 113 stations in Canada by the Climate Division of ECCC were followed (ECCC, 2013b).

114 The cavity ring-down spectrometer was calibrated every few days with calibrated standard gas mixtures
 115 (Scott-Marrin); a target background mixture (CO₂ at a mixing ratio of 379.5 parts-per-million by volume
 116 (ppmv), CH₄ at 1.976 ppmv and CO at 198.4 parts-per-billion by volume (ppbv)) and a working mixture
 117 (CO₂ = 452.15 ppmv, CH₄ = 2.988 ppmv, CO = 494.5 ppbv). The estimated precision of 1 min data was
 118 ±0.12 ppmv, ±0.6 ppbv, and ±1.89 ppbv for CO₂, CH₄ and CO respectively, while the estimated accuracy
 119 was < 1 ppmv, < 3 ppbv, and < 4 ppbv, respectively.

120 Mixing ratios of total odd nitrogen (NO_y ≡ NO + NO₂ + ΣPAN + ΣAN + HNO₃ + HONO + 2N₂O₅ + ClNO₂ + ...)

121 were measured by a chemiluminescence analyzer equipped with a heated Molybdenum converter
122 (Thermo 42i) as described elsewhere (Tokarek et al., 2014; Odame-Ankrah, 2015).

123 The total sulfur (TS) measurements were conducted using a thermal oxidizer (Thermo Scientific Model
124 CON101) to convert TS to SO₂ and detected using a pulsed-fluorescence analyzer (Thermo Scientific,
125 Model 43iTLE). SO₂ was measured directly with a second analyzer (Thermo Scientific, Model 43iTLE).
126 Total reduced sulfur (TRS) mixing ratios were calculated by subtracting mixing ratios of SO₂ from TS.

127 Concentrations of particle-surface bound polycyclic aromatic hydrocarbons (pPAH) were measured using
128 a photoelectric aerosol sensor (EcoChem Analytics, Model PAS 2000CE) (Wilson et al., 1994; Burtscher et
129 al., 1982).

130 Two soot-particle aerosol mass spectrometers (SP-AMS, Aerodyne Research, Inc.) (Onasch et al., 2012)
131 measured non-refractory PM₁ components. Both SP-AMS were high resolution time-of-flight aerosol
132 mass spectrometers (HR-ToF-AMS) fitted with a diode pumped Nd:YAG 1064 nm laser vaporizer; one SP-
133 AMS had its oven removed to measure black carbon containing particles only using the laser. Direct
134 calibrations of rBC using mono-disperse "Regal Black" (Cabot Corp. R400) particles were carried out
135 three times during the 2013 JOSM intensive study. Positive Matrix Factorization (PMF) was performed to
136 identify the potential sources of organic aerosol as described in the companion study (Adam et al., in
137 prep). Factors associated with primary aerosol, i.e., hydrocarbon-like organic aerosol (HOA), a less
138 oxidized oxygenated organic aerosol factor (LO-OOA) and measured refractory black carbon (rBC) were
139 added as variables for PCA analysis. Mass spectra associated with LO-OOA exhibited H/C, O/C and N/C
140 ratios of ~1.62, ~0.36, and ~0.004, respectively; while the O/C and N/C ratios are similar to HOA, the H/C
141 ratio of LO-OOA more resembles the more oxidized OOA factor (MO-OOA) (Adam et al., in prep.).

142 Particle volumes were calculated (assuming spherical particle shapes) from sub- and super-micron size
143 distributions acquired using a scanning mobility particle sizer (SMPS, TSI with a differential mobility

144 analyzer model 3081 and condensation particle counter model 3776; PM₁) and a 0.071 cm impactor
145 over the size range of 13.6 nm to 736.5 nm and an Aerodynamic Particle Sizer (APS, TSI 3321; PM₁₀₋₁)
146 over the size range 1.04 μm to 10.4 μm, respectively. Both instruments were operated at ambient
147 relative humidity. The SMPS sampled through conductive silicon tubing to minimize wall losses due to
148 wall charges. The APS was operated from a container located on top of the trailer and sampled from a
149 1.6 m tall, ½ o.d. aluminum tube whose tip was bent into a U-shape.

150 An ambient ion monitor – ion chromatograph (AIM-IC) (Markovic et al., 2012) was used to measure
151 hourly averaged gas-phase NH₃ and PM_{2.5} particle-phase (i.e., of particles < 2.5 μm diameter) NH₄⁺
152 concentrations. High time-resolution particle-phase NH₄⁺ measurements made by the SP-AMS were
153 scaled by interpolated phase ratios observed by AIM-IC to calculate gas-phase NH₃ concentrations at
154 high time resolution. This approach assumes the same phase ratios for PM_{2.5} as for PM₁.

155

156 **Determination of optimum PCA solution**

157 The full component pattern (before component removal, with rotation, i.e., showing 22 components for
158 22 variables) obtained for this data set is shown in Table S-2. A common challenge in PCA is the
159 determination of the maximum number of components to retain in the analysis. Several criteria are
160 used for this purpose: the latent root criterion, where only components with eigenvalues greater than 1
161 are considered significant, the 5% variance criterion, where the last component selected accounts for
162 only a small portion (<5%) of the variance, the 95% cumulative percentage of variance criterion, where
163 the extracted components account for at least 95% of the total variance, and the Scree test. In the
164 latter, the eigenvalues are plotted against the number of components in the order of extraction (Fig. S-
165 [12](#)); to avoid including too many components with unique variance, the number of acceptable
166 components is located at the point where this plot becomes horizontal. The latent root criterion is most
167 commonly used, but tends to extract too few components when the number of variables is < 20 (Hair et
168 al., 1998). The Scree test, on the other hand, often requires "some art in administering it" (Cattell, 1966),
169 i.e., is subjective, though generally results in the inclusion of two or three more components than the
170 latent root criterion (Hair et al., 1998).

171 The maximum component number for each criterion are summarized in Table S-9. The Scree test plot
172 (Fig. S-1) shows two plateaus where the slope becomes approximately horizontal: The first is located at
173 N = 5 and the second at N = 12. The latent root criterion and the <5% variance method suggests a 7-
174 component solution, whereas the >95% percentage of variance criterion suggests using a 10-component
175 solution. Hair et al. (1998) recommend to examine component solutions with differing numbers of
176 components to evaluate which best represents the structure of the variables. In the following, solutions
177 are presented in ascending order of extracted components.

178

179

180 5-component solution

181 As a first attempt at interpretation of the PCA, the first cut-off of the Scree test criterion was chosen (N
182 = 5 variables). The results (after Varimax rotation) are presented in Table S-3.

183 The 5-component solution accounts for a cumulative variance of 81.0 % after rotation. Communalities
184 for the analysis, i.e., the fraction of total pollutant observations accounted for by the PCA (Otto, 2007),
185 are greater than 70% for 18 variables. The lowest communalities were obtained for gas-phase ammonia
186 (0.40), CO (0.48) and PM₁₀₋₁ (0.51). TRS and the IVOCs were also relatively poorly represented (0.63 and
187 0.73, respectively). All eigenvalues are greater than 1.

188 The component accounting for most of the variance of the data, component 1, is strongly associated
189 with all of the anthropogenic VOCs (with correlations of $r > 0.8$) and TRS ($r = 0.76$), moderateweakly
190 associated with CH₄ ($r = 0.62$), HOA ($r = 0.44$), LO-OOA ($r = 0.59$), IVOCs ($r = 0.47$), and CO ($r = 0.53$), and
191 weakpoorly associated with NO_y and TS ($r = 0.25$ and $r = 0.28$, respectively). Component 1 is consistent
192 with tailings ponds emissions with potentially small contributions from nearby facilities (interpreted
193 from moderateweak and weakpoor correlations with rBC ($r = 0.33$) and NO_y ($r = 0.25$)), which would
194 otherwise remain unexplained. Component 2 is strongly associated with the combustion tracers NO_y ($r =$
195 0.83), rBC ($r = 0.89$) and pPAH ($r = 0.83$) and moderateweakly associated with IVOCs ($r = 0.61$), gas-phase
196 ammonia ($r = 0.34$), undecane ($r = 0.31$), and CH₄ (0.38), but weakpoorly and not significantly with CO or
197 CO₂ ($r = 0.19$ and 0.06 , respectively); this component is identified as mine fleet emissions. Component 3
198 is strongly associated ($r > 0.9$) with the biogenic VOCs and moderateweakly ($r = 0.55$) associated with
199 CO₂ and is identified as a biogenic component. Component 4 is strongly associated with SO₂ and TS ($r =$
200 0.93 and 0.91 , respectively) and is consistent with emissions from upgrader facilities. These four
201 components persisted, with little variation, in all solutions with a greater number of selected
202 components (see below).

203 Component 5 is strongly associated with CO₂ ($r = 0.71$), and moderateweakly associated with PM₁₀₋₁ ($r =$

204 0.57), CH₄ (r = 0.53) and CO (r = 0.40). We are not aware of a source type that would fit this profile, i.e.,
205 combine this particular set of pollutants without also being associated with NO_y (r = 0.02). This suggests
206 that this component is an artifact arising from an insufficient number of components used in the
207 analysis and motivates the inclusion of more components.

208

209 **6-component solution**

210 A 6-component solution is shown in Table S-4. Satisfying the percentage of variance criterion of the last
211 component accounting for less than 5% of the variance (4.6% in this case, Table S-2) was selected.

212 This solution accounts for a total variance of 85.23%. The first four components are essentially
213 unchanged from the 5-component solution (with the exception of LO-OOA in component 2 becoming
214 more weakpoorly correlated (r = 0.22)). Component 5 is strongly associated with IVOCs (r = 0.70) and
215 moderateweakly associated with LO-OOA (r = 0.60), and TRS (r = 0.56). Component 6 is strongly
216 associated with PM₁₀₋₁ (r = 0.81) and moderateweakly associated with CO₂ (r = 0.62), CH₄ (r = 0.41), HOA
217 (r = 0.30) and NH₃ (r = 0.36) and, unlike the 5-component solution, not associated with CO.

218

219 **7-component solution**

220 Next, the latent root criterion gives a 7-component solution. The PCA results (after Varimax rotation) are
221 presented in Table S-5. The seven components account for a cumulative variance of 88.7% after
222 rotation. Communalities for the analysis are all greater than 60%, with the lowest communality obtained
223 for CO (0.61). All eigenvalues are greater than 1.

224 Components 1 through 4 have the same associations with similar r values as those in the 5-component
225 analysis, with the only significant exception a weakpoorer association (r = 0.20) of component 2 with
226 gas-phase ammonia.

227 The identifications of components 5 through 7 of the 7-component solution are murky at best.

228 Component 5 is moderateweakly associated with TRS ($r = 0.56$) and IVOCs ($r = 0.66$). Component 6 is
229 strongly associated with PM_{10-1} volume ($r = 0.89$), and moderateweakly with CO_2 ($r = 0.54$), and CH_4 ($r =$
230 0.36) and appears to be combination of a dust component with a source of greenhouse gases, whereas
231 component 7 is strongly associated with gas-phase ammonia ($r = 0.82$) and weakpoorly associated with
232 CO ($r = 0.29$). Both appear to be amalgamations of distinct sources and suggest that too few
233 components were selected. Hair et al. (1998) note that the latent root criterion has a tendency to
234 extract a conservative number of components if the number of variables is < 20 , close to the 22
235 variables in this analysis, consistent with what is observed here. Hence, the 7-component solution is
236 sub-optimal.

237

238 **8-component solution**

239 An 8-component solution is presented in Table S-6. Not satisfying any criterion, it is included here for
240 the sake of completeness. Owing to the inclusion of an additional component, the cumulative variance
241 improved to 91.6%. The greatest improvement was seen for CO, gas-phase ammonia, as well as the
242 IVOCs, whose communalities increased from 0.61, 0.91, and 0.80 (for the 7-component solution) to 0.96,
243 0.96 and 0.84, respectively.

244 The main effect of the inclusion of an additional component was the separation of component 7 into
245 two distinct components: one of these was strongly associated with gas-phase ammonia ($r = 0.92$), and
246 the other was strongly associated with CO ($r = 0.85$). A considerable fraction of the CO observed in the
247 region is generated as a byproduct of the photochemical oxidation of hydrocarbons (Shephard et al.,
248 2015); component 8 appears to capture this source, whereas component 1 captures the anthropogenic
249 emissions. The area near the oil sands mining operations is enriched in ammonia, which originates from
250 multiple sources: it is used as a floating agent to separate and recover bitumen from tar and is
251 generated during bitumen upgrading (called hydrotreating) in which N is removed as NH_3 , and can be

252 present as a contaminant in tailing ponds. Other sources, such as agricultural activities, biological decay
253 processes, and smoldering fires are relatively minor in the region (Bytnerowicz et al., 2010). The
254 weakpoor association of component 2 with ammonia ($r = 0.22$) may capture the use of ammonia as a
255 floating agent, whereas component 8 embodies the remaining sources.

256 Component 5 is strongly associated with IVOCs ($r = 0.71$), and moderateweakly associated with LO-
257 OOA($r = 0.65$) and TRS ($r = 0.40$). It is unclear if these variables originate from the same source or are
258 forced together as a result of having chosen too few components. Considering that component 7 is split
259 when an additional component is used (see below), the latter is more likely. Component 6 remains
260 strongly associated with PM_{10-1} volume ($r = 0.89$), and moderateweakly associated with CO_2 ($r = 0.53$),
261 and CH_4 ($r = 0.35$) and is difficult to interpret. Because of the unclear classification of components 5
262 through 8, the 8-component solution is rejected.

263

264 **9-component solution**

265 A 9-component solution is presented in Table S-7. Components 1 through 8 describe sources that are
266 qualitatively similar to those provided by the 8-component solution. Component 9 is strongly associated
267 with TRS ($r = 0.71$) and weakpoorly associated with o-xylene ($r = 0.30$); its profile is consistent with
268 tailings ponds emission, where the presence of naphtha as a diluent gives rise to BTEX emissions and
269 bacteria produce reduced sulfur compounds (Small et al., 2015; Warren et al., 2016). Component 6 is
270 strongly associated with PM_{10-1} ($r = 0.89$) and moderateweakly associated with CO_2 ($r = 0.54$) and CH_4 ($r =$
271 0.41). We have decided to reject this solution on the basis that $< 95\%$ cumulative variance is observed.

272

273 **10-component solution**

274 Next, a 10-component solution with cumulative variance of 95.5%, satisfying the 95% criterion, was
275 considered. With this solution, all communalities are >0.85 (Table 3). Component 6 is strongly associated

276 with CO₂ (r = 0.77) and moderateweakly associated with CH₄ (r = 0.59) but is not associated with other
277 combustion tracers and is identified as inactive open-pit mines (see main text). Component 7 is strongly
278 correlated with PM₁₀₋₁ (r = 0.93) and is identified as wind-blown dust. Component 8 and 9 are strongly
279 associated with a single variable each, gas-phase ammonia (r = 0.94) and CO (r = 0.87), respectively.
280 Component 10 is strongly associated with TRS (r = 0.71) and moderateweakly associated with o-xylene (r
281 = 0.32). Overall, this component is most consistent with a tailings ponds source, where the presence of
282 naphtha as diluent gives rise to BTEX emissions, and sulfur-reducing bacteria are at work (Small et al.,
283 2015; Warren et al., 2016). Overall, the 10-component solution was judged to be optimal.

284

285 **11-component solution**

286 The 11-component analysis is presented in Table S-8. Component 10 is now strongly associated with LO-
287 OOA (r = 0.72) and moderateweakly with rBC (r = 0.34), and has a low eigenvalue of 0.87. This solution is
288 therefore rejected as we believe it contains too many components.

289

290 **Discussion of low-eigenvalue components**

291

292 **Component 6: A non-combustion source of CO₂ and CH₄**

293 Component 6 of the analysis has a strong association with the greenhouse gases CO₂ (r = 0.77) and a
294 ~~moderate~~weak association with CH₄ (r = 0.59) but is not associated with tracers of combustion (i.e., NO_y,
295 pPAH, rBC) or naphtha (i.e., anthropogenic VOCs).

296 A significant amount of carbon is stored in bitumen, which, on geological time scales, conduces
297 formation of CO₂ and CH₄ (i.e., natural gas) reservoirs and pools. When bitumen is mined, substantial
298 emissions of CO₂ and, in particular, of CH₄ occur (Johnson et al., 2016). It is unclear, though, to what
299 extent these greenhouse gases are released from "hot spots" (i.e., from a small number of locations)
300 through surface cracks and fissures in the mine faces, or from new material that is exposed and then
301 releases greenhouse gases during material handling, transport and processing (Johnson et al., 2016). The
302 PCA analysis presented here would be more consistent with the "hot spots" hypothesis since
303 component 6 is not associated with NO_y, PAHs, or CO, which are expected to be emitted by the Diesel
304 machinery involved in surface mining (i.e., active disturbance of the bitumen).

305 Another potential source contribution to component 6 is the degradation of peat and surface soil.
306 Peatland soils, as they occur in the boreal forest surrounding the AMS 13 site, have long been
307 recognized as important contributors to greenhouse gas fluxes and may also be contributing to
308 component 6 (Miller et al., 2014; Gorham, 1991; Warner et al., 2017). The fixation and/or release of CO₂
309 as well as consumption and/or production of CH₄ through root, anaerobic and aerobic microbial
310 respiration are dependent on soil conditions such as water table position, temperature, soil pH, and
311 plant community composition (Yavitt et al., 2005; Oertel et al., 2016; Whalen, 2005). Emissions from
312 peat and surface soil that was stripped as part of surface mining is expected to release between

313 1.1×10^{10} and 4.7×10^{10} kg stored carbon (Rooney et al., 2012), though it is unclear on what time scale this
314 release will occur. Some of this historical peat material is used for land reclamation. However, a
315 preliminary assessment of greenhouse gas fluxes from such a site gave no indication of significant
316 emissions, at least in the short term (Nwaishi et al., 2016). The bivariate polar plot shows that
317 component 6 is associated with no particular wind direction but with relatively low wind speeds ($<$
318 1.5 m/s; Figure S-7C), consistent with a dispersed surface source. Further, when variables associated
319 with secondary processes were added to the analysis (Table 7), component 6 anticorrelates with O_x ($r = -$
320 0.41). Dry deposition is a significant O_3 and NO_2 , and therefore O_x , loss process (Wesely and Hicks, 2000;
321 Zhang et al., 2002).

322 Overall, we have too little information to constrain soil fluxes for this data set. Considering the large CH_4
323 and CO_2 concentrations observed in this study, it is more likely that anthropogenic sources dominate
324 over natural soil emissions (Thompson et al., 2017). Future field campaigns at AMS 13 would benefit
325 from N_2O measurements to constrain contributions of natural sources to greenhouse gas
326 concentrations, such as those produced by microbes in water-logged soil.

327

328 **Component 7: Wind-blown dust**

329 Component 7 is correlated with PM_{10-1} ($r = 0.93$) and, weakpoorly, with CO_2 ($r = 0.25$), CH_4 ($r = 0.11$),
330 HOA ($r = 0.23$), and LO-OOA ($r = 0.25$). In the Athabasca oil sands region, surface mining has created
331 large portions of land whose surface is void of vegetation and is covered by sand and soil particles,
332 which are readily suspended by wind and vehicle traffic. Other mining activities add to the PM_{10-1}
333 emissions, including combustion processes, tailings sands, and mine haul roads, though the
334 contributions of each of these to the overall PM_{10-1} burden is uncertain (Wang et al., 2015). Recently,
335 Phillips-Smith et al. investigated metal species found in $PM_{2.5}$ aerosol at AMS 13 and found haul road

336 dust and soil from mine faces to be important sources of PM_{2.5} (Phillips-Smith et al., 2017) and, likely,
337 PM₁₀₋₁ as well. The very **weakpoor** associations of this component with CO₂ and CH₄ and lack of
338 association with NO_y (r = 0.02) suggest contributions of open mine face soil in addition to dust
339 suspended by vehicles travelling on unpaved roads.

340 The size range captured by PM₁₀₋₁ may also include bioaerosol, including bacteria, fungal spores and
341 plant pollen, which constitute the "natural" background aerosol over vegetated continental regions,
342 typically contributing a few µg m⁻³ of aerosol mass (Huffman et al., 2010). Considering the large PM₁₀₋₁
343 volumes observed in this work (Table 3), the contribution of bioaerosol is likely minor.

344

345 **Component 8: Ammonia**

346 Component 8 is a single variable component strongly associated with NH₃ (r = 0.94) but with no other
347 variables: the second largest correlation coefficient is that of rBC (r = 0.13).

348 Bytnerowicz et al. (2010) reported larger concentrations of NH₃ in the oil sands region than the
349 provincial average. More recently, Shephard et al. (2015) reported enhancements of NH₃ in the general
350 area as judged from satellite observations. Both studies hence suggest the existence of anthropogenic
351 sources, though Shephard et al. (2015) speculated that biomass burning can contribute to the ammonia
352 burden in the region. A recent modelling study by Whaley et al. (2017) estimated that around half of
353 near-surface NH₃ during the study was likely from bi-directional exchange (i.e., re-emission from soil and
354 plants).

355 In the oil sands, NH₃ is used as a floating agent for the separation and recovery of bitumen from tar,
356 during bitumen upgrading in a process called "hydrotreating", and in tailing ponds, which, on occasion,
357 have been contaminated with NH₃ to such a degree that they outgas it (Bytnerowicz et al., 2010).

358 Ammonia is also used for flue gas de-sulfurization by Syncrude; emission inventories (NPRI, 2013; ECCC,
359 2013a) suggest their fugitive emissions are the largest anthropogenic source in the region, though it is
360 not clear if all sources are accurately inventoried.

361 The lack of association of ammonia with other variables in this component and the bivariate polar plots
362 (Figure S-9) are consistent with an NH₃-specific source profile, such as fugitive emissions from one or
363 more point sources that emit independently from other activities (i.e., ammonia storage tanks) and
364 natural emissions from soil and trees.

365

366 **Component 9: ~~Background CO from VOC oxidation~~Incomplete hydrocarbon oxidation**

367 Component 9 is another single variable component and strongly correlates with CO ($r = 0.87$). The
368 variables with the next largest correlation coefficients are CH₄ ($r = 0.17$), 1,2,3- and 1,2,4-TMB (both $r =$
369 0.18), and o-xylene ($r = 0.16$).

370 The conventional interpretation of CO is as a byproduct of incomplete VOC oxidation, as it is found in
371 fossil fuel combustion exhaust or in biomass burning plumes. Component 9, however, is not associated
372 with NO_y ($r = -0.08$) or CO₂ ($r = 0.05$), which rules out this conventional interpretation.

373 Recently, Marey et al. (2015) examined the spatial distribution of CO in Northern Alberta using a
374 combination of satellite and ground station data and found that most CO is derived from anthropogenic
375 sources, biomass burning and the photochemical oxidation of methane and other VOCs. During the 2013
376 JOSM study, there was no obvious (i.e., tracer) evidence for fire emissions impacting the measurements
377 at AMS 13 (Phillips-Smith et al., 2017), though an impact from distant sources (such as fires located
378 1,000s of km upwind in British Columbia or Washington State) cannot be entirely ruled out. We
379 therefore interpret component 9 as a VOC oxidation product component.

380 **Component 10: Dry tailings**

381 Component 10 is strongly associated with TRS ($r = 0.71$) and moderateweakly with o-xylene ($r = 0.32$).
382 There are weakpoor correlations with CH_4 ($r = 0.14$) and IVOCs ($r = 0.20$). This component is qualitatively
383 similar to component 1, in that the presence of o-xylene suggests emission of naphtha, and the
384 presence of TRS and CH_4 suggests anaerobic sulfur reducing bacteria and methanogens as they occur in
385 tailings ponds (Holowenko et al., 2000; Percy, 2013; Quagraine et al., 2005). However, the absence of
386 correlations with NO_y , rBC, and CO suggests that this source is not in spatial proximity with a
387 continuously operating combustion source. The much weakpoorer correlations of o-xylene, CH_4 , and
388 IVOCs than for component 1 suggests that this component is much more "aged", i.e., emits less naphtha
389 and bitumen.

390 As part of the reclamation process, tailings ponds in the Alberta oil sands region are converted into
391 "composite tailings", which consist of a consolidated alkaline, saline mixture of processed sand, residual
392 bitumen, clay fines, and gypsum (CaSO_4). This mixture settles and releases water, forming shallow pools
393 of surface water (Figure 4J). Due to intensive microbial activity, composite tailings deposits are strong
394 sources of H_2S and, likely, other reduced sulfur species (Warren et al., 2016; Bradford et al., 2017).
395 Composite tailings are a source consistent with the emission profile of component 10. The association
396 with TRS is explained by its production from biological activity and the presence of IVOCs by outgassing
397 from the residual bitumen. Syncrude (the company operating closest to AMS 13) has been undertaking a
398 pilot scale wetland reclamation project in the Athabasca Oil Sands Region to allow the development of a
399 fen wetland above composite tailings (Bradford et al., 2017). Component 10 is hence interpreted as a
400 dry tailings pond component, though the confidence in this interpretation is somewhat marginal as
401 judged, for example, from the low eigenvalue of 0.74.

402

403 **Bivariate polar plots**

404 Bivariate polar plots map a surface using wind direction and wind speed and then model pollutant
405 concentrations. While PCA is good at showing the temporal distribution of sources, bivariate polar plots
406 help to show the spatial distribution of sources.

407 Figure S-[32](#) shows a sample of variables associated with component 1. This component appears to
408 dominate when winds are from the SSE and E and of moderate wind speeds (2-3 m/s).

409 Figure S-[43](#) shows a sample of dominant variables associated with component 2. This component
410 appears to dominate when winds are from the E at low wind speeds (1-2 m/s). The map appears to track
411 the location of the Athabasca river and highway 63, corroborating that this source is from vehicular
412 emissions.

413 Figure S-[54](#) shows a sample of dominant variables associated with component 3. This component
414 appears to dominate when winds are stagnant and local. This is unsurprising because biogenic emissions
415 are expected to be emitted in great concentrations locally since our site is surrounded on all sides by
416 forest.

417 Figure S-[65](#) shows a sample of dominant variables associated with component 4 (or with component 2 in
418 the secondary processes PCA). This component appears to dominate when winds are moderate (2-3
419 m/s) and from the SE and E.

420 Figure S-[76](#) shows a sample of dominant variables associated with component 5. This component
421 appears to dominate when winds are from the E at moderate wind speeds (2-3 m/s).

422 Figure S-[87](#) shows a sample of dominant variables associated with component 6. This component
423 appears to dominate when winds are stagnant and local. This suggests that this source is biogenic and
424 may be due to emissions from trees.

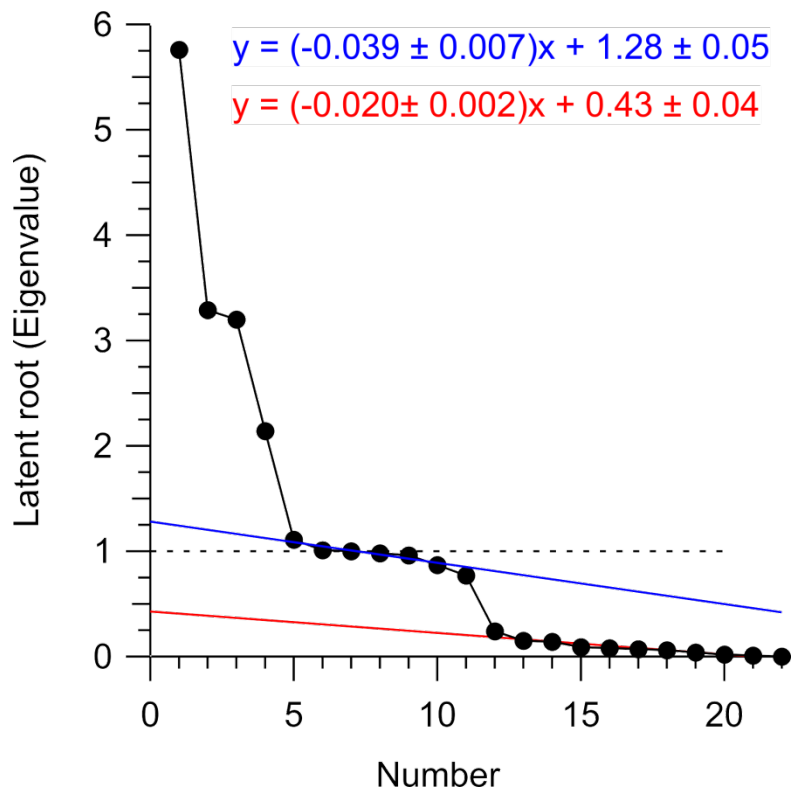
425 Figure S-[98](#) shows a sample of dominant variables associated with component 7. This component
426 appears to dominate when winds are from the SE and E at moderate wind speeds (1-3 m/s).

427 Figure S-9-10 shows a sample of dominant variables associated with component 8. This component does
428 not appear to have a specific direction associated with it and is observed in all directions. This
429 component is observed when winds are at moderate to high speeds (2-4 m/s).

430 Figure S-10-11 shows a sample of dominant variables associated with component 9. This component is
431 observed when winds are from the S, SE, and E. This component is observed when winds are at low to
432 moderate speeds (1-3 m/s).

433 Figure S-11-12 shows a sample of dominant variables associated with component 10. This component is
434 observed when winds are from the SSE. This component is observed when winds are around 1.5 m/s.
435 This source is very likely a point source due to its consistency with wind direction and speed.

436



437

438 **Figure S-12.** Scree plot used to consider the number of components to retain. Dashed line represents
439 the latent root criterions (eigenvalues > 1). Blue line represents the first instance of eigenvalues
440 becoming horizontal. Red line represents the second instance of eigenvalues becoming horizontal.

441 **Table S-1.** Ionimed Analytical GCU Standard.-

Compound	Volume mixing ratio (ppmv)	Uncertainty (%)
Formaldehyde	1.01	±8
Methanol	1.01	±8
Acetonitrile	1.01	±6
Acetaldehyde	1.01	±5
Ethanol	1.01	±8
Acrolein	0.98	±5
Acetone	1.02	±5
Isoprene	0.99	±5
Crotonaldehyde	0.92	±6
2-Butanone	1.01	±5
Benzene	1.01	±5
Toluene	1.02	±5
o-xylene	1.03	±6
Chlorobenzene	1.02	±5
α-pinene	0.93	±5
1,2, Dichlorobenzene	1.03	±7
1,2,4-Trichlorobenzene	1.01	±9

442

443

444 **Table S-2.** The component pattern after Varimax rotation. Correlations greater than 0.30 or less than -0.30 are bolded.

	1	2	3	4	5	6	7	8	9	10	11	12	13	14	15	16	17	18	19	20	21	22
Anthropogenic VOCs																						
o-xylene	0.89	0.07	0.03	0.10	0.09	0.06	-0.03	0.11	0.15	0.06	0.26	0.11	0.00	0.04	-0.08	0.24	0.00	-0.01	-0.02	0.00	-0.01	0.00
1,2,3 - TMB	0.94	0.15	0.07	0.06	0.05	0.08	-0.01	0.06	0.17	0.01	-0.01	0.02	-0.04	0.01	-0.08	-0.14	0.03	0.00	-0.09	0.00	-0.07	0.00
1,2,4 - TMB	0.94	0.13	0.01	0.11	0.08	0.05	-0.02	0.09	0.17	0.04	0.12	0.03	-0.01	0.02	-0.06	0.03	0.01	0.00	-0.04	0.00	0.09	0.00
decane	0.91	0.22	-0.02	0.15	0.05	0.00	0.04	0.15	0.05	0.15	0.07	-0.02	0.04	-0.01	0.07	-0.03	-0.03	0.02	0.16	0.00	-0.01	0.00
undecane	0.85	0.27	-0.08	0.23	0.08	-0.03	0.06	0.05	0.00	0.20	0.01	-0.10	0.09	0.00	0.26	-0.05	-0.02	0.02	0.02	0.00	0.00	0.00
Biogenic VOCs																						
α-pinene	-0.03	-0.08	0.98	-0.11	0.02	0.05	-0.08	0.02	0.01	0.00	-0.01	0.02	0.00	0.00	-0.01	0.01	-0.08	-0.01	0.00	0.09	0.00	0.00
β-pinene	-0.02	-0.08	0.97	-0.12	0.01	0.05	-0.08	0.01	0.01	0.01	0.01	-0.02	0.00	-0.02	0.02	0.00	-0.10	0.01	0.01	-0.09	0.00	0.00
limonene	0.08	-0.02	0.92	-0.08	0.06	0.23	-0.11	0.08	0.02	0.07	-0.05	0.02	-0.03	0.03	-0.02	0.00	0.23	0.00	-0.01	0.00	0.00	0.00
Combustion tracers																						
NO _y	0.26	0.80	-0.25	0.21	0.03	-0.05	0.10	0.19	-0.04	0.07	0.04	0.01	0.34	0.00	0.04	0.00	-0.01	-0.01	0.01	0.00	0.00	0.00
rBC	0.31	0.80	0.03	0.05	0.08	0.07	0.11	0.24	0.12	0.34	-0.03	0.02	-0.02	-0.05	0.02	-0.01	0.00	0.22	0.01	0.00	0.00	0.00
CO	0.41	0.18	0.04	0.02	0.08	0.07	0.05	0.03	0.88	0.06	0.00	0.02	0.00	0.01	0.00	0.00	0.00	0.00	0.00	0.00	0.00	0.00
CO ₂	0.10	0.09	0.46	-0.12	0.23	0.82	-0.14	-0.03	0.07	0.00	-0.05	0.02	-0.01	0.01	0.00	0.00	0.00	0.00	0.00	0.00	0.00	0.00
Aerosol species																						
pPAH	0.07	0.94	-0.08	-0.11	0.02	0.06	0.14	0.00	0.09	-0.15	0.00	0.01	-0.14	-0.07	-0.02	0.00	0.00	-0.10	0.00	0.00	0.00	0.00
PM ₁₀₋₁	0.18	0.13	0.07	0.10	0.94	0.16	-0.03	0.04	0.07	0.10	0.08	0.02	0.00	0.01	0.00	0.00	0.00	0.00	0.00	0.00	0.00	0.00
HOA	0.41	0.74	0.02	0.11	0.21	0.11	-0.04	0.13	0.15	0.19	0.10	0.05	0.01	0.35	0.00	0.01	0.01	-0.01	0.00	0.00	0.00	0.00
LO-OOA	0.45	0.17	0.13	0.25	0.19	0.01	-0.04	0.28	0.10	0.73	0.16	0.02	0.01	0.03	0.01	0.00	0.00	0.00	0.00	0.00	0.00	0.00
Sulfur																						
TS	0.25	0.04	-0.16	0.94	0.07	-0.05	-0.02	0.02	0.01	0.09	0.14	0.00	0.01	0.01	0.01	0.00	0.00	0.00	0.00	0.00	0.00	0.01
SO ₂	0.11	0.02	-0.15	0.98	0.04	-0.04	-0.03	-0.02	0.01	0.05	-0.05	-0.01	0.01	0.01	0.00	0.00	0.00	0.00	0.00	0.00	0.00	-0.01
TRS	0.57	0.05	-0.08	0.11	0.14	-0.05	0.03	0.16	-0.01	0.13	0.77	0.02	0.00	0.01	0.00	0.00	0.00	0.00	0.00	0.00	0.00	0.00
Other																						
IVOCs	0.34	0.34	0.12	-0.03	0.05	-0.02	-0.02	0.84	0.04	0.18	0.13	0.01	0.01	0.01	0.00	0.00	0.00	0.00	0.00	0.00	0.00	0.00
NH ₃	0.01	0.19	-0.23	-0.04	-0.03	-0.09	0.95	-0.01	0.04	-0.01	0.01	0.00	0.01	0.00	0.00	0.00	0.00	0.00	0.00	0.00	0.00	0.00
CH ₄	0.60	0.39	0.10	-0.05	0.14	0.44	0.00	0.06	0.16	0.08	0.09	0.46	0.01	0.03	-0.02	0.01	0.00	0.00	0.00	0.00	0.00	0.00
Eigenvalues	5.76	3.29	3.20	2.14	1.11	1.01	1.00	0.98	0.96	0.87	0.77	0.24	0.15	0.14	0.09	0.08	0.07	0.06	0.04	0.02	0.01	0.00
% of variance	26.17	14.97	14.55	9.75	5.06	4.60	4.53	4.46	4.34	3.94	3.51	1.09	0.69	0.63	0.42	0.37	0.33	0.28	0.17	0.08	0.06	0.00
% cum. var.	26.17	41.14	55.69	65.43	70.49	75.09	79.62	84.07	88.42	92.36	95.87	96.97	97.66	98.29	98.71	99.08	99.41	99.69	99.86	99.94	100.0	100

445 **Table S-3.** The pattern after Varimax rotation with 5 components selected.

	1	2	3	4	5	Communalities
<u>Anthropogenic VOCs</u>						
o-xylene	0.94	0.08	0.03	0.09	0.15	0.93
1,2,3 - TMB	0.90	0.14	0.04	0.01	0.23	0.89
1,2,4 - TMB	0.95	0.14	-0.01	0.09	0.18	0.97
decane	0.91	0.27	-0.03	0.16	0.05	0.93
undecane	0.82	0.31	-0.10	0.26	0.05	0.84
<u>Biogenic VOCs</u>						
α-pinene	-0.03	-0.05	0.94	-0.15	0.04	0.91
β-pinene	-0.02	-0.06	0.94	-0.15	0.03	0.90
limonene	0.07	0.02	0.94	-0.10	0.18	0.93
<u>Combustion tracers</u>						
NO _y	0.25	0.83	-0.29	0.22	0.02	0.89
rBC	0.33	0.89	0.04	0.07	0.13	0.92
CO	0.53	0.19	-0.02	-0.08	0.40	0.48
CO ₂	0.07	0.06	0.55	-0.13	0.71	0.83
<u>Aerosol species</u>						
pPAH	0.01	0.83	-0.20	-0.20	0.27	0.84
PM ₁₀₋₁	0.21	0.19	0.15	0.29	0.57	0.51
HOA	0.44	0.75	0.03	0.15	0.32	0.88
LO-OOA	0.59	0.37	0.28	0.41	-0.06	0.74
<u>Sulfur</u>						
TS	0.28	0.04	-0.18	0.91	0.01	0.94
SO ₂	0.10	0.01	-0.18	0.93	0.05	0.91
TRS	0.76	0.10	-0.04	0.17	-0.13	0.63
<u>Other</u>						
IVOCs	0.47	0.61	0.28	0.03	-0.25	0.73
NH ₃	0.02	0.34	-0.47	-0.21	-0.14	0.40
CH ₄	0.62	0.38	0.12	-0.09	0.53	0.84
Eigenvalues	6.42	3.79	3.56	2.34	1.70	
% of variance	29.20	17.25	16.20	10.63	7.74	
Cumulative variance	29.20	46.45	62.65	73.28	81.01	

446

447 **Table S-4.** The pattern after Varimax rotation with 6 components selected.

	1	2	3	4	5	6	Communalities
<u>Anthropogenic VOCs</u>							
o-xylene	0.92	0.04	0.01	0.08	0.24	0.13	0.93
1,2,3 - TMB	0.94	0.16	0.08	0.07	0.06	0.05	0.92
1,2,4 - TMB	0.95	0.13	0.00	0.11	0.16	0.08	0.97
decane	0.88	0.23	-0.02	0.18	0.28	0.00	0.94
undecane	0.79	0.28	-0.09	0.29	0.25	0.00	0.85
<u>Biogenic VOCs</u>							
α-pinene	-0.02	-0.09	0.96	-0.12	0.04	0.01	0.95
β-pinene	-0.02	-0.10	0.96	-0.12	0.05	0.01	0.94
limonene	0.09	-0.01	0.95	-0.09	0.04	0.15	0.95
<u>Combustion tracers</u>							
NO _y	0.22	0.81	-0.27	0.23	0.25	0.00	0.89
rBC	0.31	0.85	0.07	0.08	0.28	0.10	0.92
CO	0.64	0.29	0.09	0.02	-0.23	0.09	0.56
CO ₂	0.17	0.12	0.57	-0.17	-0.23	0.62	0.84
<u>Aerosol species</u>							
pPAH	0.09	0.90	-0.10	-0.14	-0.10	0.05	0.87
PM ₁₀₋₁	0.19	0.14	0.03	0.12	0.17	0.81	0.76
HOA	0.44	0.73	0.04	0.13	0.22	0.30	0.88
LO-OOA	0.46	0.22	0.17	0.32	0.60	0.21	0.79
<u>Sulfur</u>							
TS	0.25	0.02	-0.18	0.92	0.12	0.06	0.97
SO ₂	0.10	0.03	-0.15	0.97	-0.02	0.02	0.98
TRS	0.62	-0.04	-0.17	0.06	0.56	0.14	0.75
<u>Other</u>							
IVOCs	0.31	0.43	0.17	-0.06	0.70	0.02	0.80
NH ₃	0.06	0.41	-0.36	-0.11	-0.11	-0.36	0.46
CH ₄	0.68	0.42	0.15	-0.10	0.00	0.41	0.84
Eigenvalues	6.09	3.60	3.47	2.25	1.76	1.58	
% of variance	27.70	16.38	15.78	10.22	7.98	7.18	
Cumulative variance	27.70	44.07	59.85	70.08	78.06	85.23	

448

449 **Table S-5.** The pattern after Varimax rotation with 7 components selected.

	1	2	3	4	5	6	7	Communalities
<u>Anthropogenic VOCs</u>								
o-xylene	0.93	0.07	0.01	0.08	0.21	0.12	-0.05	0.93
1,2,3 - TMB	0.94	0.18	0.08	0.06	0.03	0.03	-0.03	0.93
1,2,4 - TMB	0.96	0.15	0.00	0.11	0.14	0.07	-0.02	0.98
decane	0.88	0.26	-0.02	0.18	0.26	0.00	0.01	0.94
undecane	0.79	0.30	-0.09	0.28	0.23	0.00	0.03	0.85
<u>Biogenic VOCs</u>								
α -pinene	-0.03	-0.09	0.96	-0.11	0.04	0.00	-0.05	0.96
β -pinene	-0.02	-0.10	0.96	-0.11	0.06	0.01	-0.05	0.95
limonene	0.09	0.01	0.95	-0.08	0.03	0.12	-0.13	0.95
<u>Combustion tracers</u>								
NO _y	0.22	0.83	-0.28	0.22	0.20	-0.02	0.06	0.91
rBC	0.31	0.85	0.07	0.08	0.25	0.11	0.13	0.92
CO	0.62	0.22	0.13	0.03	-0.21	0.19	0.29	0.61
CO ₂	0.17	0.17	0.56	-0.18	-0.28	0.54	-0.27	0.84
<u>Aerosol species</u>								
pPAH	0.08	0.89	-0.10	-0.15	-0.14	0.03	0.15	0.88
PM ₁₀₋₁	0.18	0.12	0.06	0.13	0.18	0.89	0.01	0.89
HOA	0.44	0.76	0.03	0.12	0.16	0.27	-0.03	0.89
LO-OOA	0.46	0.23	0.18	0.33	0.59	0.25	0.01	0.81
<u>Sulfur</u>								
TS	0.25	0.04	-0.18	0.92	0.12	0.06	-0.02	0.97
SO ₂	0.10	0.04	-0.15	0.97	-0.02	0.02	-0.03	0.98
TRS	0.62	-0.03	-0.16	0.07	0.56	0.19	0.02	0.77
<u>Other</u>								
IVOCs	0.32	0.48	0.16	-0.07	0.66	0.00	-0.05	0.80
NH ₃	0.01	0.20	-0.26	-0.06	0.00	-0.05	0.89	0.91
CH ₄	0.68	0.45	0.15	-0.11	-0.05	0.36	-0.10	0.85
Eigenvalues	6.09	3.65	3.42	2.23	1.61	1.46	1.03	
% of variance	27.70	16.60	15.57	10.14	7.33	6.66	4.70	
Cumulative variance	27.70	44.30	59.86	70.01	77.34	84.00	88.70	

450 **Table S-6.** The pattern after Varimax rotation with 8 components selected.

	1	2	3	4	5	6	7	8	Communalities
<u>Anthropogenic VOCs</u>									
o-xylene	0.93	0.08	0.03	0.07	0.14	0.13	-0.03	0.11	0.93
1,2,3 - TMB	0.91	0.19	0.09	0.06	-0.01	0.02	-0.04	0.21	0.93
1,2,4 - TMB	0.95	0.16	0.01	0.11	0.09	0.07	-0.03	0.18	0.98
decane	0.90	0.26	-0.01	0.17	0.19	0.01	0.03	0.08	0.95
undecane	0.82	0.30	-0.07	0.28	0.15	0.01	0.06	0.03	0.87
<u>Biogenic VOCs</u>									
α-pinene	-0.04	-0.10	0.97	-0.11	0.06	0.00	-0.05	0.00	0.96
β-pinene	-0.02	-0.10	0.96	-0.11	0.06	0.00	-0.04	-0.01	0.96
limonene	0.07	0.00	0.95	-0.08	0.06	0.11	-0.14	0.05	0.95
<u>Combustion tracers</u>									
NO _y	0.25	0.83	-0.26	0.22	0.19	-0.01	0.10	-0.08	0.92
rBC	0.28	0.83	0.06	0.07	0.33	0.10	0.09	0.17	0.93
CO	0.42	0.18	0.04	0.01	0.07	0.11	0.06	0.85	0.96
CO ₂	0.13	0.19	0.58	-0.17	-0.28	0.53	-0.27	0.10	0.86
<u>Aerosol species</u>									
pPAH	0.06	0.91	-0.08	-0.14	-0.11	0.03	0.16	0.06	0.89
PM ₁₀₋₁	0.18	0.12	0.07	0.12	0.16	0.89	0.01	0.06	0.89
HOA	0.42	0.75	0.03	0.12	0.21	0.26	-0.06	0.15	0.89
LO-OOA	0.46	0.19	0.15	0.30	0.65	0.24	-0.04	0.15	0.87
<u>Sulfur</u>									
TS	0.28	0.03	-0.18	0.92	0.09	0.07	-0.01	-0.02	0.97
SO ₂	0.11	0.04	-0.15	0.97	-0.01	0.02	-0.04	0.03	0.98
TRS	0.72	-0.03	-0.13	0.06	0.40	0.23	0.11	-0.20	0.80
<u>Other</u>									
IVOCs	0.35	0.43	0.13	-0.09	0.71	0.00	-0.07	0.01	0.84
NH ₃	0.01	0.22	-0.24	-0.05	-0.05	-0.04	0.92	0.05	0.96
CH ₄	0.65	0.47	0.17	-0.11	-0.08	0.35	-0.10	0.16	0.86
Eigenvalues	5.99	3.58	3.40	2.20	1.52	1.43	1.03	1.00	
% of variance	27.23	16.28	15.44	10.01	6.90	6.52	4.70	4.53	
Cumulative variance	27.23	43.51	58.95	68.96	75.86	82.37	87.08	91.61	

452 **Table S-7.** The pattern after Varimax rotation with 9 components selected.

	1	2	3	4	5	6	7	8	9	Communalities
<u>Anthropogenic VOCs</u>										
o-xylene	0.89	0.09	0.03	0.09	0.11	0.11	-0.05	0.16	0.30	0.95
1,2,3 - TMB	0.93	0.16	0.08	0.05	0.05	0.05	-0.02	0.17	-0.02	0.94
1,2,4 - TMB	0.94	0.15	0.01	0.11	0.11	0.08	-0.02	0.18	0.12	0.98
decane	0.91	0.22	-0.03	0.16	0.25	0.04	0.05	0.03	0.03	0.97
undecane	0.85	0.25	-0.10	0.25	0.24	0.06	0.10	-0.05	-0.08	0.94
<u>Biogenic VOCs</u>										
α-pinene	-0.04	-0.09	0.97	-0.10	0.05	0.00	-0.06	0.02	0.02	0.97
β-pinene	-0.03	-0.10	0.97	-0.11	0.05	0.00	-0.05	0.00	0.02	0.96
limonene	0.09	-0.01	0.94	-0.09	0.08	0.13	-0.13	0.03	-0.06	0.95
<u>Combustion tracers</u>										
NO _y	0.26	0.82	-0.26	0.22	0.22	0.00	0.11	-0.09	0.02	0.92
rBC	0.31	0.79	0.04	0.05	0.41	0.12	0.12	0.12	-0.10	0.94
CO	0.42	0.19	0.05	0.02	0.08	0.10	0.06	0.87	-0.02	0.98
CO ₂	0.16	0.17	0.56	-0.18	-0.22	0.56	-0.25	0.06	-0.17	0.86
<u>Aerosol species</u>										
pPAH	0.06	0.93	-0.07	-0.12	-0.11	0.01	0.14	0.09	0.03	0.93
PM ₁₀₋₁	0.16	0.11	0.06	0.12	0.17	0.89	0.02	0.06	0.10	0.89
HOA	0.41	0.75	0.03	0.13	0.23	0.25	-0.06	0.16	0.08	0.90
LO-OOA	0.46	0.14	0.13	0.28	0.70	0.26	-0.01	0.10	0.05	0.90
<u>Sulfur</u>										
TS	0.25	0.04	-0.17	0.93	0.08	0.06	-0.02	0.00	0.13	0.99
SO ₂	0.11	0.03	-0.15	0.97	0.01	0.02	-0.03	0.01	-0.05	0.99
TRS	0.59	0.05	-0.09	0.11	0.24	0.14	0.04	-0.04	0.71	0.96
<u>Other</u>										
IVOCs	0.32	0.41	0.12	-0.09	0.70	-0.01	-0.08	0.02	0.20	0.84
NH ₃	0.01	0.21	-0.24	-0.05	-0.04	-0.04	0.93	0.04	0.01	0.97
CH ₄	0.65	0.47	0.16	-0.10	-0.06	0.36	-0.10	0.17	0.07	0.86
Eigenvalues	5.84	3.44	3.37	2.19	1.58	1.47	1.03	0.95	0.74	
% of variance	26.54	15.63	15.30	9.98	7.19	6.66	4.69	4.31	3.38	
Cumulative variance	26.54	42.17	57.47	67.44	74.63	81.29	85.98	90.29	93.67	

454 **Table S-8.** The factor pattern after Varimax rotation with 11 factors selected.

	Factor 1	Factor 2	Factor 3	Factor 4	Factor 5	Factor 6	Factor 7	Factor 8	Factor 9	Factor 10	Factor 11	Commu- nalities
<u>Anthropogenic VOCs</u>												
o-xylene	0.88	0.08	0.03	0.10	0.13	0.07	-0.04	0.17	0.11	0.04	0.32	0.95
1,2,3 - TMB	0.94	0.16	0.07	0.05	0.11	0.05	-0.01	0.18	0.06	-0.01	-0.02	0.96
1,2,4 - TMB	0.94	0.15	0.01	0.11	0.08	0.08	-0.02	0.18	0.09	0.03	0.13	0.99
decane	0.92	0.24	-0.02	0.15	0.00	0.05	0.04	0.04	0.13	0.16	0.05	0.97
undecane	0.87	0.29	-0.08	0.22	-0.06	0.09	0.05	-0.05	0.03	0.22	-0.05	0.96
<u>Biogenic VOCs</u>												
α-pinene	-0.03	-0.08	0.98	-0.11	0.04	0.01	-0.08	0.02	0.02	0.00	0.00	0.98
β-pinene	-0.02	-0.08	0.98	-0.12	0.02	0.02	-0.07	0.00	0.00	0.02	0.01	0.98
limonene	0.08	-0.02	0.93	-0.08	0.24	0.05	-0.11	0.03	0.09	0.06	-0.05	0.95
<u>Combustion tracers</u>												
NO _y	0.27	0.83	-0.26	0.21	-0.04	0.03	0.10	-0.08	0.18	0.07	0.01	0.92
rBC	0.30	0.81	0.04	0.04	0.09	0.07	0.12	0.12	0.23	0.34	-0.05	0.95
CO	0.41	0.19	0.04	0.02	0.08	0.08	0.05	0.87	0.03	0.06	-0.01	0.99
CO ₂	0.09	0.08	0.48	-0.12	0.77	0.25	-0.14	0.05	-0.04	-0.01	-0.09	0.95
<u>Aerosol species</u>												
pPAH	0.06	0.93	-0.07	-0.12	0.07	0.02	0.14	0.10	-0.02	-0.20	0.01	0.95
PM ₁₀₋₁	0.18	0.14	0.08	0.10	0.17	0.94	-0.03	0.07	0.04	0.09	0.08	1.00
HOA	0.40	0.77	0.03	0.11	0.14	0.20	-0.07	0.16	0.09	0.19	0.13	0.92
LO-OOA	0.45	0.19	0.13	0.25	0.03	0.19	-0.04	0.11	0.27	0.72	0.16	0.98
<u>Sulfur</u>												
TS	0.26	0.05	-0.16	0.93	-0.05	0.07	-0.02	0.01	0.02	0.08	0.13	0.26
SO ₂	0.12	0.03	-0.15	0.98	-0.04	0.04	-0.03	0.01	-0.02	0.05	-0.05	0.12
TRS	0.58	0.06	-0.08	0.10	-0.04	0.14	0.03	-0.03	0.16	0.13	0.74	0.58
<u>Other</u>												
IVOCs	0.34	0.37	0.13	-0.03	-0.01	0.05	-0.03	0.03	0.82	0.18	0.12	1.00
NH ₃	0.01	0.20	-0.24	-0.04	-0.08	-0.03	0.94	0.04	-0.02	-0.01	0.01	1.00
CH ₄	0.59	0.40	0.10	-0.06	0.59	0.10	0.00	0.17	0.05	0.07	0.15	0.93
Eigenvalues	5.75	3.43	3.24	2.13	1.12	1.10	0.99	0.96	0.93	0.87	0.79	
% var.	26.14	15.61	14.72	9.66	5.11	4.99	4.51	4.35	4.22	3.95	3.60	
% Cum. var.	26.14	41.74	56.46	66.12	71.23	76.22	80.73	85.09	89.31	93.26	96.86	

455 **Table S-9.** The pattern with mixing height included after Varimax rotation with 10 components.

	1	2	3	4	5	6	7	8	9	10	Communalities
<u>Anthropogenic VOCs</u>											
o-xylene	0.89	0.04	0.03	0.10	0.29	0.10	-0.01	-0.06	0.17	0.16	0.95
1,2,3 - TMB	0.94	0.17	0.10	0.04	-0.04	0.01	-0.03	-0.04	0.17	0.06	0.95
1,2,4 - TMB	0.94	0.13	0.03	0.10	0.11	0.09	-0.02	-0.06	0.18	0.07	0.98
decane	0.92	0.25	0.03	0.15	0.11	0.11	0.01	0.04	0.03	-0.04	0.97
undecane	0.87	0.31	-0.05	0.23	-0.03	0.17	0.03	0.10	-0.05	-0.11	0.96
<u>Biogenic VOCs</u>											
α-pinene	-0.02	-0.08	0.96	-0.10	0.03	0.01	-0.05	-0.11	0.01	0.02	0.96
β-pinene	-0.01	-0.08	0.96	-0.11	0.04	0.02	-0.05	-0.12	-0.01	0.02	0.96
limonene	0.11	0.02	0.95	-0.08	0.04	0.02	-0.11	-0.06	0.03	0.12	0.96
<u>Combustion tracers</u>											
NO _y	0.21	0.86	-0.25	0.21	0.11	0.06	0.10	0.01	-0.08	-0.02	0.92
rBC	0.29	0.89	0.12	0.02	0.10	0.19	0.03	0.09	0.10	-0.01	0.95
CO	0.43	0.20	0.04	0.01	0.00	0.08	0.02	0.05	0.86	0.07	0.98
CO ₂	0.15	0.17	0.56	-0.13	-0.12	0.13	-0.14	-0.12	0.08	0.68	0.91
<u>Aerosol species</u>											
pPAH	0.01	0.86	-0.09	-0.13	-0.08	-0.03	0.23	-0.18	0.12	0.17	0.90
PM ₁₀₋₁	0.31	0.22	0.05	0.15	0.12	0.88	0.04	-0.01	0.08	0.10	0.97
HOA	0.45	0.79	0.02	0.14	0.16	0.15	-0.02	-0.02	0.16	0.10	0.93
LO-OOA	0.52	0.30	0.21	0.26	0.37	0.36	-0.17	0.27	0.04	-0.18	0.88
<u>Sulfur</u>											
TS	0.27	0.06	-0.16	0.93	0.10	0.10	-0.03	0.04	-0.01	-0.02	1.00
SO ₂	0.11	0.05	-0.14	0.97	-0.06	0.06	-0.05	0.05	0.01	-0.05	0.99
TRS	0.64	0.01	-0.12	0.11	0.63	0.20	0.09	-0.04	-0.09	0.12	0.91
<u>Other</u>											
IVOCs	0.28	0.50	0.22	-0.07	0.66	0.08	-0.13	0.04	0.06	-0.18	0.87
NH ₃	0.00	0.22	-0.20	-0.07	-0.03	0.03	0.92	0.11	0.02	-0.06	0.96
CH ₄	0.64	0.43	0.15	-0.07	0.09	0.10	0.00	-0.07	0.17	0.50	0.92
Mixing height	-0.04	-0.07	-0.35	0.07	0.01	0.00	0.12	0.90	0.04	-0.07	0.96
Eigenvalues	6.06	3.81	3.51	2.16	1.19	1.12	1.03	1.02	0.94	0.92	
% var.	26.35	16.57	15.27	9.39	5.19	4.86	4.48	4.42	4.08	3.98	
% Cum. var.	26.35	42.92	58.19	67.58	72.77	77.63	82.11	86.53	90.61	94.60	

456

457

458 **Table S-10.** Criteria for number of components extracted by PCA.

Criterion	Number of components extracted	% Variance explained (after rotation)
Scree test 1	5	81.0%
< 5% variance	6	85.2%
Latent root	7	88.7%
≥ 95% cumulative variance	10	95.5%
Scree test 2	11	96.9%

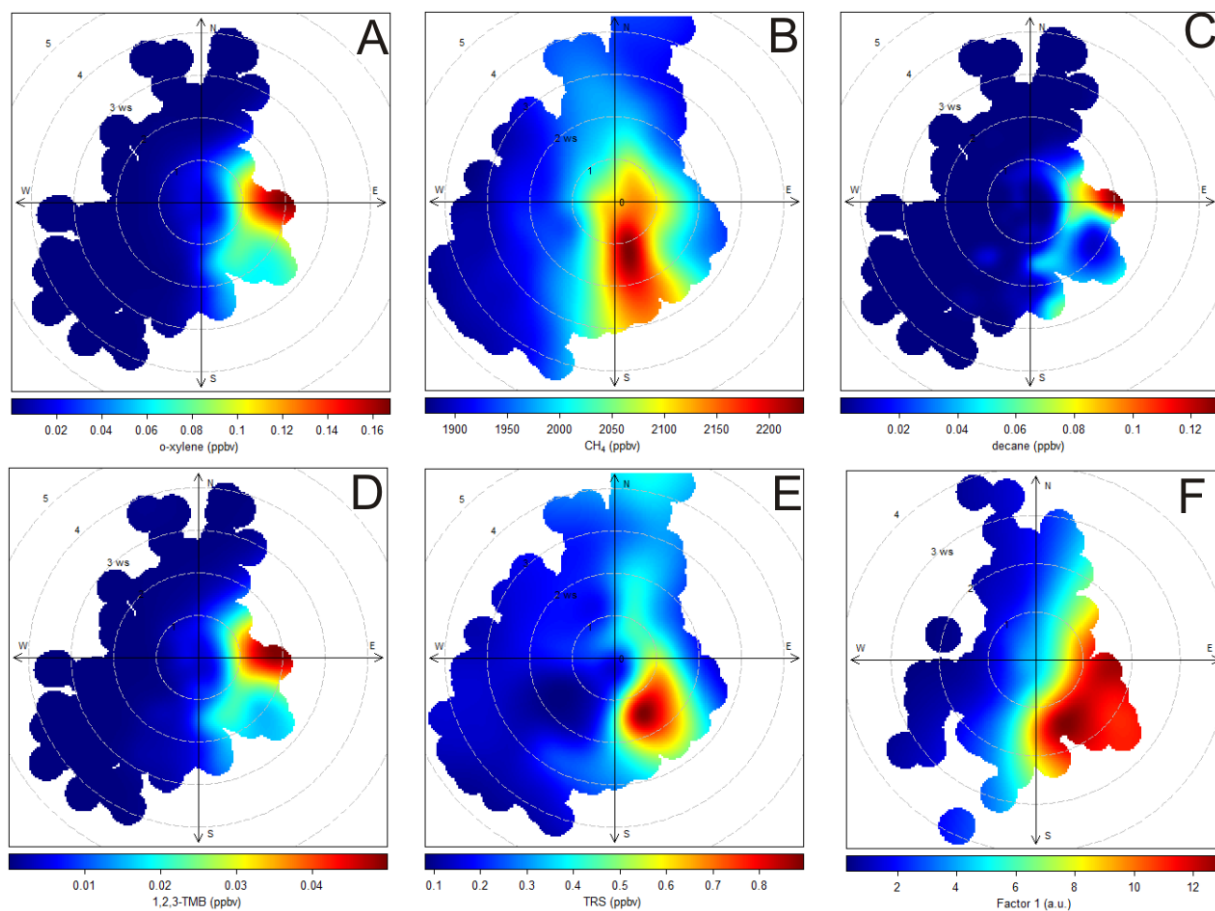
459

460

461 **Table S-11.** Association of IVOCs with relevant components.

# of components in solution	Oil sands surface mining facilities (Component 1)	Mine fleet and operations (Component 2)	Mine face (Component 5)
5	0.47	0.61	n/a
6	0.31	0.43	n/a
7	0.32	0.48	0.66
8	0.35	0.43	0.71
9	0.32	0.41	0.70
10	0.31	0.39	0.74
11	0.34	0.37	n/a

462



463

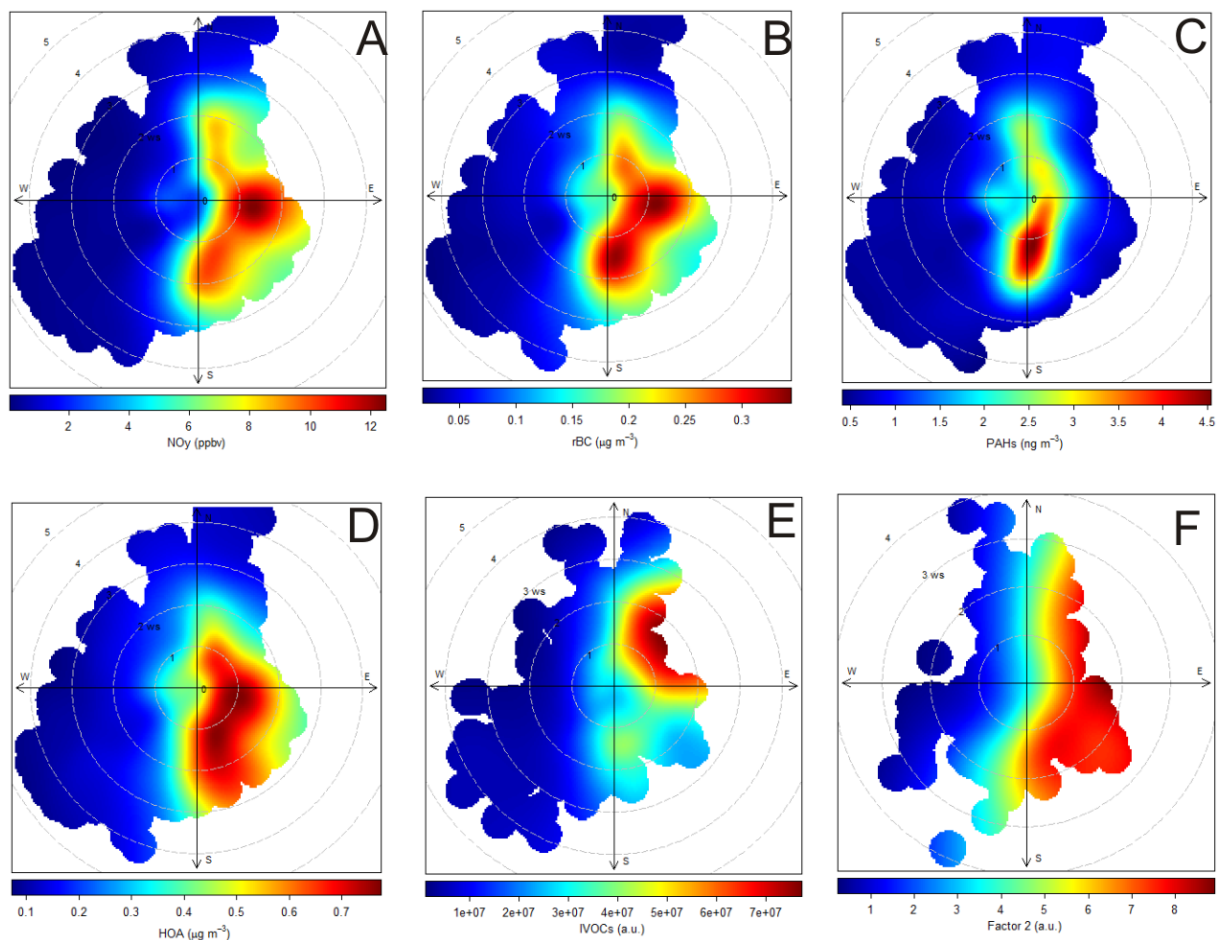
464

465

466

Figure S-23. Bivariate polar plots associated with component 1 for the optimum primary pollutant solution (Table 54.). (A) o-xylene, (B) CH₄, (C) decane, (D) 1, 2, 3-TMB, (E) TRS, (F) and component 1.

467



468

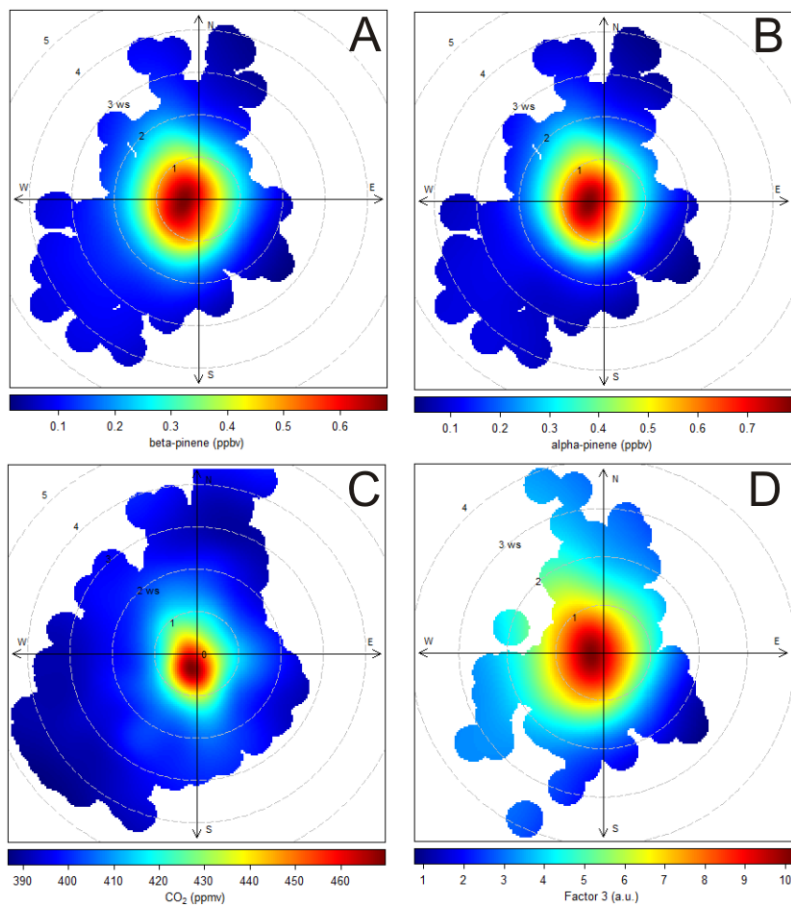
469

470

471

Figure S-34. Bivariate polar plots associated with component 2 for the optimum primary pollutant solution (Table 54.). (A) NO_y , (B) rBC, (C) PAHs, (D) HOA, (E) IVOCs, (F) and component 2.

472



473

474

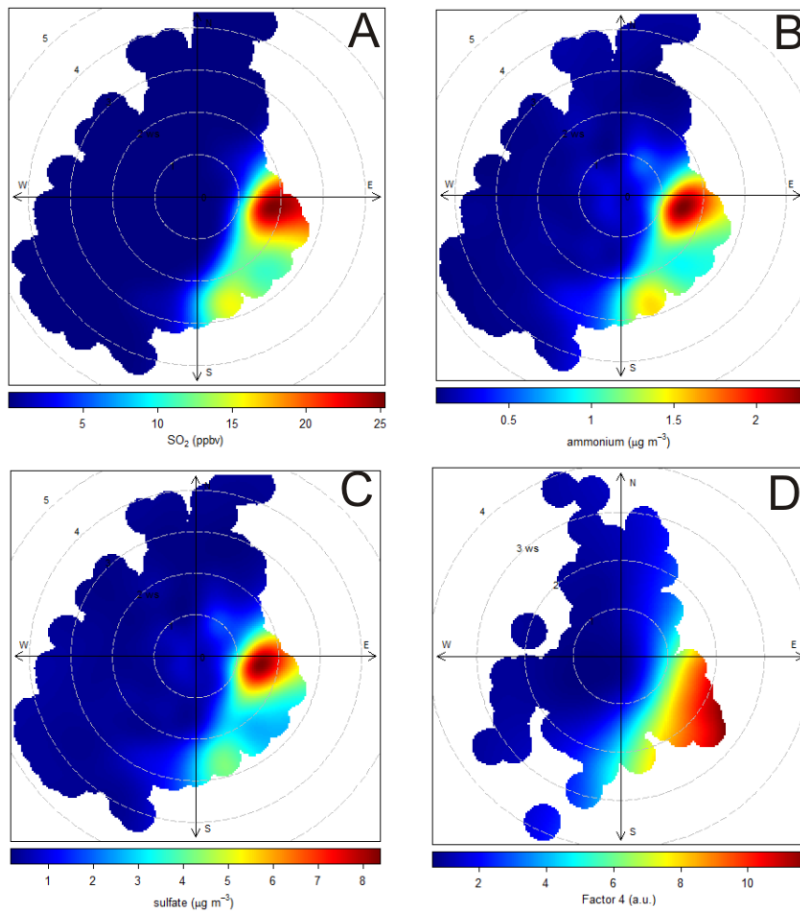
475

476

Figure S-45. Bivariate polar plots associated with component 3 for the optimum primary pollutant solution (Table 54.). (A) β -pinene, (B) α -pinene, (C) CO_2 , (D) and component 3.

477

478



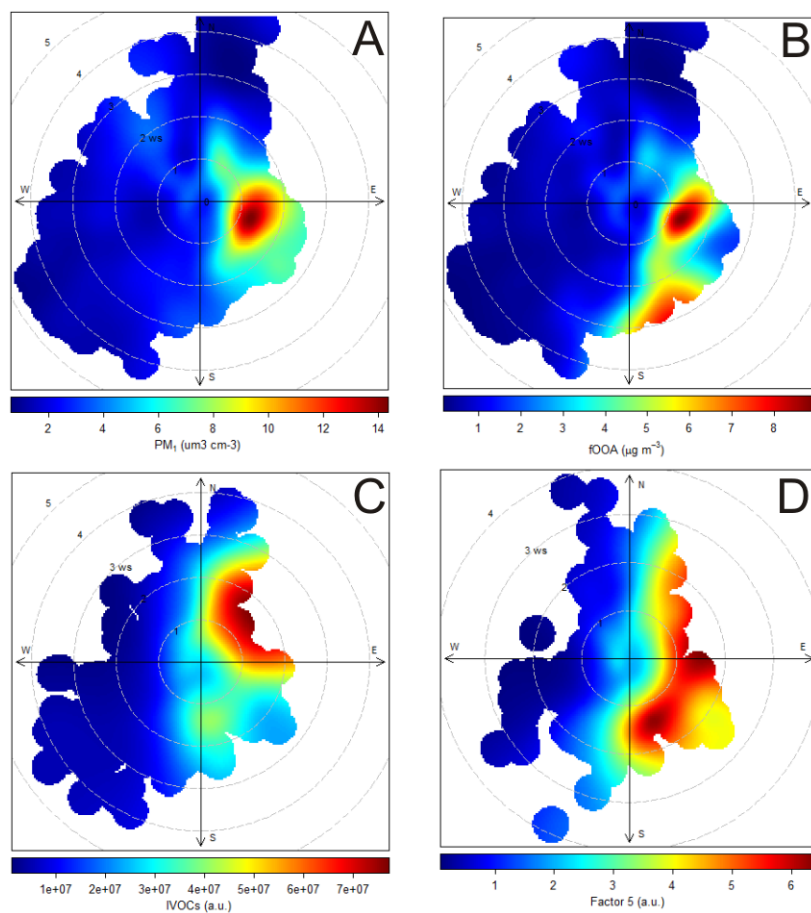
479

480

481

482

Figure S-56. Bivariate polar plots associated with component 4 for the optimum [primary-secondary](#) pollutant solution (Table [Z4](#)). **(A)** SO₂, **(B)** NH₄⁺(p), **(C)** SO₄²⁻(p), **(D)** and component 4.

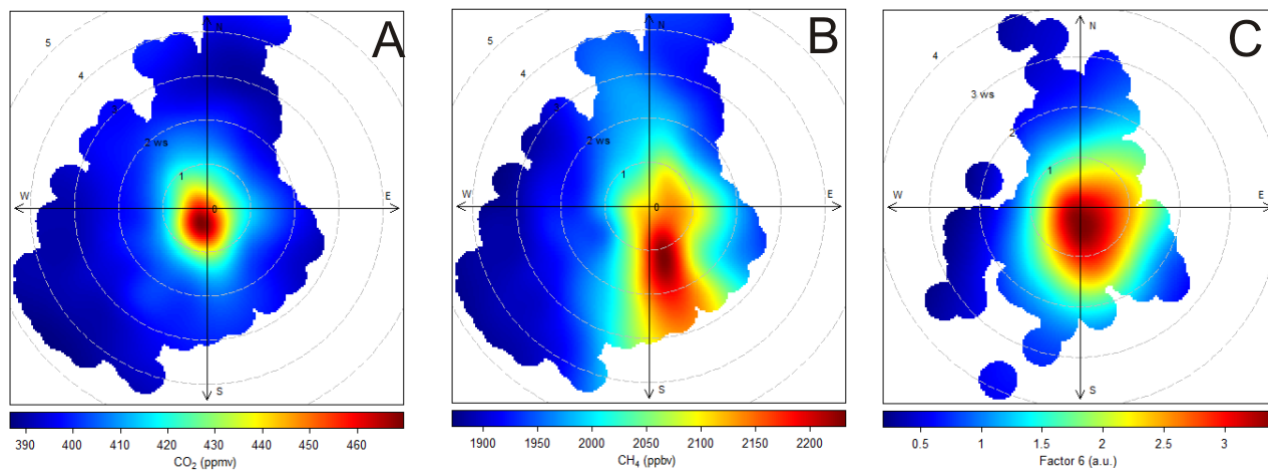


484

485 **Figure S-67.** Bivariate polar plots associated with component 5 for the optimum [primary-secondary](#)
 486 pollutant solution (Table [Z4-](#)). **(A)** PM_{10} (11-component solution), **(B)** LO-OA, **(C)** IVOCs, and **(D)**
 487 component 5.

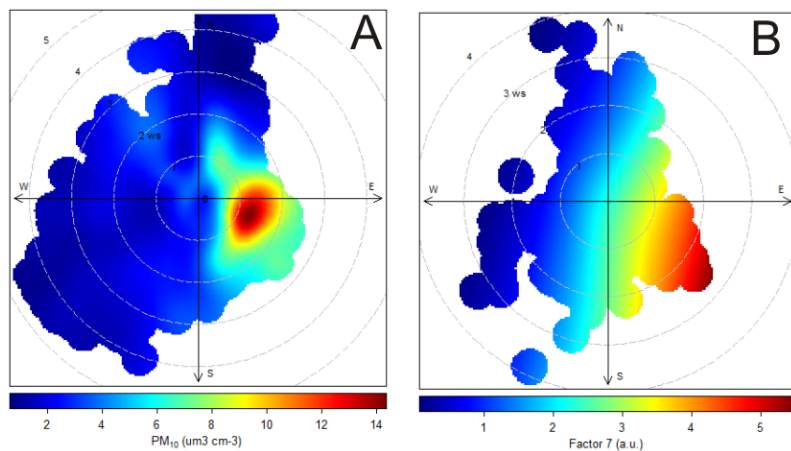
488

489
490



491
492
493
494
495

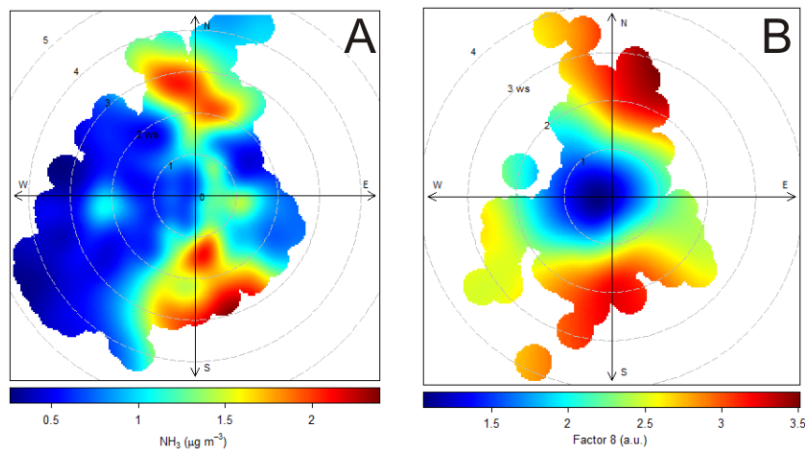
Figure S-78. Bivariate polar plots associated with component 6 for the optimum primary pollutant solution (Table 54). (A) CO₂, (B) CH₄, and (C) component 6.



496
497
498
499

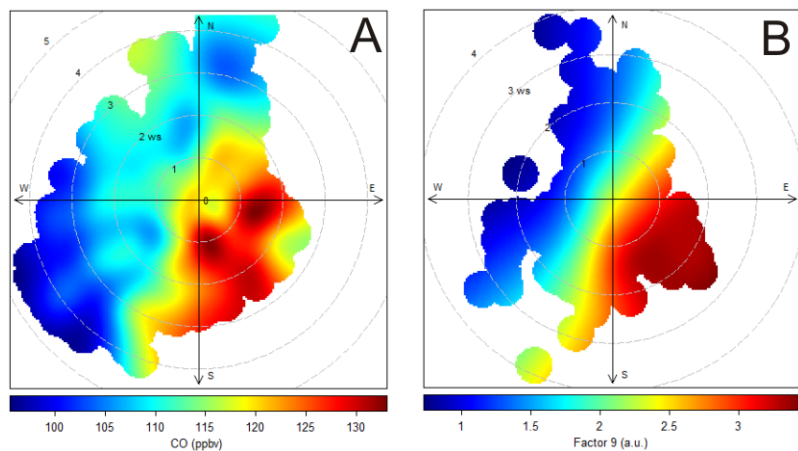
Figure S-89. Bivariate polar plots associated with component 7 for the optimum primary pollutant solution (Table 54). (A) PM₁₀₋₁, (B) and component 7.

500
501



502
503
504
505
506

Figure S-109. Bivariate polar plots associated with component 8 for the optimum primary pollutant solution (Table 54). (A) NH_3 , (B) and component 8.

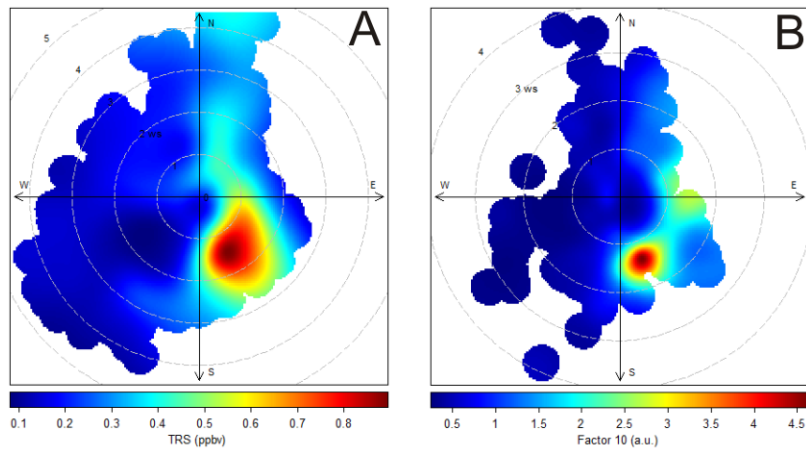


507
508
509
510

Figure S-1011. Bivariate polar plots associated with component 9 for the optimum primary pollutant solution (Table 54). (A) CO, and (B) component 9.

511

512



513

514 **Figure S-121.** Bivariate polar plots associated with component 10 for the optimum primary pollutant
515 solution (Table S-54). (A) TRS, (B) and component 10.

516

517 **References**

- 518
- 519 Bradford, L. M., Ziolkowski, L. A., Goad, C., Warren, L. A., and Slater, G. F.: Elucidating carbon sources
520 driving microbial metabolism during oil sands reclamation, *Journal of Environmental Management*,
521 188, 246-254, 10.1016/j.jenvman.2016.11.029, 2017.
- 522 Burtscher, H., Scherrer, L., Siegmann, H. C., Schmidtott, A., and Federer, B.: Probing aerosols by
523 photoelectric charging, *J. Appl. Phys.*, 53, 3787-3791, 10.1063/1.331120, 1982.
- 524 Bytnerowicz, A., Fraczek, W., Schilling, S., and Alexander, D.: Spatial and temporal distribution of
525 ambient nitric acid and ammonia in the Athabasca Oil Sands Region, Alberta, *J. Limnol.*, 69, 11-21,
526 10.3274/jl10-69-s1-03, 2010.
- 527 Cattell, R. B.: The Scree Test For The Number Of Factors, *Multivariate Behavioral Research*, 1, 245-276,
528 10.1207/s15327906mbr0102_10, 1966.
- 529 Chen, H., Karion, A., Rella, C. W., Winderlich, J., Gerbig, C., Filges, A., Newberger, T., Sweeney, C., and
530 Tans, P. P.: Accurate measurements of carbon monoxide in humid air using the cavity ring-down
531 spectroscopy (CRDS) technique, *Atmos. Meas. Tech.*, 6, 1031-1040, 10.5194/amt-6-1031-2013, 2013.
- 532 National pollutant release inventory (NPRI): [http://open.canada.ca/data/en/dataset/e40099ae-b116-](http://open.canada.ca/data/en/dataset/e40099ae-b116-4c48-9475-f3806fe5a6a6)
533 [4c48-9475-f3806fe5a6a6](http://open.canada.ca/data/en/dataset/e40099ae-b116-4c48-9475-f3806fe5a6a6), access: October 5, 2016, 2013a.
- 534 Measurement instrumentation: carbon dioxide: [https://www.ec.gc.ca/mges-](https://www.ec.gc.ca/mges-ghgm/default.asp?lang=En&n=7903528C-1)
535 [ghgm/default.asp?lang=En&n=7903528C-1](https://www.ec.gc.ca/mges-ghgm/default.asp?lang=En&n=7903528C-1), access: April 25, 2017, 2013b.
- 536 Gorham, E.: Northern peatlands - role in the carbon-cycle and probable responses to climatic warming,
537 *Ecol. Appl.*, 1, 182-195, 10.2307/1941811, 1991.
- 538 Hair, J. F., Anderson, R. E., Tatham, R. L., and Black, W. C.: *Multivariate data analysis*, in, 7th edition ed.,
539 Prentice-Hall, Upper Saddle River, NJ, pp. 108 -110, 1998.
- 540 Holowenko, F. M., MacKinnon, M. D., and Fedorak, P. M.: Methanogens and sulfate-reducing bacteria in
541 oil sands fine tailings waste, *Canadian Journal of Microbiology*, 46, 927-937, 10.1139/cjm-46-10-927,
542 2000.
- 543 Huffman, J. A., Treutlein, B., and Pöschl, U.: Fluorescent biological aerosol particle concentrations and
544 size distributions measured with an Ultraviolet Aerodynamic Particle Sizer (UV-APS) in Central
545 Europe, *Atmos. Chem. Phys.*, 10, 3215-3233, 10.5194/acp-10-3215-2010, 2010.
- 546 Johnson, M. R., Crosland, B. M., McEwen, J. D., Hager, D. B., Armitage, J. R., Karimi-Golpayegani, M., and
547 Picard, D. J.: Estimating fugitive methane emissions from oil sands mining using extractive core
548 samples, *Atmos. Environ.*, 144, 111-123, 10.1016/j.atmosenv.2016.08.073, 2016.
- 549 Liggio, J., Li, S.-M., Hayden, K., Taha, Y. M., Stroud, C., Darlington, A., Drollette, B. D., Gordon, M., Lee, P.,
550 Liu, P., Leithead, A., Moussa, S. G., Wang, D., O'Brien, J., Mittermeier, R. L., Brook, J., Lu, G., Staebler,
551 R., Han, Y., Tokarek, T. W., Osthoff, H. D., Makar, P. A., Zhang, J., Plata, D., and Gentner, D. R.: Oil
552 Sands Operations as a Large Source of Secondary Organic Aerosols, *Nature*, 534, 91-94,
553 10.1038/nature17646, 2016.
- 554 Marey, H. S., Hashisho, Z., Fu, L., and Gille, J.: Spatial and temporal variation in CO over Alberta using
555 measurements from satellites, aircraft, and ground stations, *Atmos. Chem. Phys.*, 15, 3893-3908,
556 10.5194/acp-15-3893-2015, 2015.
- 557 Markovic, M. Z., VandenBoer, T. C., and Murphy, J. G.: Characterization and optimization of an online
558 system for the simultaneous measurement of atmospheric water-soluble constituents in the gas and
559 particle phases, *J. Environ. Monit.*, 14, 1872-1884, 2012.
- 560 Miller, S. M., Worthy, D. E. J., Michalak, A. M., Wofsy, S. C., Kort, E. A., Havice, T. C., Andrews, A. E.,
561 Dlugokencky, E. J., Kaplan, J. O., Levi, P. J., Tian, H. Q., and Zhang, B. W.: Observational constraints on
562 the distribution, seasonality, and environmental predictors of North American boreal methane
563 emissions, *Glob. Biogeochem. Cycle*, 28, 146-160, 10.1002/2013gb004580, 2014.

564 Nara, H., Tanimoto, H., Tohjima, Y., Mukai, H., Nojiri, Y., Katsumata, K., and Rella, C. W.: Effect of air
565 composition (N₂, O₂, Ar, and H₂O) on CO₂ and CH₄ measurement by wavelength-scanned cavity
566 ring-down spectroscopy: calibration and measurement strategy, *Atmos. Meas. Tech.*, 5, 2689-2701,
567 10.5194/amt-5-2689-2012, 2012.

568 Detailed facility information: [http://www.ec.gc.ca/inrp-npri/donnees-](http://www.ec.gc.ca/inrp-npri/donnees-data/index.cfm?do=facility_information&lang=En&opt_npri_id=0000002274&opt_report_year=2013)
569 [data/index.cfm?do=facility_information&lang=En&opt_npri_id=0000002274&opt_report_year=2013](http://www.ec.gc.ca/inrp-npri/donnees-data/index.cfm?do=facility_information&lang=En&opt_npri_id=0000002274&opt_report_year=2013)
570 , access: April 13, 2017, 2013.

571 Nwaishi, F., Petrone, R. M., Macrae, M. L., Price, J. S., Strack, M., and Andersen, R.: Preliminary
572 assessment of greenhouse gas emissions from a constructed fen on post-mining landscape in the
573 Athabasca oil sands region, Alberta, Canada, *Ecol. Eng.*, 95, 119-128, 10.1016/j.ecoleng.2016.06.061,
574 2016.

575 Odame-Ankrah, C. A.: Improved detection instrument for nitrogen oxide species, Ph.D., Chemistry,
576 University of Calgary, <http://hdl.handle.net/11023/2006>, Calgary, 2015.

577 Oertel, C., Matschullat, J., Zurba, K., Zimmermann, F., and Erasmi, S.: Greenhouse gas emissions from
578 soils A review, *Chem Erde-Geochem.*, 76, 327-352, 10.1016/j.chemer.2016.04.002, 2016.

579 Onasch, T. B., Trimborn, A., Fortner, E. C., Jayne, J. T., Kok, G. L., Williams, L. R., Davidovits, P., and
580 Worsnop, D. R.: Soot Particle Aerosol Mass Spectrometer: Development, Validation, and Initial
581 Application, *Aerosol Sci. Technol.*, 46, 804-817, 10.1080/02786826.2012.663948, 2012.

582 Percy, K. E.: Ambient Air Quality and Linkage to Ecosystems in the Athabasca Oil Sands, Alberta, *Geosci.*
583 *Can.*, 40, 182-201, 2013.

584 Phillips-Smith, C., Jeong, C. H., Healy, R. M., Dabek-Zlotorzynska, E., Celio, V., Brook, J. R., and Evans, G.:
585 Sources of Particulate Matter in the Athabasca Oil Sands Region: Investigation through a Comparison
586 of Trace Element Measurement Methodologies, *Atmos. Chem. Phys. Discuss.*, 2017, 1-34,
587 10.5194/acp-2016-966, 2017.

588 Quagraine, E. K., Headley, J. V., and Peterson, H. G.: Is biodegradation of bitumen a source of recalcitrant
589 naphthenic acid mixtures in oil sands tailing pond waters?, *J. Environ. Sci. Health Part A-Toxic/Hazard.*
590 *Subst. Environ. Eng.*, 40, 671-684, 10.1081/ese-200046637, 2005.

591 Rooney, R. C., Bayley, S. E., and Schindler, D. W.: Oil sands mining and reclamation cause massive loss of
592 peatland and stored carbon, *Proc. Natl. Acad. Sci. U.S.A.*, 109, 4933-4937, 10.1073/pnas.1117693108,
593 2012.

594 Shephard, M. W., McLinden, C. A., Cady-Pereira, K. E., Luo, M., Moussa, S. G., Leithead, A., Liggio, J.,
595 Staebler, R. M., Akingunola, A., Makar, P., Lehr, P., Zhang, J., Henze, D. K., Millet, D. B., Bash, J. O.,
596 Zhu, L., Wells, K. C., Capps, S. L., Chaliyakunnel, S., Gordon, M., Hayden, K., Brook, J. R., Wolde, M.,
597 and Li, S. M.: Tropospheric Emission Spectrometer (TES) satellite observations of ammonia,
598 methanol, formic acid, and carbon monoxide over the Canadian oil sands: validation and model
599 evaluation, *Atmospheric Measurement Techniques*, 8, 5189-5211, 10.5194/amt-8-5189-2015, 2015.

600 Small, C. C., Cho, S., Hashisho, Z., and Ulrich, A. C.: Emissions from oil sands tailings ponds: Review of
601 tailings pond parameters and emission estimates, *Journal of Petroleum Science and Engineering*, 127,
602 490-501, 10.1016/j.petrol.2014.11.020, 2015.

603 Thompson, R. L., Sasakawa, M., Machida, T., Aalto, T., Worthy, D., Lavric, J. V., Myhre, C. L., and Stohl, A.:
604 Methane fluxes in the high northern latitudes for 2005-2013 estimated using a Bayesian atmospheric
605 inversion, *Atmos. Chem. Phys.*, 17, 3553-3572, 10.5194/acp-17-3553-2017, 2017.

606 Tokarek, T. W., Huo, J. A., Odame-Ankrah, C. A., Hammoud, D., Taha, Y. M., and Osthoff, H. D.: A gas
607 chromatograph for quantification of peroxy-carboxylic nitric anhydrides calibrated by thermal
608 dissociation cavity ring-down spectroscopy, *Atmos. Meas. Tech.*, 7, 3263-3283, 10.5194/amt-7-3263-
609 2014, 2014.

610 Tokarek, T. W., Brownsey, D. K., Jordan, N., Garner, N. M., Ye, C. Z., Assad, F. V., Peace, A., Schiller, C. L.,
611 Mason, R. H., Vingarzan, R., and Osthoff, H. D.: Biogenic Emissions and Nocturnal Ozone Depletion

612 Events at the Amphitrite Point Observatory on Vancouver Island, Atmosphere-Ocean, 1-12,
613 10.1080/07055900.2017.1306687, 2017.

614 Wang, X. L., Chow, J. C., Kohl, S. D., Percy, K. E., Legge, A. H., and Watson, J. G.: Characterization of
615 PM_{2.5} and PM₁₀ fugitive dust source profiles in the Athabasca Oil Sands Region, J. Air Waste Manag.
616 Assoc., 65, 1421-1433, 10.1080/10962247.2015.1100693, 2015.

617 Warner, D. L., Villarreal, S., McWilliams, K., Inamdar, S., and Vargas, R.: Carbon Dioxide and Methane
618 Fluxes From Tree Stems, Coarse Woody Debris, and Soils in an Upland Temperate Forest, Ecosystems,
619 10.1007/s10021-016-0106-8, 2017.

620 Warren, L. A., Kendra, K. E., Brady, A. L., and Slater, G. F.: Sulfur Biogeochemistry of an Oil Sands
621 Composite Tailings Deposit, Front. Microbiol., 6, 14, 10.3389/fmicb.2015.01533, 2016.

622 Wesely, M. L., and Hicks, B. B.: A review of the current status of knowledge on dry deposition, Atmos.
623 Environm., 34, 2261-2282, 10.1016/S1352-2310(99)00467-7, 2000.

624 Whalen, S. C.: Biogeochemistry of methane exchange between natural wetlands and the atmosphere,
625 Environ. Eng. Sci., 22, 73-94, 10.1089/ees.2005.22.73, 2005.

626 Whaley, C., Makar, P. A., Shephard, M. W., Zhang, L., Zhang, J., Zheng, Q., Akingunola, A., Wentworth, G.
627 R., Murphy, J. G., Kharol, S. K., and Cady-Pereira, K. E.: Contributions of natural and anthropogenic
628 sources to ambient ammonia in the Athabasca Oil Sands and north-western Canada, Atmos. Chem.
629 Phys., submitted, 2017.

630 Wilson, N. K., Barbour, R. K., Chuang, J. C., and Mukund, R.: Evaluation of a real-time monitor for fine
631 particle-bound PAH in air, Polycycl. Aromat. Compd., 5, 167-174, 10.1080/10406639408015168,
632 1994.

633 Yavitt, J. B., Williams, C. J., and Wieder, R. K.: Soil chemistry versus environmental controls on
634 production of CH₄ and CO₂ in northern peatlands, Eur. J. Soil Sci., 56, 169-178, 10.1111/j.1365-
635 2389.2004.00657.x, 2005.

636 Zhang, L. M., Brook, J. R., and Vet, R.: On ozone dry deposition - with emphasis on non-stomatal uptake
637 and wet canopies, Atmos. Environm., 36, 4787-4799, 10.1016/s1352-2310(02)00567-8, 2002.

638

639